

## Contents

General information .....	S1
Synthesis .....	S4
NMR spectra .....	S15
Thermal stabilities.....	S48
Single-crystal X-ray diffraction .....	S49
Photophysical properties .....	S52
Cyclic voltammetry .....	S64
TD-DFT calculations.....	S68
Cartesian coordinates in the structures optimized by DFT calculation .....	S77
References .....	S81

## General information

All starting materials were purchased from commercial sources and used without further purification or prepared following reported procedures. All solvents for synthetic reactions and for photophysical were HPLC grade and spectrographic grade, respectively. The solvents used in this study are bought from Shanghai Aladdin Biochemical Technology Co., Ltd. or J&K Scientific Ltd. and used without further purification. Manipulations and synthesis of all complexes were performed inside a nitrogen gas-filled glovebox (MBRAUN Labmaster 130) or under an argon atmosphere using standard Schlenk techniques.

## General characterization

$^1\text{H}$ ,  $^{13}\text{C}\{^1\text{H}\}$ ,  $^{11}\text{B}\{^1\text{H}\}$ ,  $^{19}\text{F}\{^1\text{H}\}$  heteronuclear correlation spectra were measured at 298 K using a Bruker Avance III 400 MHz, 500 MHz or 600 MHz spectrometers. Chemical shifts ( $\delta$ ) were referenced to solvent peaks as follows:  $^1\text{H}$  NMR spectra were referenced to residual  $\text{CHCl}_3$  in  $\text{CDCl}_3$  (7.26 ppm);  $^{13}\text{C}\{^1\text{H}\}$  NMR spectra were referenced to  $\text{CDCl}_3$  (77.16 ppm);  $^{11}\text{B}\{^1\text{H}\}$  NMR signals were referenced to external  $\text{BF}_3\cdot\text{OEt}_2$  and  $^{19}\text{F}\{^1\text{H}\}$  NMR signals were referenced to  $\text{CFCl}_3$ . High resolution mass spectrometry (HRMS) was performed with a Thermo Fisher Scientific Q Exactive mass spectrometer with the orbitrap as the analyzer.

## Photophysical measurements

All measurements were performed with a standard quartz cuvette (1 cm  $\times$  1 cm cross-section) in the air. UV-visible absorption spectra were recorded using a Thermo Scientific Evolution 201 UV-Visible Spectrophotometer. Emission spectra were performed via Edinburgh spectrometer FLS-980 equipped with MCP-PMT and NIR-PMT detectors. Absolute luminescent quantum yields were recorded with Hamamatsu absolute PL quantum yield spectrometer C11347. Emission lifetime measurements were performed with Hamamatsu compact fluorescence lifetime spectrometer C11367.

## Electrochemical measurements

Cyclic voltammetry experiments were performed using a Gamry Instruments Metrohm Autolab PGSTAT204 in a glovebox. A standard three-electrode cell configuration was

employed using a platinum disk working electrode, a platinum wire counter electrode, and a silver wire, separated by a Vycor tip, serving as the reference electrode. The CH<sub>2</sub>Cl<sub>2</sub> was deoxygenated by bubbling Ar for 10 min before transfer into a glovebox. Tetra-n-butylammonium hexafluorophosphate ([n-Bu<sub>4</sub>N][PF<sub>6</sub>]) was employed as the supporting electrolyte at a concentration of 0.1 mol L<sup>-1</sup> in a 5.0 mL cell. All the cyclic voltammetry measurements were performed at r.t. Before starting the measurements of the complexes, a blank scan was performed to check the purity of the background. Then a small amount (ca. 1 mg) of complex was added and starting the measurements. After recording the cyclic voltammograms of the complexes, another small amount of ferrocene was added and the formal redox potentials are referenced to the ferrocene/ferrocenium redox couple. After each measurement, the working electrode was polished with alumina (first 1.0 micron and then 0.05 micron) by using a smooth, circular motion to regenerate the electrode surface.

### **Single-crystal X-ray diffraction**

The diffraction data were collected by a 'Bruker APEX-II CCD' diffractometer. The crystal was kept at 100 K during data collection. Using Olex2,<sup>[1]</sup> the structure was solved with the SHELXT<sup>[2]</sup> structure solution program using Direct Methods and refined with the SHELXL<sup>[3]</sup> refinement package using Least Squares minimization. Crystal data and experimental details are listed in Table S1-S3; full structural information has been deposited with Cambridge Crystallographic Data Centre CCDC-2373158 (**1**), CCDC-2372887 (**3**), CCDC-2372893 (**4**) and CCDC-2372895(**6**).

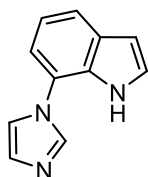
### **Theoretical studies**

DFT and TD-DFT calculations were carried out with the program package Gaussian 16 (A.03) and were performed on a parallel cluster system. GaussView (6.0.16) was used to visualize the results, to measure calculated structural parameters, and to plot orbital surfaces (isovalue:  $\pm 0.020 [e a_0^{-3}]^{1/2}$ ). The ground-state geometries were optimized using the B3LYP functional<sup>4</sup> in combination with the 6-31+g(d,p) basis set.<sup>5</sup> Frequency calculation were performed on the optimized structures to confirm them to be local minima showing no negative (imaginary) frequencies. Based on these optimized structures, the lowest-energy vertical transitions (gas-phase) were calculated (singlets, 20 states for **1–6** and 30 states for **7**) by TD-DFT, using the

Coulomb attenuated functional B3LYP. The program package Multiwfn\_3.7 was used to plot the UV-vis absorption spectra.<sup>6</sup>

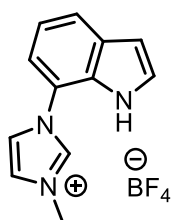
## Synthesis

### 7-(1*H*-imidazol-1-yl)-1*H*-indole



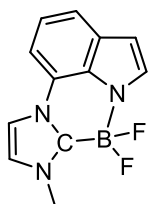
To a pressure-resistant tube was added 7-bromo-1*H*-indole (970 mg, 5 mmol, 1.0 equiv), imidazole (510 mg, 7.5 mmol, 1.5 equiv), CuSO<sub>4</sub>•5H<sub>2</sub>O (249 mg, 1 mmol, 0.2 equiv), K<sub>2</sub>CO<sub>3</sub> (1.38 g, 10 mmol, 2 equiv) and anhydrous DMSO (20 mL) under Ar. The resulting mixture was stirred at 140 °C for 5 days. After cooling to r.t., 100 mL water was added to the mixture and a solid precipitate out. The solid was filtrated and washed by another 100 mL of water. The resulting solid was then extracted by CH<sub>2</sub>Cl<sub>2</sub> and dried over anhydrous Na<sub>2</sub>SO<sub>4</sub>. The collected organic layers were concentrated under reduced pressure and then re-dissolved in CH<sub>2</sub>Cl<sub>2</sub>. After adding hexane, a brown solid precipitate out and the solid was collected (550 mg, 60%) by filtration. <sup>1</sup>H NMR (500 MHz, DMSO-*d*<sub>6</sub>, ppm) δ 11.28 (s, 1H), 8.07 (s, 1H), 7.63 (d, *J* = 7.7 Hz, 1H), 7.60 (s, 1H), 7.38 (t, *J* = 2.8 Hz, 1H), 7.19 (s, 1H), 7.17–7.08 (m, 2H), 6.59 (dd, *J* = 2.8, 1.8 Hz, 1H); <sup>13</sup>C{<sup>1</sup>H} NMR (125 MHz, DMSO-*d*<sub>6</sub>, ppm): δ 137.1, 130.3, 129.20, 129.17, 127.0, 122.3, 120.2, 120.0, 119.2, 116.5, 102.3. HRMS (ESI<sup>+</sup>): *m/z* calcd for [C<sub>11</sub>H<sub>10</sub>N<sub>3</sub>]<sup>+</sup>: 184.0869; Found: 184.0872 [M+H]<sup>+</sup>.

### 1-(1*H*-Indol-7-yl)-3-methyl-1*H*-imidazol-3-ium tetrafluoroborate



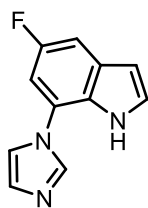
To a round flask was added 7-(1*H*-imidazol-1-yl)-1*H*-indole (183 mg, 1.0 mmol, 1.0 equiv), Me<sub>3</sub>O•BF<sub>4</sub> (148 mg, 1.0 mmol, 1.0 equiv) and anhydrous CH<sub>3</sub>CN (8 mL) under Ar. After stirring at room temperature for 3 hours, the resulting solution was dried under reduced pressure and dissolved in CH<sub>2</sub>Cl<sub>2</sub>. Then hexane was added and a brown solid (231 mg, 81% yield) was obtained by filtration. <sup>1</sup>H NMR (500 MHz, DMSO-*d*<sub>6</sub>) δ 11.56 (s, 1H), 9.65 (s, 1H), 8.14 (t, *J* = 1.8 Hz, 1H), 7.99 (t, *J* = 1.8 Hz, 1H), 7.81 (d, *J* = 7.7 Hz, 1H), 7.57 (t, *J* = 2.8 Hz, 1H), 7.33 (d, *J* = 7.7 Hz, 1H), 7.21 (t, *J* = 7.7 Hz, 1H), 6.68 (dd, *J* = 2.8, 1.8 Hz, 1H), 3.98 (s, 3H); <sup>13</sup>C{<sup>1</sup>H} NMR (125 MHz, DMSO-*d*<sub>6</sub>) δ 137.7, 130.5, 129.7, 127.5, 123.9, 123.6, 122.5, 119.7, 119.2, 117.8, 102.6, 36.1; <sup>11</sup>B{<sup>1</sup>H} NMR (160 MHz, DMSO-*d*<sub>6</sub>, ppm): δ -1.3 (s); <sup>19</sup>F{<sup>1</sup>H} NMR (376 MHz, DMSO-*d*<sub>6</sub>, ppm): δ -148.18, -148.24. HRMS (ESI<sup>+</sup>): *m/z* calcd for [C<sub>12</sub>H<sub>12</sub>N<sub>3</sub>]<sup>+</sup>: 198.1026; Found: 198.1028 [M]<sup>+</sup>.

**7,7-Difluoro-8-methyl-7*H*,8*H*-7λ<sup>4</sup>,7aλ<sup>3</sup>-imidazo[2',1':3,4][1,4,2]diazaborinino[5,6,1-*h*]indole (1)**



To a suspension of 1-(1*H*-indol-7-yl)-3-methyl-1*H*-imidazol-3-ium tetrafluoroborate (143 mg, 0.5 mmol, 1.0 equiv) in toluene (5.0 mL) was added LDA (2.4 equiv) at -78 °C. The resulting mixture was kept stirring at -78 °C for 1 hour and then warmed to r.t. for another 1 hour. The mixture was re-cooled to -78 °C and then BF<sub>3</sub>•Et<sub>2</sub>O (0.5 mmol, 1.0 equiv) was added. The solution was slowly warmed to r.t. and kept stirring at r.t. overnight. The volatiles were removed under reduced pressure and then purified by column chromatography on silica gel (CH<sub>2</sub>Cl<sub>2</sub>). The target compound was obtained as a white solid in 36% yield. <sup>1</sup>H NMR (500 MHz, DMSO-*d*<sub>6</sub>, ppm) δ 8.62 (d, *J* = 2.0 Hz, 1H), 7.89 (d, *J* = 2.0 Hz, 1H), 7.74 (d, *J* = 7.8 Hz, 1H), 7.61 (d, *J* = 7.8 Hz, 1H), 7.54 (d, *J* = 3.0 Hz, 1H), 7.14 (t, *J* = 7.8 Hz, 1H), 6.64 (d, *J* = 3.0 Hz, 1H), 4.01 (s, 3H); <sup>13</sup>C{<sup>1</sup>H} NMR (125 MHz, DMSO-*d*<sub>6</sub>, ppm): δ 129.4, 128.6, 128.3, 124.9, 119.8, 119.7, 118.4, 115.7, 107.2, 104.0, 35.5; <sup>11</sup>B{<sup>1</sup>H} NMR (160 MHz, CDCl<sub>3</sub>, ppm): δ 0.43 (t, *J* = 42.2 Hz); <sup>19</sup>F{<sup>1</sup>H} NMR (376 MHz, CDCl<sub>3</sub>, ppm): δ -136.4–(-137.3) (m). HRMS (ESI<sup>+</sup>): *m/z* calcd for [C<sub>12</sub>H<sub>10</sub>BF<sub>2</sub>N<sub>3</sub>Na]<sup>+</sup>: 268.0828; Found: 268.0832 [M+Na]<sup>+</sup>.

**4-Fluoro-7-(1*H*-imidazol-1-yl)-1*H*-indole**

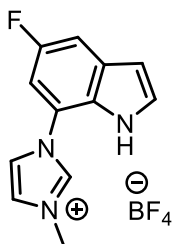


To a pressure-resistant tube was added 7-bromo-4-fluoro-1*H*-indole (1 g, 4.7 mmol, 1.0 equiv), imidazole (476 mg, 7.0 mmol, 1.5 equiv), CuSO<sub>4</sub>•5H<sub>2</sub>O (234 mg, 0.94 mmol, 0.2 equiv), K<sub>2</sub>CO<sub>3</sub> (1.3 g, 9.4 mmol, 2 equiv) and anhydrous DMSO (20 mL) under Ar. The resulting mixture was stirred at 140 °C for 5 days. After cooling to r.t., 100 mL water was added to the mixture and a solid precipitate out. The solid was filtrated and washed by another 100 mL of water. The resulting solid was then extracted by CH<sub>2</sub>Cl<sub>2</sub> and dried over anhydrous Na<sub>2</sub>SO<sub>4</sub>. The collected organic layers were concentrated and washed by Et<sub>2</sub>O. The resulting brown solid were further dried under reduced pressure (422 mg, 45%). <sup>1</sup>H NMR (500 MHz, DMSO-*d*<sub>6</sub>, ppm) δ 11.38 (s, 1H), 8.13 (s, 1H), 7.66 (s, 1H), 7.46 (t, *J* = 2.4 Hz, 1H), 7.43 (dd, *J* = 9.4, 2.4 Hz, 1H), 7.20 (s, 1H), 7.15 (dd, *J* = 9.4, 2.4 Hz, 1H), 6.59 (d, *J* = 1.6 Hz, 1H); <sup>13</sup>C NMR (126 MHz, DMSO-*d*<sub>6</sub>, ppm) δ 156.1 (d, *J*<sub>C-F</sub> =

233 Hz), 137.1, 130.0 (d,  $J_{C-F} = 10.4$  Hz), 129.4, 128.9, 125.8, 122.4 (d,  $J_{C-F} = 12.8$  Hz), 120.1, 105.0 (d,  $J_{C-F} = 29.5$  Hz), 104.4 (d,  $J_{C-F} = 23.3$  Hz), 102.6 (d,  $J_{C-F} = 5.5$  Hz);  $^{19}F\{^1H\}$  NMR (376 MHz, DMSO- $d_6$ , ppm):  $\delta$  -124.2. HRMS (ESI $^+$ ):  $m/z$  calcd for  $[C_{11}H_9FN_3]^+$ : 202.0775; Found: 202.0777 [M+H] $^+$ .

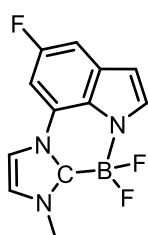
### 1-(5-Fluoro-1H-indol-7-yl)-3-methyl-1H-imidazol-3-ium tetrafluoroborate

To a round flask was added 4-fluoro-7-(1H-imidazol-1-yl)-1H-indole (201 mg, 1.0 mmol, 1.0 equiv),  $Me_3O \cdot BF_4$  (148 mg, 1.0 mmol, 1.0 equiv) and anhydrous  $CH_3CN$  (8 mL) under Ar. After stirring at room temperature for 3 hours, the resulting solution was dried under reduced pressure and a light yellow oil (276 mg, 91% yield) was obtained.  $^1H$  NMR (500 MHz, DMSO- $d_6$ )  $\delta$  11.66 (s, 1H), 9.70



(d,  $J = 1.8$  Hz, 1H), 8.17 (t,  $J = 1.8$  Hz, 1H), 8.00 (t,  $J = 1.8$  Hz, 1H), 7.69–7.63 (m, 2H), 7.39 (dd,  $J = 9.4, 2.4$  Hz, 1H), 6.68 (d,  $J = 3.1$  Hz, 1H), 3.98 (s, 3H);  $^{13}C\{^1H\}$  NMR (125 MHz, DMSO- $d_6$ )  $\delta$  155.6 (d,  $J_{C-F} = 234$  Hz), 138.0, 130.3 (d,  $J_{C-F} = 10.9$  Hz), 129.5, 126.7, 124.0, 123.6, 119.4 (d,  $J_{C-F} = 12.6$  Hz), 107.3 (d,  $J_{C-F} = 23.1$  Hz), 106.8 (d,  $J_{C-F} = 29.9$  Hz), 103.0 (d,  $J_{C-F} = 5.1$  Hz), 36.2;  $^{11}B\{^1H\}$  NMR (160 MHz, DMSO- $d_6$ , ppm):  $\delta$  -1.3 (s);  $^{19}F\{^1H\}$  NMR (376 MHz, DMSO- $d_6$ , ppm):  $\delta$  -124.0 (t,  $J = 9.5$  Hz), -148.18, -148.23. HRMS (ESI $^+$ ):  $m/z$  calcd for  $[C_{12}H_{12}N_3]^+$ : 216.0932; Found: 216.0934 [M] $^+$ .

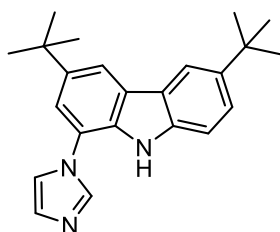
### 3,7,7-Trifluoro-8-methyl-7H,8H-7 $\lambda^4$ ,7a $\lambda^3$ -imidazo[2',1':3,4][1,4,2]diazaborinino[5,6,1-*hi*]indole (2)



To a suspension of 1-(5-fluoro-1H-indol-7-yl)-3-methyl-1H-imidazol-3-ium tetrafluoroborate (152 mg, 0.5 mmol, 1.0 equiv) in toluene (5.0 mL) was added LDA (2.4 equiv) at -78 °C. The resulting mixture was kept stirring at -78 °C for 1 hour and then warmed to room temperature for another 1 hour. The mixture was re-cooled to -78 °C and then  $BF_3 \cdot Et_2O$  (0.5 mmol, 1.0 equiv) was added. The solution was slowly warmed to r.t. and stirring at r.t. overnight. The volatiles were removed under reduced pressure and then purified by column chromatography on silica gel ( $CH_2Cl_2$ :MeOH = 30:1). The target compound was obtained as a white solid in 6% yield.  $^1H$  NMR (500 MHz, DMSO- $d_6$ , ppm)  $\delta$  8.61 (d,  $J = 2.0$  Hz, 1H), 7.90 (d,  $J = 2.0$  Hz, 1H), 7.79 (dd,  $J = 10.0,$

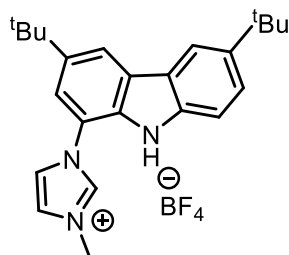
2.2 Hz, 1H), 7.61 (d,  $J = 2.8$  Hz, 1H), 7.41 (dd,  $J = 10.0, 2.2$  Hz, 1H), 6.63 (d,  $J = 2.8$  Hz, 1H), 4.00 (s, 3H);  $^{13}\text{C}\{^1\text{H}\}$  NMR (125 MHz, DMSO- $d_6$ , ppm):  $\delta$  156.3 (d,  $J_{\text{C-F}} = 231$  Hz), 130.3, 128.8 (d,  $J_{\text{C-F}} = 11.4$  Hz), 125.10, 125.06, 119.4 (d,  $J_{\text{C-F}} = 13.4$  Hz), 116.1, 104.5 (d,  $J_{\text{C-F}} = 23.7$  Hz), 104.3 (d,  $J_{\text{C-F}} = 4.7$  Hz), 97.0 (d,  $J_{\text{C-F}} = 32.5$  Hz), 35.6;  $^{11}\text{B}\{^1\text{H}\}$  NMR (160 MHz, DMSO- $d_6$ , ppm):  $\delta$  0.35 (t,  $J = 42.4$  Hz);  $^{19}\text{F}\{^1\text{H}\}$  NMR (376 MHz, DMSO- $d_6$ , ppm):  $\delta$  -124.0, -136.9–(-136.8) (m). HRMS (ESI $^+$ ):  $m/z$  calcd for  $[\text{C}_{12}\text{H}_{10}\text{BF}_3\text{N}_3]^+$ : 264.0914; Found: 264.0914  $[\text{M}+\text{H}]^+$ .

### 3,6-Di-*tert*-butyl-1-(1H-imidazol-1-yl)-9H-carbazole



To a pressure-resistant tube was added 1-bromo-3,6-di-*tert*-butyl-9H-carbazole (2.8 g, 7.9 mmol, 1.0 equiv), imidazole (0.81 g, 11.9 mmol, 1.5 equiv),  $\text{CuSO}_4 \cdot 5\text{H}_2\text{O}$  (0.4 g, 1.58 mmol, 0.2 equiv),  $\text{K}_2\text{CO}_3$  (1.7 g, 15.8 mmol, 2 equiv) and anhydrous DMSO (20 mL) under Ar. The resulting mixture was stirred at 140 °C for 5 days. After cooling to r.t., 100 mL water was added to the mixture and light yellow a solid precipitate out. The solid was filtrated and washed by another 100 mL of water. The resulting solid was then washed by ca. 20 mL ethanol and then 100 mL of  $\text{CH}_2\text{Cl}_2/\text{P.E.}$  (1:1). The collected solid was dried under reduced pressure and a light yellow solid (2.2 g, 81% yield) was obtained.  $^1\text{H}$  NMR (500 MHz, DMSO- $d_6$ , ppm):  $\delta$  11.04 (s, 1H), 8.26 (d,  $J = 1.7$  Hz, 1H), 8.22 (d,  $J = 1.5$  Hz, 1H), 8.13 (s, 1H), 7.68 (s, 1H), 7.48 (dd,  $J = 8.6, 1.9$  Hz, 1H), 7.44–7.37 (m, 2H), 7.23 (s, 1H), 1.43 (s, 9H), 1.40 (s, 9H);  $^{13}\text{C}\{^1\text{H}\}$  NMR (125 MHz, DMSO- $d_6$ , ppm): 141.8, 141.6, 138.9, 137.2, 131.6, 129.2, 125.1, 124.0, 122.3, 120.9, 120.3, 118.4, 116.4, 116.2, 111.2, 34.6, 34.5, 31.9, 31.8. HRMS (ESI $^+$ ):  $m/z$  calcd for  $[\text{C}_{23}\text{H}_{28}\text{N}_3]^+$ : 346.2278; Found: 346.2281  $[\text{M}+\text{H}]^+$ .

### 1-(3,6-Di-*tert*-butyl-9H-carbazol-1-yl)-3-methyl-1H-imidazol-3-ium tetrafluoroborate

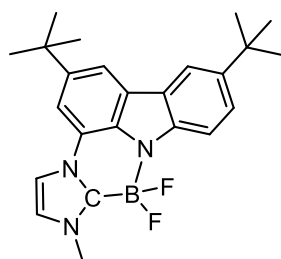


To a round flask was added 3,6-di-*tert*-butyl-1-(1H-imidazol-1-yl)-9H-carbazole (345 mg, 1.0 mmol, 1.0 equiv),  $\text{Me}_3\text{O} \cdot \text{BF}_4$  (148 mg, 1.0 mmol, 1.0 equiv) and anhydrous  $\text{CH}_3\text{CN}$  (8 mL) under Ar. After stirring at r.t. for 3 hours, the resulting solution was dried under reduced pressure and dissolved in  $\text{CH}_2\text{Cl}_2$ . Then hexane was added and a brown solid (281 mg, 63% yield) was obtained by filtration (For further purification, it



can be crystallized by CH<sub>2</sub>Cl<sub>2</sub>/hexane to give a white solid). <sup>1</sup>H NMR (500 MHz, DMSO-*d*<sub>6</sub>) δ 11.33 (s, 1H), 9.70 (s, 1H), 8.47 (d, *J* = 1.7 Hz, 1H), 8.31 (d, *J* = 1.8 Hz, 1H), 8.22 (t, *J* = 1.8 Hz, 1H), 8.03 (t, *J* = 1.8 Hz, 1H), 7.62 (d, *J* = 1.7 Hz, 1H), 7.54 (dd, *J* = 8.6, 1.8 Hz, 1H), 7.43 (d, *J* = 8.6 Hz, 1H), 4.01 (s, 3H), 1.45 (s, 9H), 1.41 (s, 9H); <sup>13</sup>C{<sup>1</sup>H} NMR (125 MHz, DMSO-*d*<sub>6</sub>) δ 142.2, 142.0, 138.7, 137.9, 132.1, 125.5, 124.6, 123.9, 123.7, 122.2, 119.5, 118.8, 118.2, 116.9, 110.9, 36., 34.7, 34.6, 31.8, 31.7; <sup>11</sup>B{<sup>1</sup>H} NMR (160 MHz, DMSO-*d*<sub>6</sub>, ppm): δ -1.3 (s); <sup>19</sup>F{<sup>1</sup>H} NMR (376 MHz, DMSO-*d*<sub>6</sub>, ppm): -148.2, -148.3. HRMS (ESI<sup>+</sup>): *m/z* calcd for [C<sub>24</sub>H<sub>30</sub>N<sub>3</sub>]<sup>+</sup>: 360.2434; Found: 360.2438 [M]<sup>+</sup>.

**2,12-Di-*tert*-butyl-8,8-difluoro-7-methyl-7*H*,8*H*-7a<sup>3</sup>,8l<sup>4</sup>-imidazo[2',1':3,4][1,4,2]diazaborini no[5,6,1-*jk*]carbazole (3)**

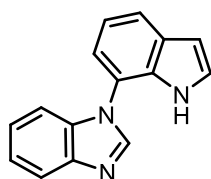


To a suspension of 1-(3,6-di-*tert*-butyl-9*H*-carbazol-1-yl)-3-methyl-1*H*-imidazol-3-ium tetrafluoroborate (224, 0.5 mmol, 1.0 equiv) in toluene (5.0 mL) was added LDA (2.4 equiv) at -78 °C. The resulting mixture was kept stirring at -78 °C for 1 hour and then warmed to r.t. for another 1 hour. The mixture was re-cooled to -78 °C and then BF<sub>3</sub>•Et<sub>2</sub>O (0.5 mmol, 1.0 equiv) was added. The solution was warmed to r.t. and kept stirring at r.t. overnight. The volatiles were removed under reduced pressure and then purified by column chromatography on silica gel (CH<sub>2</sub>Cl<sub>2</sub>). The target compound was obtained as a white solid in 42% yield. <sup>1</sup>H NMR (500 MHz, CDCl<sub>3</sub>, ppm) δ 8.12–8.10 (m, 1H), 8.10 (d, *J* = 1.5 Hz, 1H), 7.86 (d, *J* = 8.5 Hz, 1H), 7.80 (d, *J* = 1.9 Hz, 1H), 7.58 (dd, *J* = 8.5, 2.0 Hz, 1H), 7.49 (d, *J* = 1.5 Hz, 1H), 7.07 (d, *J* = 1.9 Hz, 1H), 4.08 (s, 3H), 1.50 (s, 10H), 1.47 (s, 9H); <sup>13</sup>C{<sup>1</sup>H} NMR (125 MHz, CDCl<sub>3</sub>, ppm): δ 142.6, 141.5, 140.9, 131.66, 125.7, 124.6, 124.5, 123.0, 118.1, 116.4, 116.3, 114.1, 113.6, 107.5, 36.1, 35.2, 34.9, 32.4, 32.2; <sup>11</sup>B{<sup>1</sup>H} NMR (160 MHz, CDCl<sub>3</sub>, ppm): δ 1.3 (t, *J* = 42.2 Hz); <sup>19</sup>F{<sup>1</sup>H} NMR (376 MHz, CDCl<sub>3</sub>, ppm): δ -142.5–(-141.5) (m). HRMS (ESI<sup>+</sup>): *m/z* calcd for [C<sub>24</sub>H<sub>28</sub>BF<sub>2</sub>N<sub>3</sub>Na]<sup>+</sup>: 430.2237; Found: 430.2242 [M+Na]<sup>+</sup>.

**1-(1*H*-indol-7-yl)-1*H*-benzo[*d*]imidazole**

To a pressure-resistant tube was added 7-bromo-1*H*-indole (0.97 g, 5 mmol, 1.0 equiv), benzimidazole (885 mg, 7.5 mmol, 1.5 equiv), CuSO<sub>4</sub>•5H<sub>2</sub>O (249 mg, 1 mmol, 0.2 equiv), K<sub>2</sub>CO<sub>3</sub>

(1.38 g, 10 mmol, 2 equiv) and anhydrous DMSO (20 mL) under Ar. The resulting mixture was



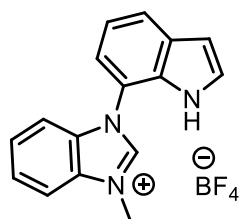
stirred at 140 °C for 5 days. After cooling to r.t., 100 mL water was added to the mixture and a solid precipitate out. The solid was filtrated and washed by another 100 mL of water. The resulting solid was then

extracted by CH<sub>2</sub>Cl<sub>2</sub> and dried over anhydrous Na<sub>2</sub>SO<sub>4</sub>. The collected organic layers were concentrated under reduced pressure and then re-dissolved in CH<sub>2</sub>Cl<sub>2</sub>. After adding hexane, a brown solid starting to precipitate out and the solid was collected (410 mg, 35%) by filtration.

<sup>1</sup>H NMR (500 MHz, DMSO-*d*<sub>6</sub>, ppm) δ 11.23 (s, 1H), 8.53 (s, 1H), 7.82 (d, *J* = 7.8 Hz, 1H), 7.74 (d, *J* = 7.8 Hz, 1H), 7.37 (t, *J* = 2.8 Hz, 1H), 7.34–7.25 (m, 2H), 7.25–7.21 (m, 1H), 7.21–7.16 (m, 2H), 6.63 (dd, *J* = 3.0, 1.8 Hz, 1H); <sup>13</sup>C NMR (126 MHz, DMSO-*d*<sub>6</sub>, ppm) δ 144.1, 143.4, 134.5, 130.9, 130.3, 126.9, 123.2, 122.2, 120.8, 120.2, 119.8, 119.3, 118.7, 110.6, 102.2. HRMS (ESI<sup>+</sup>): *m/z* calcd for [C<sub>15</sub>H<sub>12</sub>N<sub>3</sub>]<sup>+</sup>: 234.1026; Found: 234.1024 [M+H]<sup>+</sup>.

#### 1-(1*H*-indol-7-yl)-3-methyl-1*H*-benzo[*d*]imidazol-3-ium tetrafluoroborate

To a round flask was added 1-(1*H*-indol-7-yl)-1*H*-benzo[*d*]imidazole (233 mg, 1.0 mmol, 1.0



equiv), Me<sub>3</sub>O•BF<sub>4</sub> (148 mg, 1.0 mmol, 1.0 equiv) and anhydrous CH<sub>3</sub>CN (8 mL) under Ar. After stirring at room temperature for 3 hours, the resulting solution was dried under reduced pressure and a light yellow oil (278 mg, 83% yield) was obtained. <sup>1</sup>H NMR (500 MHz, DMSO-*d*<sub>6</sub>,

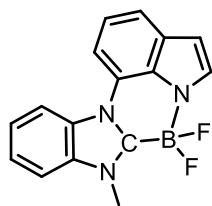
ppm) δ 11.44 (s, 1H), 10.20 (s, 1H), 8.21 (d, *J* = 8.4 Hz, 1H), 7.92 (d, *J* = 7.9 Hz, 1H), 7.84–7.77 (m, 1H), 7.71–7.64 (m, 1H), 7.55 (t, *J* = 2.8 Hz, 1H), 7.50–7.45 (m, 2H), 7.30 (t, *J* = 7.9 Hz, 1H), 6.72 (dd, *J* = 2.8, 1.8 Hz, 1H), 4.23 (s, 3H); <sup>13</sup>C{<sup>1</sup>H} NMR (125 MHz, DMSO-*d*<sub>6</sub>) δ 144.0, 132.1, 131.8, 131.0, 130.6, 127.5, 127.4, 127.0, 123.1, 119.42, 119.41, 116.8, 113.9, 113.2, 102.7, 33.6; <sup>11</sup>B{<sup>1</sup>H} NMR (160 MHz, DMSO-*d*<sub>6</sub>, ppm): δ -1.3 (s); <sup>19</sup>F{<sup>1</sup>H} NMR (376 MHz, DMSO-*d*<sub>6</sub>, ppm): δ -148.20, -148.26. HRMS (ESI<sup>+</sup>): *m/z* calcd for [C<sub>16</sub>H<sub>14</sub>N<sub>3</sub>]<sup>+</sup>: 248.1182; Found: 248.1184 [M]<sup>+</sup>.

#### 7,7-Difluoro-8-methyl-7*H*,8*H*-7*λ*<sup>4</sup>,7*aλ*<sup>3</sup>-

#### benzo[4',5']imidazo[2',1':3,4][1,4,2]diazaborinino[5,6,1-*hi*]indole (4)

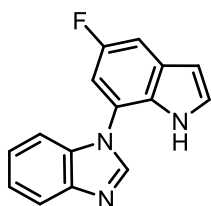
To a suspension of 1-(1*H*-indol-7-yl)-3-methyl-1*H*-benzo[*d*]imidazol-3-ium tetrafluoroborate

(168 mg, 0.5 mmol, 1.0 equiv) in toluene (5.0 mL) was added LDA (2.4 equiv) at  $-78\text{ }^{\circ}\text{C}$ . The resulting mixture was kept stirring at  $-78\text{ }^{\circ}\text{C}$  for 1 hour and then warmed to room temperature for another 1 hour. The mixture was re-cooled to  $-78\text{ }^{\circ}\text{C}$  and then  $\text{BF}_3 \cdot \text{Et}_2\text{O}$  (0.5 mmol, 1.0 equiv) was added. The solution was slowly warmed to r.t. and stirring at r.t. overnight. The volatiles were removed under reduced pressure and then purified by column chromatography on silica gel (hexane: $\text{CH}_2\text{Cl}_2 = 1:2$ ). The target compound was obtained as a white solid in 10% yield.  $^1\text{H}$  NMR (500 MHz,  $\text{CD}_2\text{Cl}_2$ , ppm)  $\delta$  8.51–8.45 (m, 1H), 7.95 (d,  $J = 7.8$  Hz, 1H), 7.78–7.74 (m, 1H), 7.72–7.65 (m, 3H), 7.61 (d,  $J = 3.0$  Hz, 1H), 7.24 (t,  $J = 7.8$  Hz, 1H), 6.72 (d,  $J = 3.0$  Hz, 1H), 4.28 (s, 3H);  $^{13}\text{C}\{^1\text{H}\}$  NMR (125 MHz,  $\text{CD}_2\text{Cl}_2$ , ppm):  $\delta$  134.3, 130.8, 130.4, 129.4, 128.6, 126.9, 126.6, 122.2, 120.5, 118.8, 115.9, 112.7, 108.6, 104.9, 33.0;  $^{11}\text{B}\{^1\text{H}\}$  NMR (160 MHz,  $\text{CD}_2\text{Cl}_2$ , ppm):  $\delta$  0.74 (t,  $J = 43.0$  Hz);  $^{19}\text{F}\{^1\text{H}\}$  NMR (376 MHz, 500 MHz,  $\text{CD}_2\text{Cl}_2$ , ppm):  $\delta$   $-138.8$ –( $-139.3$ ) (m). HRMS (ESI $^+$ ): m/z calcd for  $[\text{C}_{16}\text{H}_{13}\text{BF}_2\text{N}_3]^+$ : 296.1165; Found: 296.1158  $[\text{M}+\text{H}]^+$ .

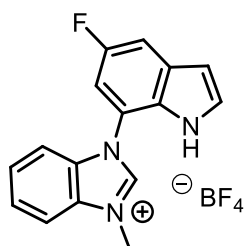


#### 1-(5-Fluoro-1H-indol-7-yl)-1H-benzo[d]imidazole

To a pressure-resistant tube was added 7-bromo-4-fluoro-1H-indole (1.05 g, 5 mmol, 1.0 equiv), benzimidazole (885 mg, 7.5 mmol, 1.5 equiv),  $\text{CuSO}_4 \cdot 5\text{H}_2\text{O}$  (249 mg, 1 mmol, 0.2 equiv),  $\text{K}_2\text{CO}_3$  (1.38 g, 10 mmol, 2 equiv) and anhydrous DMSO (20 mL) under Ar. The resulting mixture was stirred at  $130\text{ }^{\circ}\text{C}$  for 5 days. After cooling to r.t., 100 mL water was added to the mixture and a solid precipitate out. The solid was filtrated and washed by another 100 mL of water. The resulting solid was then extracted by  $\text{CH}_2\text{Cl}_2$  and dried over anhydrous  $\text{Na}_2\text{SO}_4$ . The collected organic layers were concentrated and dried under reduced pressure. The target compound was obtained as a white solid in 36% (451 mg) yield.  $^1\text{H}$  NMR (500 MHz,  $\text{DMSO}-d_6$ , ppm)  $\delta$  11.34 (s, 1H), 8.56 (s, 1H), 7.93–7.75 (m, 1H), 7.55 (dd,  $J = 9.4, 2.4$  Hz, 1H), 7.45 (t,  $J = 2.8$  Hz, 1H), 7.36–7.27 (m, 2H), 7.27–7.20 (m, 2H), 6.63 (dd,  $J = 2.8, 1.4$  Hz, 1H);  $^{13}\text{C}$  NMR (126 MHz,  $\text{DMSO}-d_6$ , ppm)  $\delta$  157.1 (d,  $J_{\text{C-F}} = 234$  Hz), 144.0, 143.4, 134.2, 130.0 (d,  $J_{\text{C-F}} = 11.2$  Hz), 128.8, 127.8, 123.4, 122.4, 120.3 (d,  $J_{\text{C-F}} = 12.2$  Hz), 119.9, 110.6, 107.3 (d,  $J_{\text{C-F}} = 27.4$  Hz), 105.5 (d,  $J_{\text{C-F}} = 23.6$  Hz), 102.5 (d,  $J_{\text{C-F}} = 4.6$  Hz);  $^{19}\text{F}\{^1\text{H}\}$  NMR (376 MHz,  $\text{DMSO}-d_6$ , ppm):  $\delta$   $-124.1$ . HRMS (ESI $^+$ ): m/z calcd for  $[\text{C}_{15}\text{H}_{11}\text{FN}_3]^+$ : 252.0932; Found: 252.0930  $[\text{M}+\text{H}]^+$ .



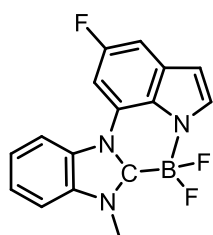
### 1-(5-Fluoro-1*H*-indol-7-yl)-3-methyl-1*H*-benzo[*d*]imidazol-3-ium tetrafluoroborate



To a round flask was added 1-(5-fluoro-1*H*-indol-7-yl)-1*H*-benzo[*d*]imidazole (251 mg, 1.0 mmol, 1.0 equiv), Me<sub>3</sub>O•BF<sub>4</sub> (148 mg, 1.0 mmol, 1.0 equiv) and anhydrous CH<sub>3</sub>CN (8 mL) under Ar. After stirring at room temperature for 3 hours, the resulting solution was dried under reduced pressure and dissolved in CH<sub>2</sub>Cl<sub>2</sub>. Then hexane was added and a white solid (307 mg, 87% yield) was obtained by filtration. <sup>1</sup>H NMR (500 MHz, DMSO-*d*<sub>6</sub>) δ 11.53 (s, 1H), 10.23 (s, 1H), 8.21 (d, *J* = 8.2 Hz, 1H), 7.81 (t, *J* = 7.8 Hz, 1H), 7.76 (dd, *J* = 9.4, 2.2 Hz, 1H), 7.69 (t, *J* = 7.8 Hz, 1H), 7.63 (t, *J* = 2.6 Hz, 1H), 7.56 (d, *J* = 8.2 Hz, 1H), 7.50 (dd, *J* = 9.4, 2.2 Hz, 1H), 6.71 (dd, *J* = 2.6, 1.9 Hz, 1H), 4.23 (s, 3H); <sup>13</sup>C{<sup>1</sup>H} NMR (125 MHz, DMSO-*d*<sub>6</sub>) δ 155.7 (d, *J*<sub>C-F</sub> = 234 Hz), 144.1, 132.0, 131.7, 130.4 (d, *J*<sub>C-F</sub> = 10.9 Hz), 129.5, 128.1, 127.6, 127.1, 116.6 (d, *J*<sub>C-F</sub> = 12.6 Hz), 113.9, 113.3, 108.2 (d, *J*<sub>C-F</sub> = 29.4 Hz), 108.1 (d, *J*<sub>C-F</sub> = 23.0 Hz) (according to the <sup>13</sup>C spectra of its precursor and its derivative below, two peaks are merged at 108.2 ppm which is caused by C–F coupling), 103.0 (d, *J*<sub>C-F</sub> = 4.5 Hz), 33.6; <sup>11</sup>B{<sup>1</sup>H} NMR (160 MHz, DMSO-*d*<sub>6</sub>, ppm): δ –1.3 (s); <sup>19</sup>F{<sup>1</sup>H} NMR (376 MHz, DMSO-*d*<sub>6</sub>, ppm): –123.6 (t, *J* = 8.4 Hz), –148.2, –148.3. HRMS (ESI<sup>+</sup>): *m/z* calcd for [C<sub>16</sub>H<sub>13</sub>FN<sub>3</sub>]<sup>+</sup>: 266.1088; Found: 266.1086 [M]<sup>+</sup>.

### 2,7,7-Trifluoro-8-methyl-7*H*,8*H*-7λ<sup>4</sup>,7aλ<sup>3</sup>-

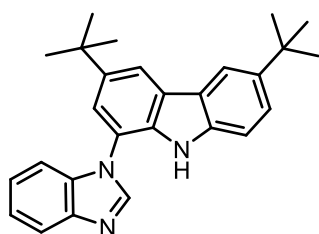
#### benzo[4',5']imidazo[2',1':3,4][1,4,2]diazaborinino[5,6,1-*hi*]indole (5)



To a suspension of 1-(5-fluoro-1*H*-indol-7-yl)-3-methyl-1*H*-benzo[*d*]imidazol-3-ium tetrafluoroborate (177 mg, 0.5 mmol, 1.0 equiv) in toluene (5.0 mL) was added LDA (2.4 equiv) at –78 °C. The resulting mixture was kept stirring at –78 °C for 1 hour and then warmed to r.t. for another 1 hour. The mixture was re-cooled to –78 °C and then BF<sub>3</sub>•Et<sub>2</sub>O (0.5 mmol, 1.0 equiv) was added. The solution was slowly warmed to r.t. and stirring at room temperature overnight. The volatiles were removed under reduced pressure and then purified by column chromatography on silica gel (hexane:CH<sub>2</sub>Cl<sub>2</sub> = 1:5). The target compound was obtained as a white solid in 12% yield. <sup>1</sup>H NMR (500 MHz, DMSO-*d*<sub>6</sub>, ppm) δ 8.85 (d, *J* = 7.6 Hz,

1H), 8.17–8.05 (m, 2H), 7.84–7.71 (m, 2H), 7.67 (d,  $J = 2.9$  Hz, 1H), 7.50 (d,  $J = 9.5$  Hz, 1H), 6.71 (d,  $J = 2.9$  Hz, 1H), 4.26 (s, 3H);  $^{13}\text{C}\{^1\text{H}\}$  NMR (125 MHz, DMSO- $d_6$ , ppm):  $\delta$  156.2 (d,  $J_{\text{C-F}} = 232$  Hz), 133.6, 129.8, 129.2, 128.8 (d,  $J_{\text{C-F}} = 11.3$  Hz), 127.0, 126.5, 125.1, 120.8 (d,  $J_{\text{C-F}} = 13.0$  Hz), 115.7, 113.7, 104.8 (d,  $J_{\text{C-F}} = 4.7$  Hz), 104.4 (d,  $J_{\text{C-F}} = 23.6$  Hz), 98.43 (d,  $J_{\text{C-F}} = 32.3$  Hz), 32.8;  $^{11}\text{B}\{^1\text{H}\}$  NMR (160 MHz, DMSO- $d_6$ , ppm):  $\delta$  0.54 (t,  $J = 42.2$  Hz);  $^{19}\text{F}\{^1\text{H}\}$  NMR (376 MHz, 500 MHz, DMSO- $d_6$ , ppm):  $\delta$  -123.1 (t,  $J = 10.1$  Hz), -141.2–(-140.6) (m). HRMS (ESI $^+$ ):  $m/z$  calcd for  $[\text{C}_{16}\text{H}_{12}\text{BF}_3\text{N}_3]^+$ : 314.1071; Found: 314.1063  $[\text{M}+\text{H}]^+$ .

### 1-(1H-benzo[d]imidazol-1-yl)-3,6-di-tert-butyl-9H-carbazole

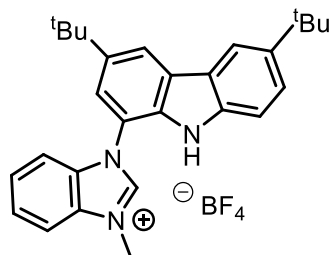


To a pressure-resistant tube was added 1-bromo-3,6-di-tert-butyl-9H-carbazole (1.6 g, 4.5 mmol, 1.0 equiv), benzimidazole (0.8 g, 6.8 mmol, 1.5 equiv),  $\text{CuSO}_4 \cdot 5\text{H}_2\text{O}$  (0.2 g, 0.9 mmol, 0.2 equiv),  $\text{K}_2\text{CO}_3$  (1.2 g, 9 mmol, 2 equiv) and anhydrous DMSO (15 mL) under Ar. The resulting mixture was stirred at 140 °C for 5 days. After cooling to r.t., 100 mL water was added to the mixture and a light yellow solid precipitate out. The solid was filtrated and washed by another 100 mL of water. The resulting solid was then washed by ca. 20 mL ethanol and then 100 mL of  $\text{CH}_2\text{Cl}_2/\text{P.E.}$  (1:1). The collected solid was dried under reduced pressure and a light yellow solid (1.3 g, 71% yield) was obtained.  $^1\text{H}$  NMR (500 MHz, DMSO- $d_6$ , ppm):  $\delta$  11.00 (s, 1H), 8.60 (s, 1H), 8.37 (s, 1H), 8.27 (s, 1H), 7.85 (d,  $J = 7.9$  Hz, 1H), 7.52 (s, 1H), 7.47 (d,  $J = 7.8$  Hz, 1H), 7.36–7.25 (m, 3H), 7.21 (d,  $J = 7.8$  Hz, 1H), 1.45 (s, 9H), 1.41 (s, 9H);  $^{13}\text{C}\{^1\text{H}\}$  NMR (125 MHz, DMSO- $d_6$ , ppm):  $\delta$  144.2, 143.5, 141.9, 141.6, 138.8, 134.4, 133.3, 125.2, 124.0, 123.3, 122.4, 122.2, 120.5, 119.9, 118.8, 117.0, 116.6, 111.1, 110.7, 34.6, 34.5, 31.9, 31.8. HRMS (ESI $^+$ ):  $m/z$  calcd for  $[\text{C}_{27}\text{H}_{30}\text{N}_3]^+$ : 396.2434; Found: 396.2438  $[\text{M}+\text{H}]^+$ .

### 1-(3,6-Di-tert-butyl-9H-carbazol-1-yl)-3-methyl-1H-benzo[d]imidazol-3-ium tetrafluoroborate

To a round flask was added 1-(1H-benzo[d]imidazol-1-yl)-3,6-di-tert-butyl-9H-carbazole (395 mg, 1.0 mmol, 1.0 equiv),  $\text{Me}_3\text{O} \cdot \text{BF}_4$  (148 mg, 1.0 mmol, 1.0 equiv) and anhydrous  $\text{CH}_3\text{CN}$  (8

mL) under Ar. After stirring at r.t. for 3 hours, the resulting solution was dried under reduced

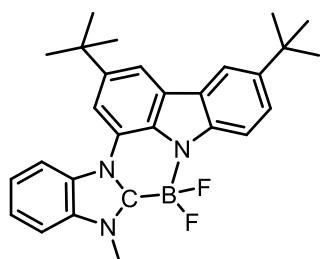


pressure and dissolved in CH<sub>2</sub>Cl<sub>2</sub>. Then hexane was added and a brown solid (402 mg, 81% yield) was obtained by filtration (For further purification, it can be crystallized by CH<sub>2</sub>Cl<sub>2</sub>/hexane and give a white solid). <sup>1</sup>H NMR (500 MHz, DMSO-*d*<sub>6</sub>) δ 11.19 (s, 1H), 10.25 (s, 1H), 8.57 (d, *J* = 0.8 Hz, 1H), 8.35 (d, *J* = 0.8 Hz, 1H),

8.23 (d, *J* = 8.4 Hz, 1H), 7.81 (t, *J* = 7.8 Hz, 1H), 7.79–7.76 (m, 1H), 7.68 (t, *J* = 7.8 Hz, 1H), 7.52 (dd, *J* = 8.6, 1.9 Hz, 1H), 7.46 (d, *J* = 8.4 Hz, 1H), 7.36 (d, *J* = 8.6 Hz, 1H), 4.26 (s, 3H), 1.46 (s, 9H), 1.42 (s, 9H); <sup>13</sup>C{<sup>1</sup>H} NMR (125 MHz, DMSO-*d*<sub>6</sub>) δ 144.0, 142.3, 142.2, 138.6, 133.4, 132.1, 131.8, 127.5, 127.0, 125.7, 124.6, 122.3, 121.0, 119.5, 117.0, 115.4, 113.9, 113.3, 110.9, 34.8, 34.6, 33.5, 31.9, 31.8; <sup>11</sup>B{<sup>1</sup>H} NMR (160 MHz, DMSO-*d*<sub>6</sub>, ppm): δ -1.3 (s); <sup>19</sup>F{<sup>1</sup>H} NMR (376 MHz, DMSO-*d*<sub>6</sub>, ppm): δ -148.2, -148.3. HRMS (ESI<sup>+</sup>): *m/z* calcd for [C<sub>28</sub>H<sub>32</sub>N<sub>3</sub>]<sup>+</sup>: 410.2591; Found: 410.2592 [M]<sup>+</sup>.

#### 2,5-Di-*tert*-butyl-9,9-difluoro-10-methyl-9H,10H-9λ<sup>4</sup>,9aλ<sup>3</sup>-

#### benzo[4',5']imidazo[2',1':3,4][1,4,2]diazaborinino[5,6,1-*jk*]carbazole (6)



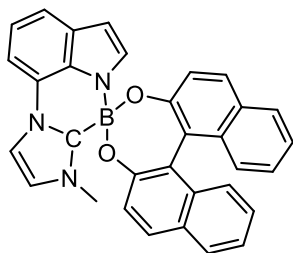
To a suspension of 1-(3,6-di-*tert*-butyl-9H-carbazol-1-yl)-3-methyl-1H-benzo[*d*]imidazol-3-ium tetrafluoroborate (248 mg, 0.5 mmol, 1.0 equiv) in toluene (5.0 mL) was added LDA (2.4 equiv) at -78 °C. The resulting mixture was kept stirring at -78 °C for 1 hour and then warmed to room temperature for another

1 hour. The mixture was re-cooled to -78 °C and then BF<sub>3</sub>•Et<sub>2</sub>O (0.5 mmol, 1.0 equiv) was added. The solution was slowly warmed to room temperature and stirring at room temperature overnight. The volatiles were removed under reduced pressure and then purified by column chromatography on silica gel (hexane:CH<sub>2</sub>Cl<sub>2</sub> = 1:2). The target compound was obtained as a white solid in 14% yield. <sup>1</sup>H NMR (500 MHz, CDCl<sub>3</sub>, ppm) δ 8.45 (d, *J* = 8.3 Hz, 1H), 8.19 (d, *J* = 0.8 Hz, 1H), 8.14 (dd, *J* = 3.9, 0.8 Hz, 2H), 7.89 (d, *J* = 8.3 Hz, 1H), 7.73–7.66 (m, 2H), 7.66–7.57 (m, 2H), 4.33 (s, 3H), 1.58 (s, 9H), 1.49 (s, 9H); <sup>13</sup>C{<sup>1</sup>H} NMR (125 MHz, CDCl<sub>3</sub>, ppm): δ 142.8, 141.1, 141.0, 134.1, 131.8, 130.1, 126.5, 126.3, 125.8, 124.7, 124.6, 120.5, 116.4, 116.0, 115.7, 113.7, 112.4, 109.6, 35.3, 34.9, 32.8, 32.5, 32.2; <sup>11</sup>B{<sup>1</sup>H} NMR (160 MHz,

CDCl<sub>3</sub>, ppm):  $\delta$  1.6 (t,  $J$  = 43.7 Hz); <sup>19</sup>F{<sup>1</sup>H} NMR (376 MHz, CDCl<sub>3</sub>, ppm):  $\delta$  -141.2–(-140.6) (m).

HRMS (ESI<sup>+</sup>):  $m/z$  calcd for [C<sub>24</sub>H<sub>28</sub>BF<sub>2</sub>N<sub>3</sub>Na]<sup>+</sup>: 480.2393; Found: 480.2398 [M+Na]<sup>+</sup>.

**8'-Methyl-8'H-4 $\lambda^4$ ,7a' $\lambda^3$ -spiro[dinaphtho[2,1-*d*:1',2'-*f*][1,3,2]dioxaborepine-4,7'-imidazo[2', 1':3,4][1,4,2]diazaborinino[5,6,1-*h*]indole] (7)**



To a suspension of **1** (25 mg, 0.1 mmol) and (*R*)- or (*S*)-BINOL (86 mg, 0.3 mmol) in CH<sub>2</sub>Cl<sub>2</sub> (4.0 mL) was added EtAlCl<sub>2</sub> (0.12 mmol) at r.t. The mixture was kept stirring for 3 hours and then the volatiles were removed under reduced pressure. The solid was washed by Et<sub>2</sub>O for three times and **7** was obtained as a white solid. <sup>1</sup>H NMR

(500 MHz, CD<sub>2</sub>Cl<sub>2</sub>, ppm)  $\delta$  7.96 (d,  $J$  = 8.1 Hz, 1H), 7.94 (d,  $J$  = 8.7 Hz, 1H), 7.90 (d,  $J$  = 8.1 Hz, 1H), 7.86–7.79 (m, 2H), 7.62 (d,  $J$  = 7.8 Hz, 1H), 7.41–7.35 (m, 3H), 7.35–7.30 (m, 2H), 7.28 (d,  $J$  = 8.7 Hz, 1H), 7.26–7.18 (m, 2H), 7.17–7.10 (m, 2H), 7.04 (d,  $J$  = 1.9 Hz, 1H), 6.76 (d,  $J$  = 3.0 Hz, 1H), 6.43 (d,  $J$  = 3.0 Hz, 1H), 3.17 (s, 3H); <sup>13</sup>C{<sup>1</sup>H} NMR (125 MHz, CD<sub>2</sub>Cl<sub>2</sub>, ppm):  $\delta$  155.3, 154.9, 133.7, 131.1, 130.6, 130.34, 130.27, 129.7, 129.5, 129.4, 128.6, 128.5, 127.1, 127.0, 125.8, 125.7, 124.20, 124.17, 123.8, 123.7, 123.4, 123.3, 122.9, 120.4, 120.3, 118.4, 114.8, 106.2, 103.5, 36.6 (except the peak of carbene carbon was not observed, one additional peak of carbon from indole moiety is missing which is similar to that of **1** in CDCl<sub>3</sub>. We also tried to measure the <sup>13</sup>C{<sup>1</sup>H} NMR in DMSO-*d*<sub>6</sub>, yet only 29 peaks from the aromatic region were observed); <sup>11</sup>B{<sup>1</sup>H} NMR (160 MHz, CD<sub>2</sub>Cl<sub>2</sub>, ppm):  $\delta$  3.73. HRMS (ESI<sup>+</sup>):  $m/z$  calcd for [C<sub>32</sub>H<sub>22</sub>BN<sub>3</sub>O<sub>2</sub>Na] 514.1697; Found: 514.1703 [M+Na]<sup>+</sup>.

## NMR spectra

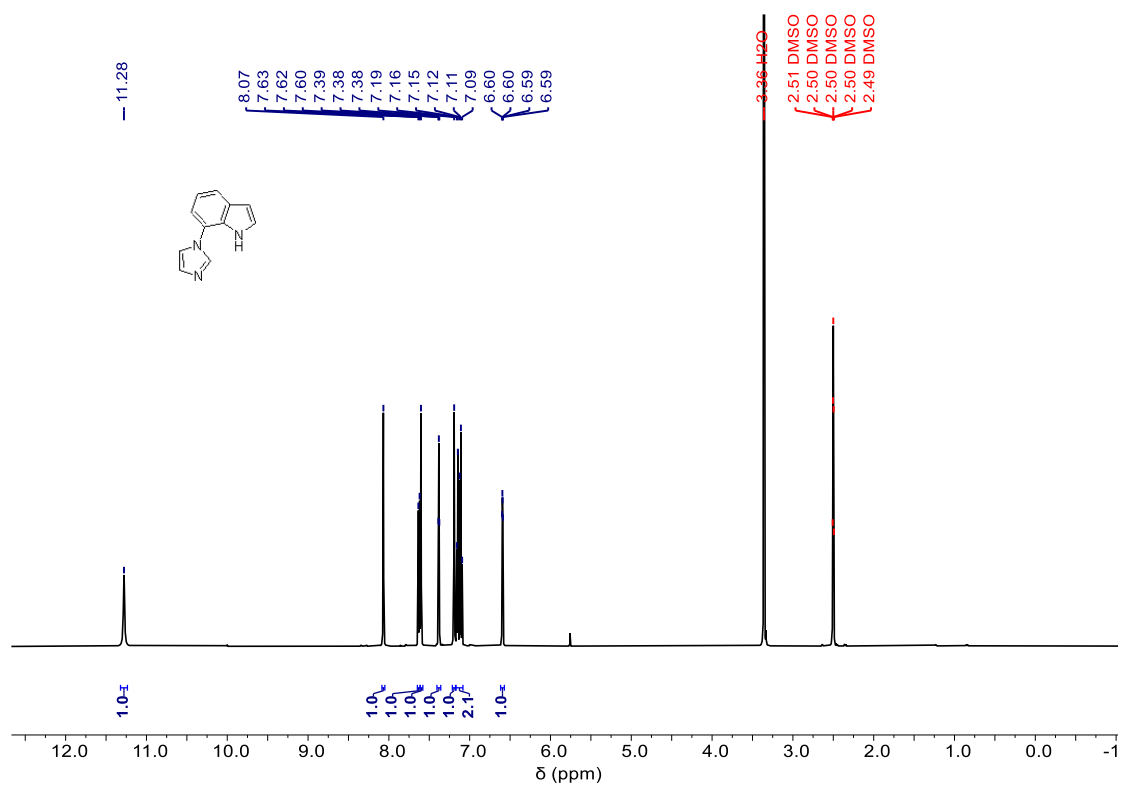


**Figure S1.**  $^1\text{H}$  NMR spectrum of 7-(1H-imidazol-1-yl)-1H-indole in DMSO- $d_6$  at 500 MHz.

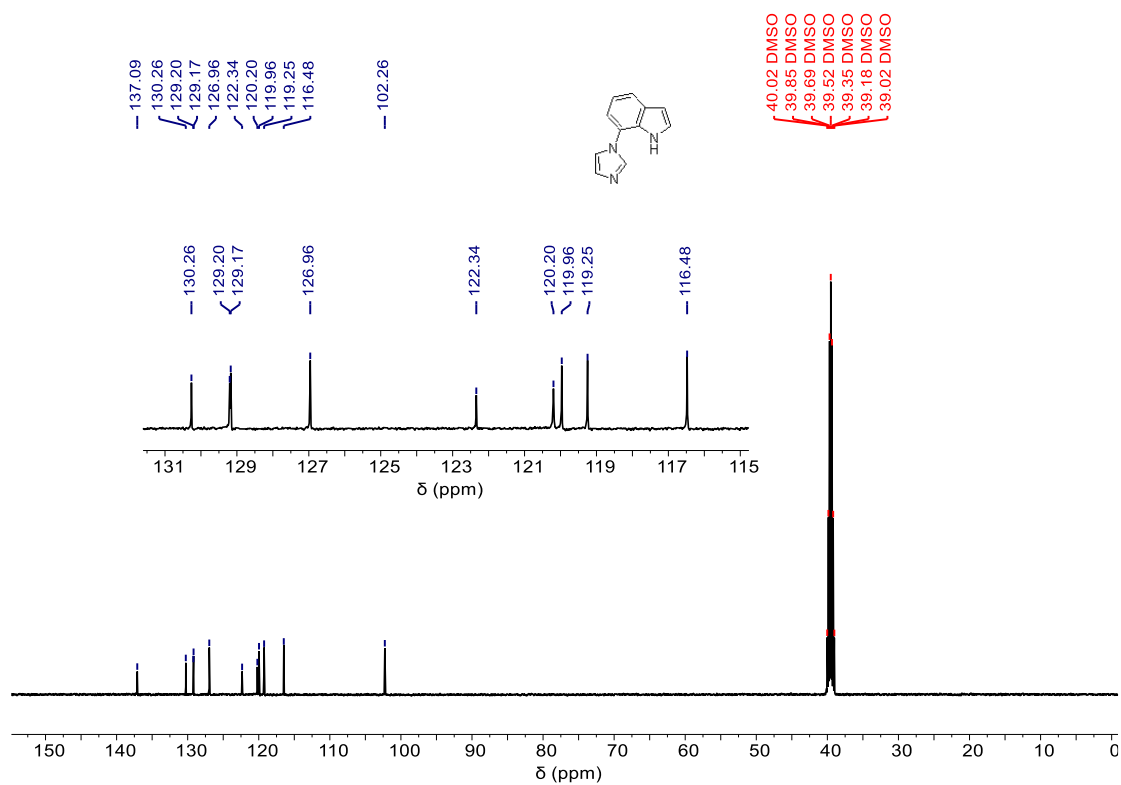


**Figure S2.**  $^{13}\text{C}\{^1\text{H}\}$  NMR spectra of 7-(1H-imidazol-1-yl)-1H-indole in DMSO- $d_6$  at 125 MHz.



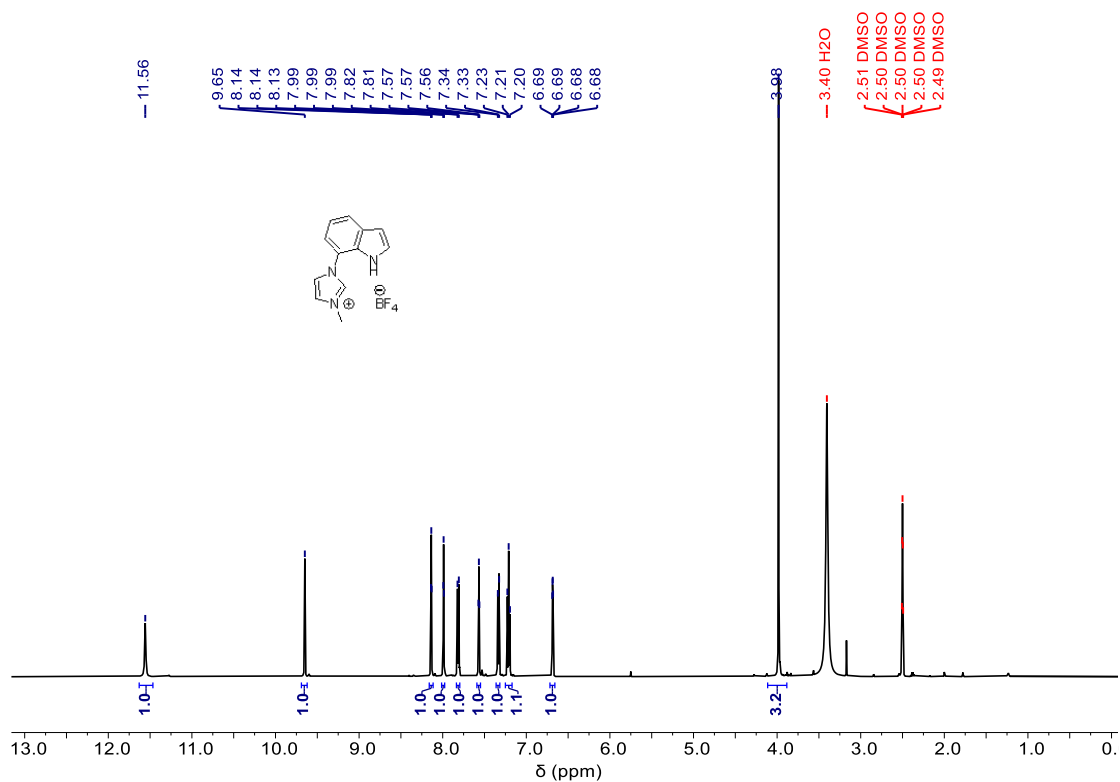


**Figure S3.**  $^1\text{H}$  NMR spectrum of 1-(1*H*-indol-7-yl)-3-methyl-1*H*-imidazol-3-ium tetrafluoroborate in  $\text{DMSO-}d_6$  at 500 MHz.

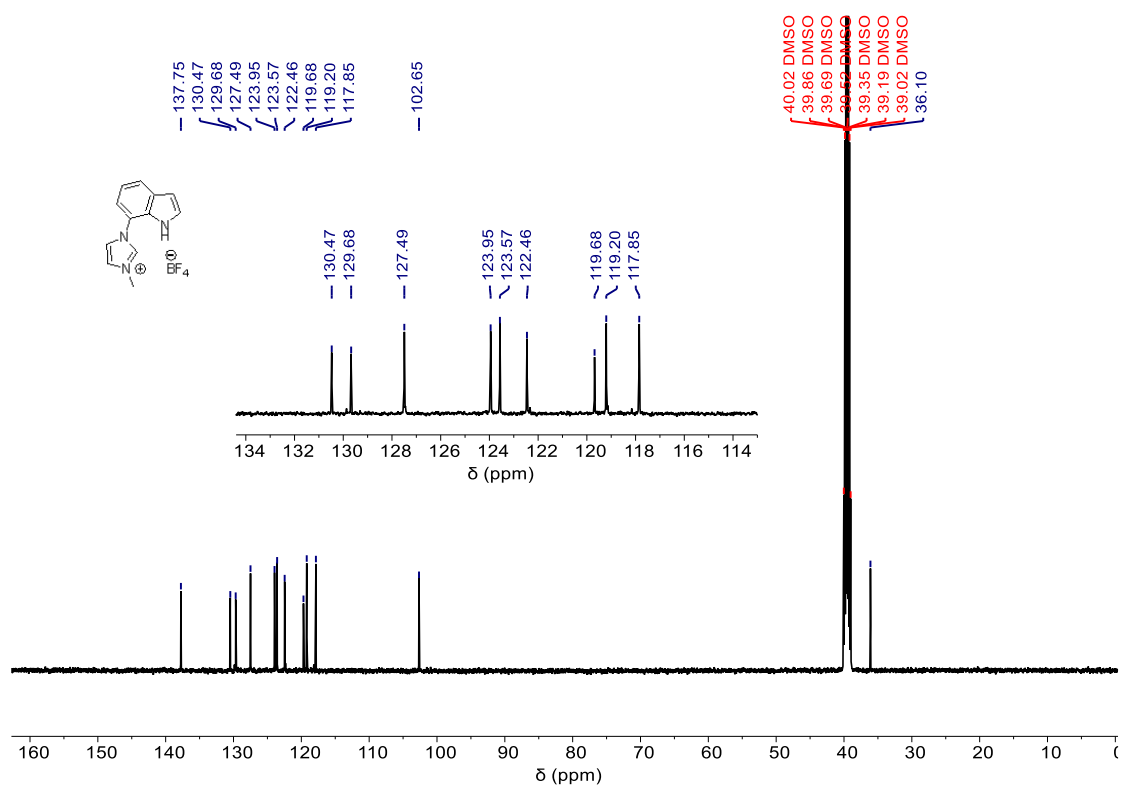


**Figure S4.**  $^{13}\text{C}\{^1\text{H}\}$  NMR spectra of 1-(1*H*-indol-7-yl)-3-methyl-1*H*-imidazol-3-ium tetrafluoroborate in  $\text{DMSO-}d_6$  at 125 MHz.

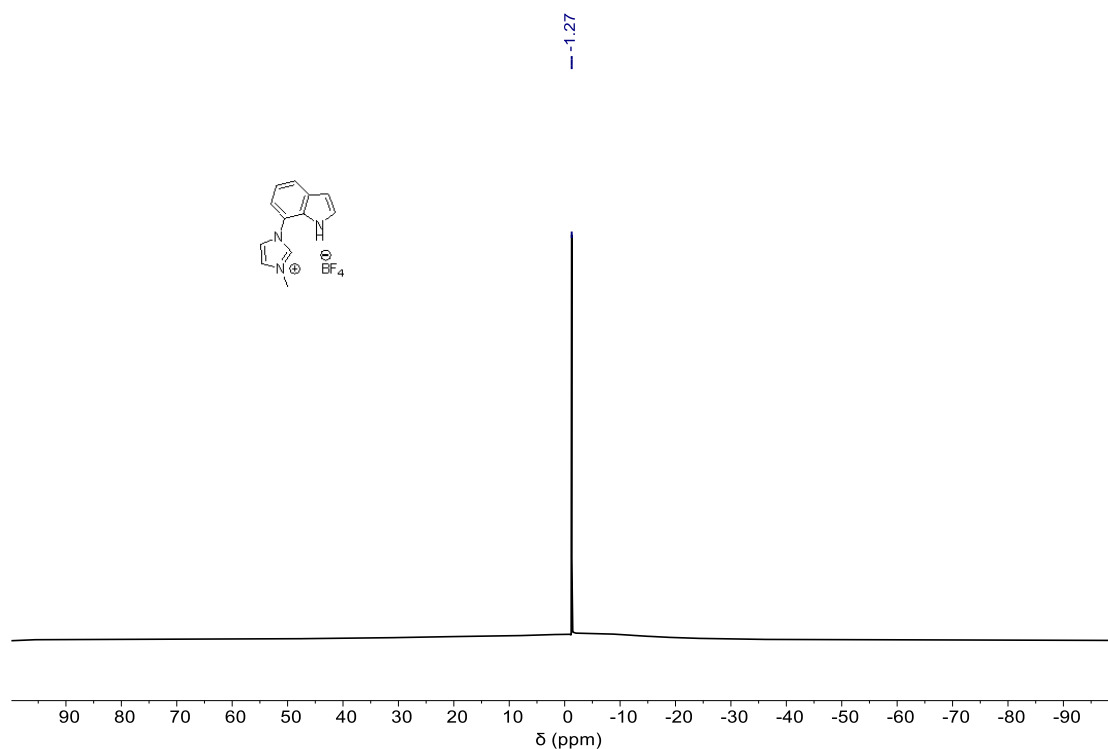


**Figure S5.**  $^{11}\text{B}\{^1\text{H}\}$  NMR spectrum of 1-(1*H*-indol-7-yl)-3-methyl-1*H*-imidazol-3-ium tetrafluoroborate in  $\text{DMSO-}d_6$  at 160 MHz.

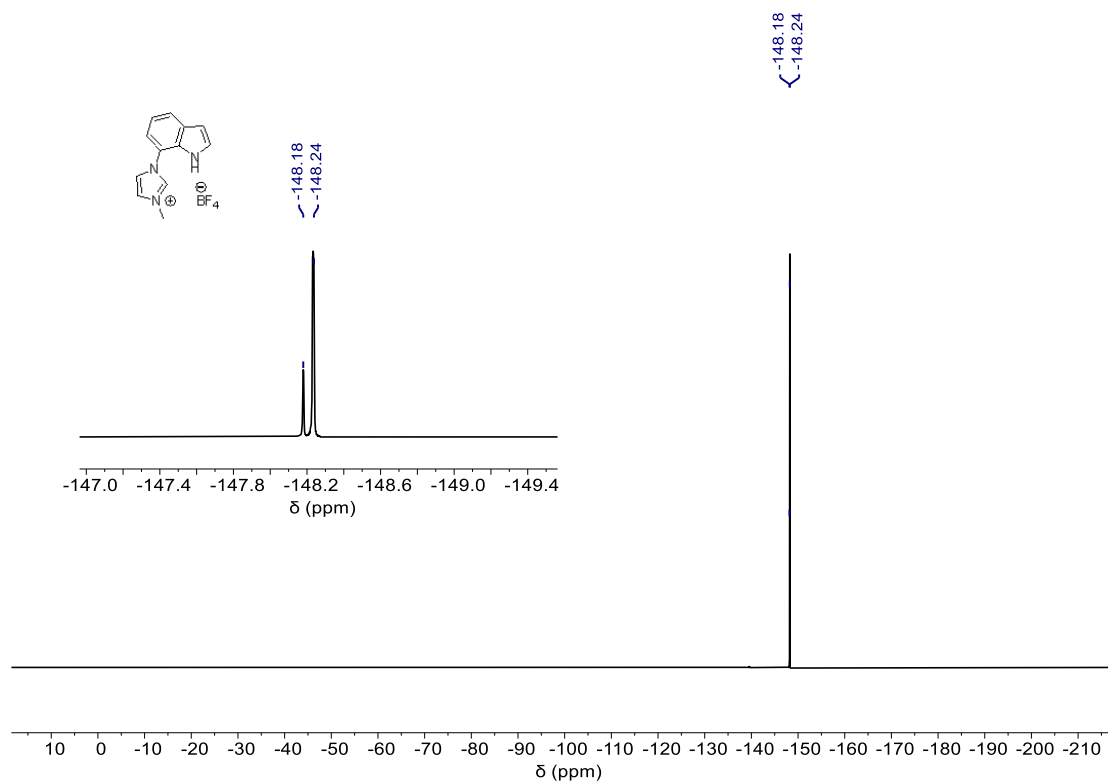


**Figure S6.**  $^{19}\text{F}\{^1\text{H}\}$  NMR spectra of 1-(1*H*-indol-7-yl)-3-methyl-1*H*-imidazol-3-ium tetrafluoroborate in  $\text{DMSO-}d_6$  at 376 MHz.

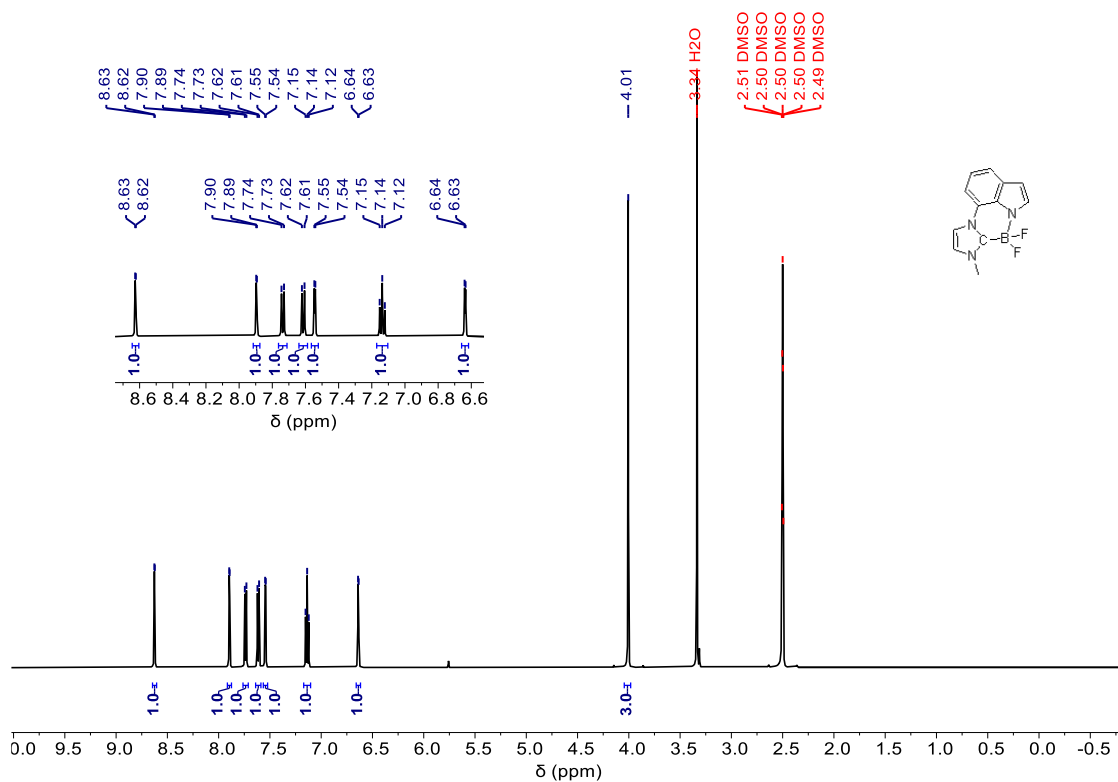


**Figure S7.**  $^1\text{H}$  NMR spectra of **1** in  $\text{DMSO-}d_6$  at 500 MHz.

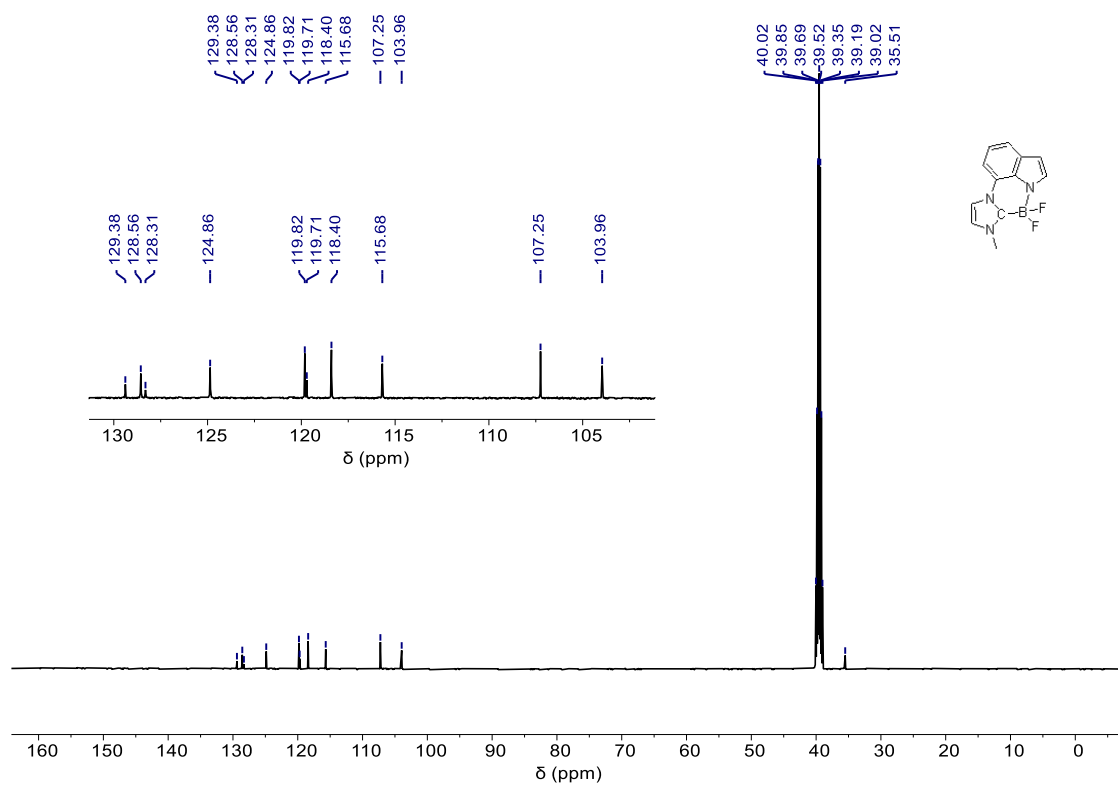


**Figure S8.**  $^{13}\text{C}\{^1\text{H}\}$  NMR spectra of **1** in  $\text{DMSO-}d_6$  at 125 MHz.

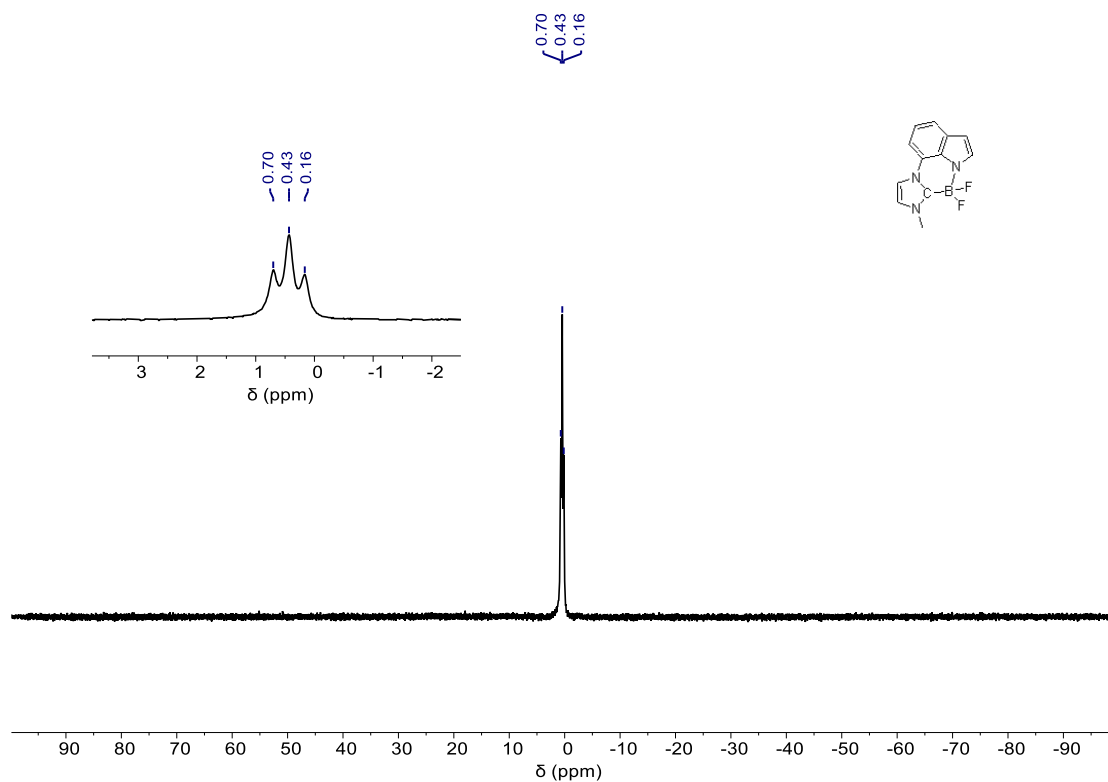


**Figure S9.**  $^{11}\text{B}\{^1\text{H}\}$  NMR spectra of **1** in  $\text{DMSO-}d_6$  at 160 MHz.

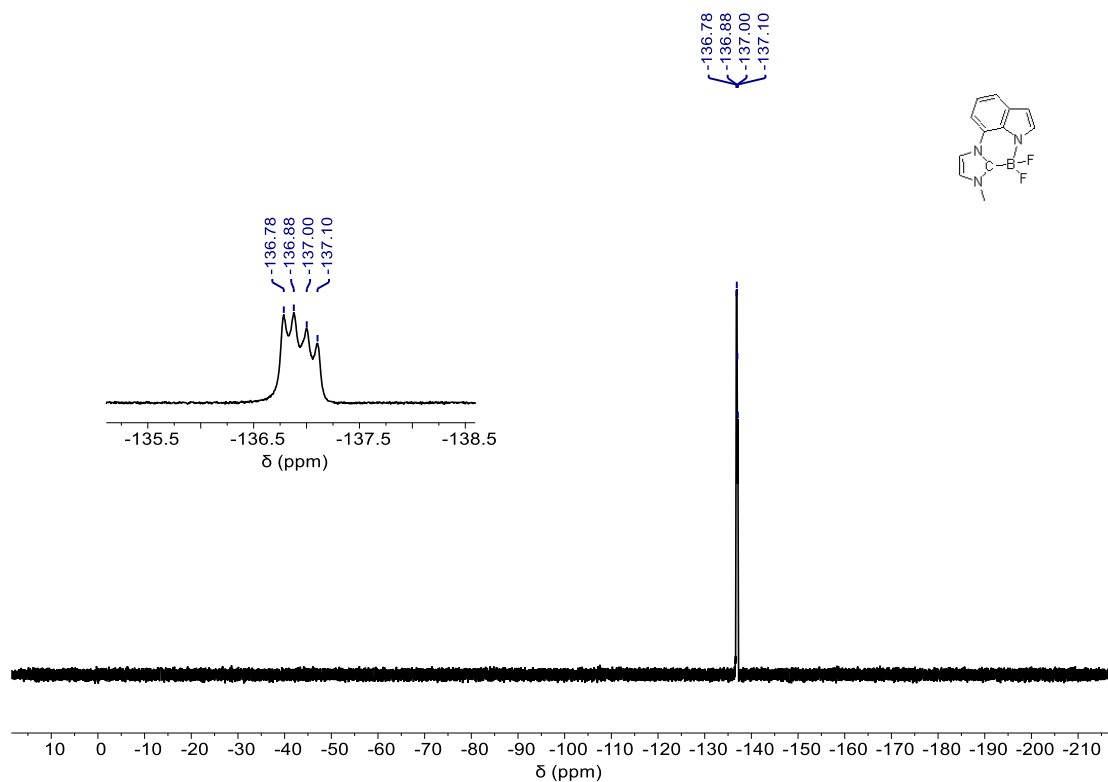


**Figure S10.**  $^{19}\text{F}\{^1\text{H}\}$  NMR spectra of **1** in  $\text{DMSO-}d_6$  at 376 MHz.

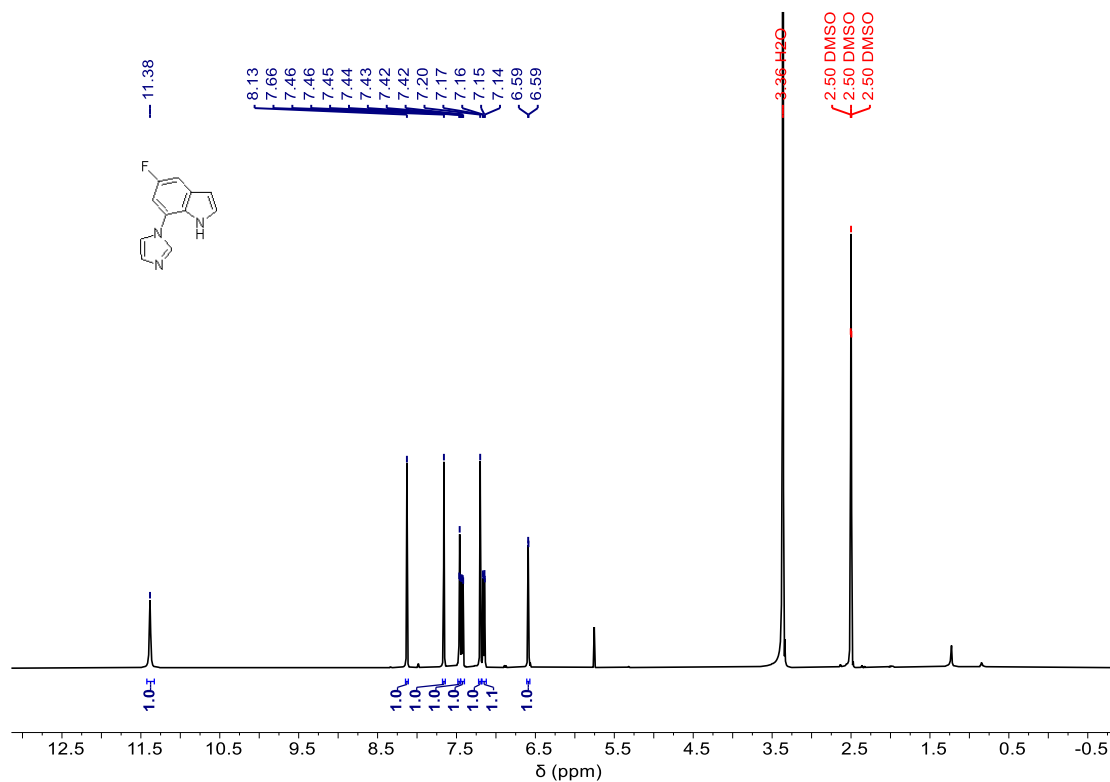


**Figure S11.**  $^1\text{H}$  NMR spectrum of 4-fluoro-7-(1*H*-imidazol-1-yl)-1*H*-indole in DMSO- $d_6$  at 500 MHz.

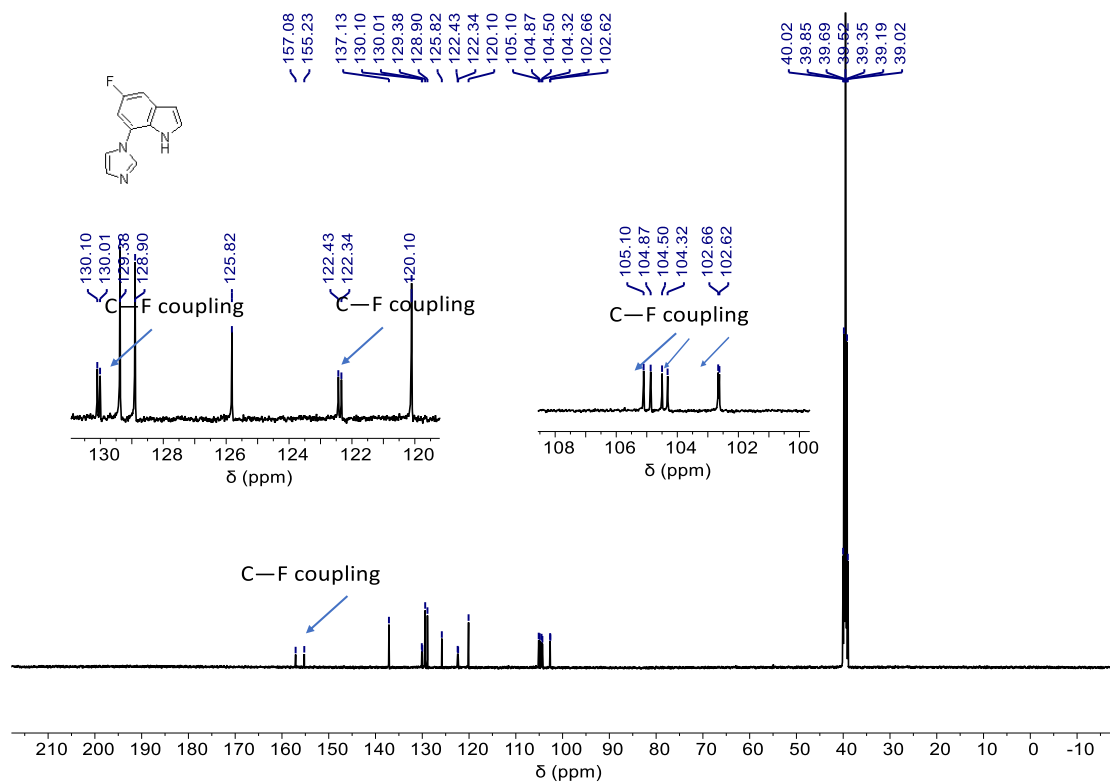


**Figure S12.**  $^{13}\text{C}\{^1\text{H}\}$  NMR spectra of 4-fluoro-7-(1*H*-imidazol-1-yl)-1*H*-indole in DMSO- $d_6$  at 125 MHz.

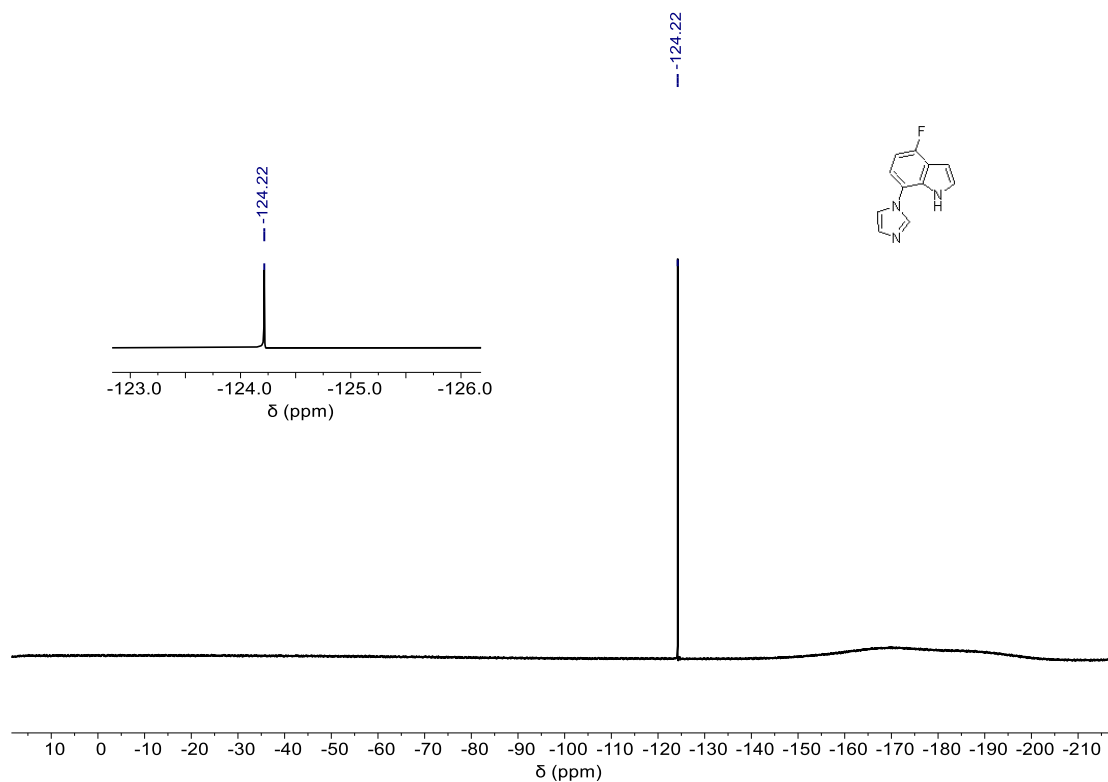


**Figure S13.**  $^{19}\text{F}\{^1\text{H}\}$  NMR spectra of 4-fluoro-7-(1H-imidazol-1-yl)-1H-indole in  $\text{DMSO-}d_6$  at 376 MHz.

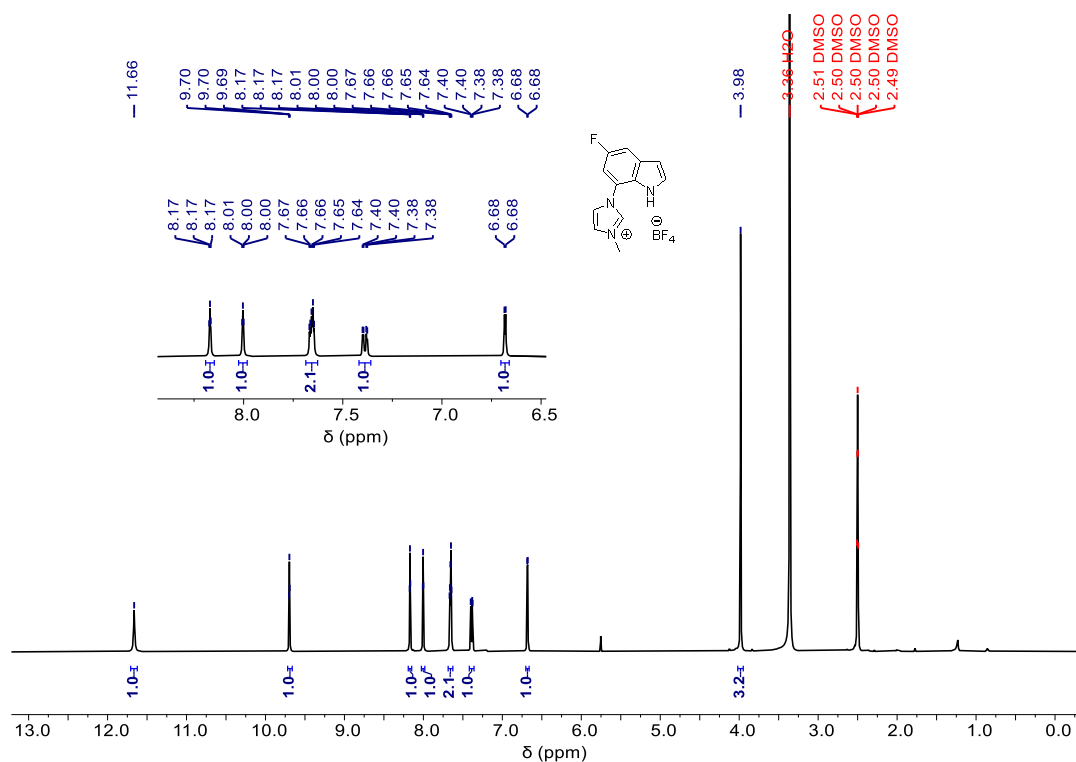


**Figure S14.**  $^1\text{H}$  NMR spectra of 1-(5-fluoro-1H-indol-7-yl)-3-methyl-1H-imidazol-3-ium tetrafluoroborate in  $\text{DMSO-}d_6$  at 500 MHz.

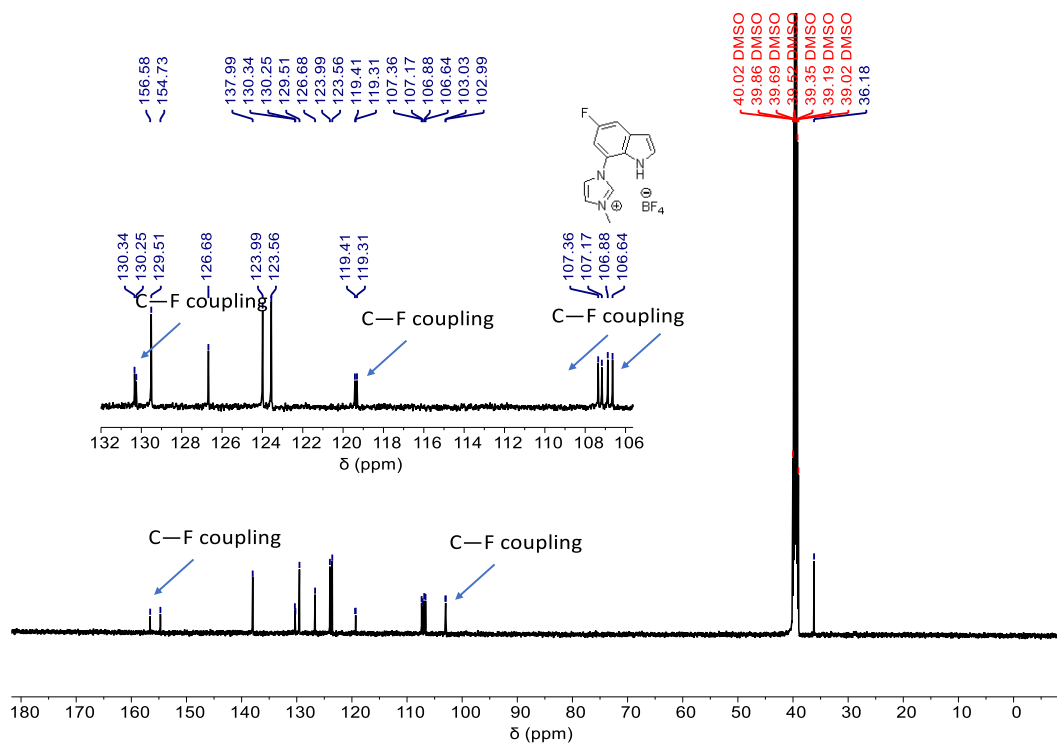


**Figure S15.**  $^{13}\text{C}\{^1\text{H}\}$  NMR spectra of 1-(5-fluoro-1*H*-indol-7-yl)-3-methyl-1*H*-imidazol-3-ium tetrafluoroborate in  $\text{DMSO-}d_6$  at 125 MHz.

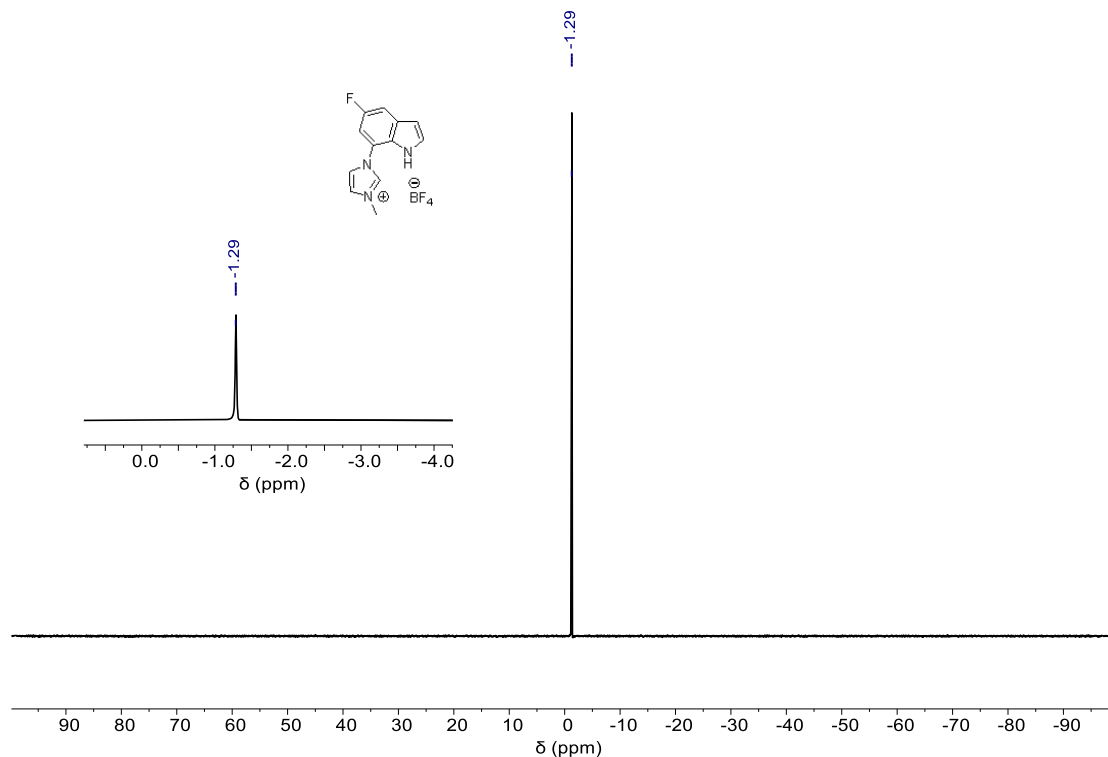


**Figure S16.**  $^{11}\text{B}\{^1\text{H}\}$  NMR spectra of 1-(5-fluoro-1*H*-indol-7-yl)-3-methyl-1*H*-imidazol-3-ium tetrafluoroborate in  $\text{DMSO-}d_6$  at 160 MHz.

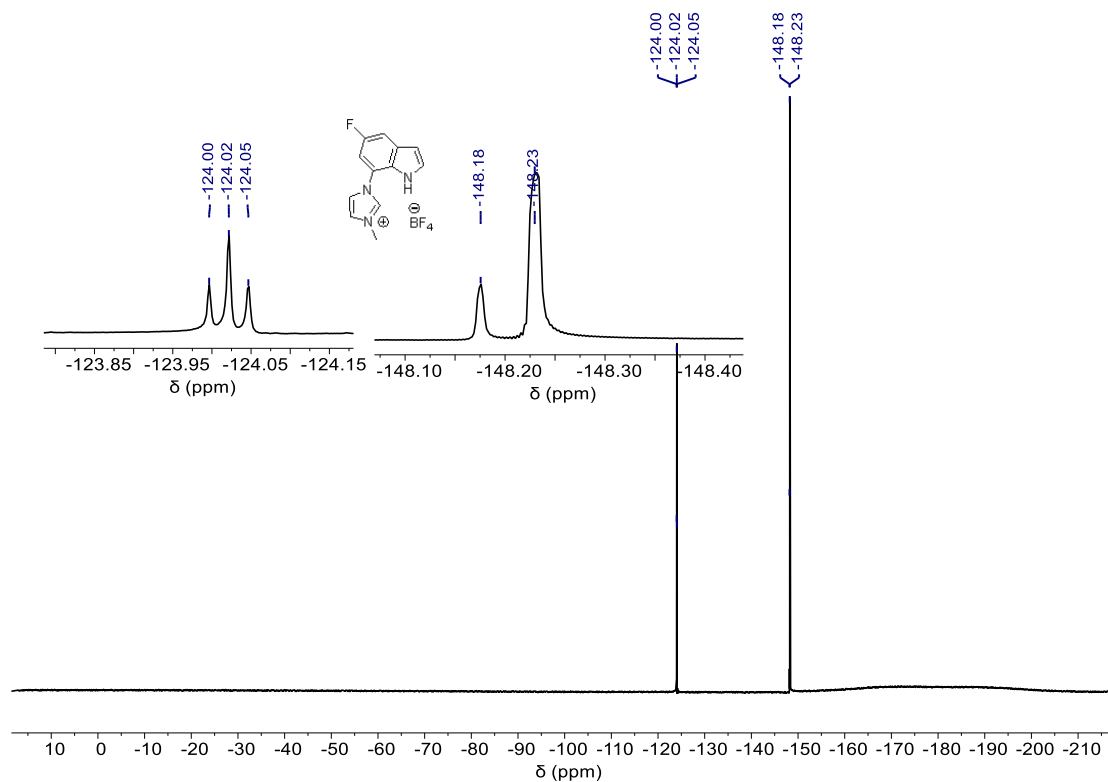


**Figure S17.**  $^{19}\text{F}\{^1\text{H}\}$  NMR spectra of 1-(5-fluoro-1H-indol-7-yl)-3-methyl-1H-imidazol-3-ium tetrafluoroborate in  $\text{DMSO-}d_6$  at 376 MHz.

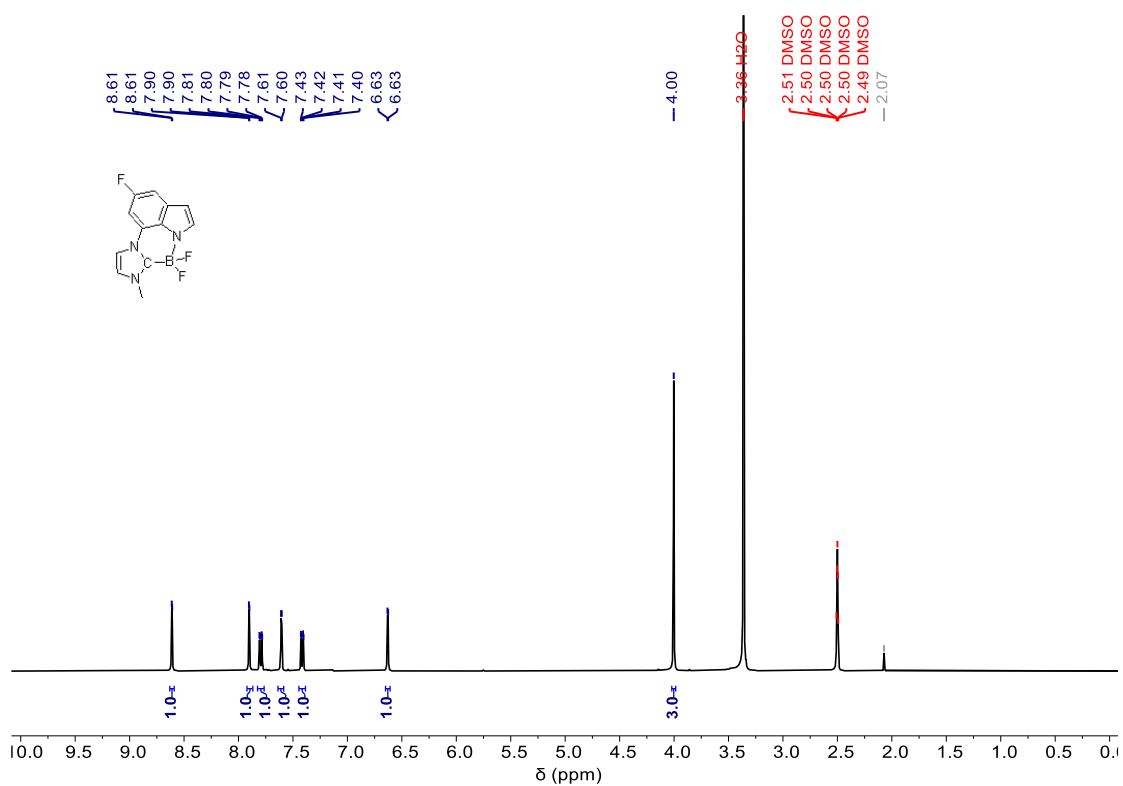
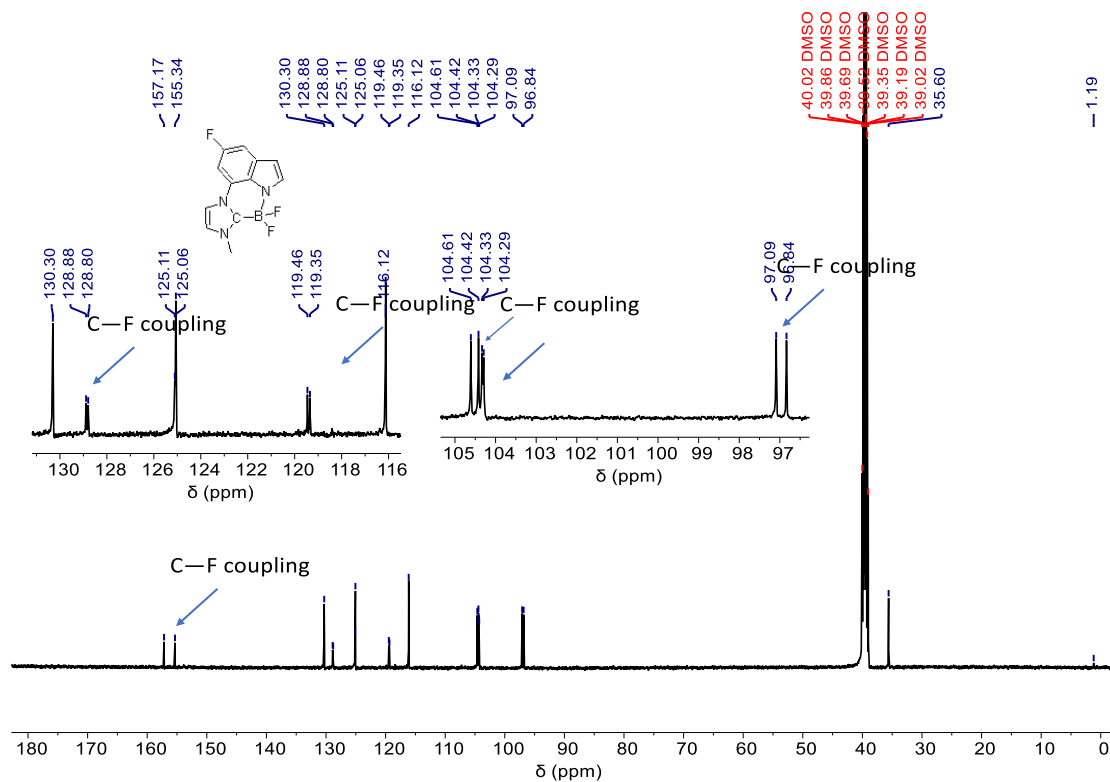


**Figure S18.**  $^1\text{H}$  NMR spectrum of **2** in  $\text{DMSO-}d_6$  at 500 MHz.





— 1.19

**Figure S19.**  $^{13}\text{C}\{^1\text{H}\}$  NMR spectra of **2** in  $\text{DMSO-}d_6$  at 125 MHz.

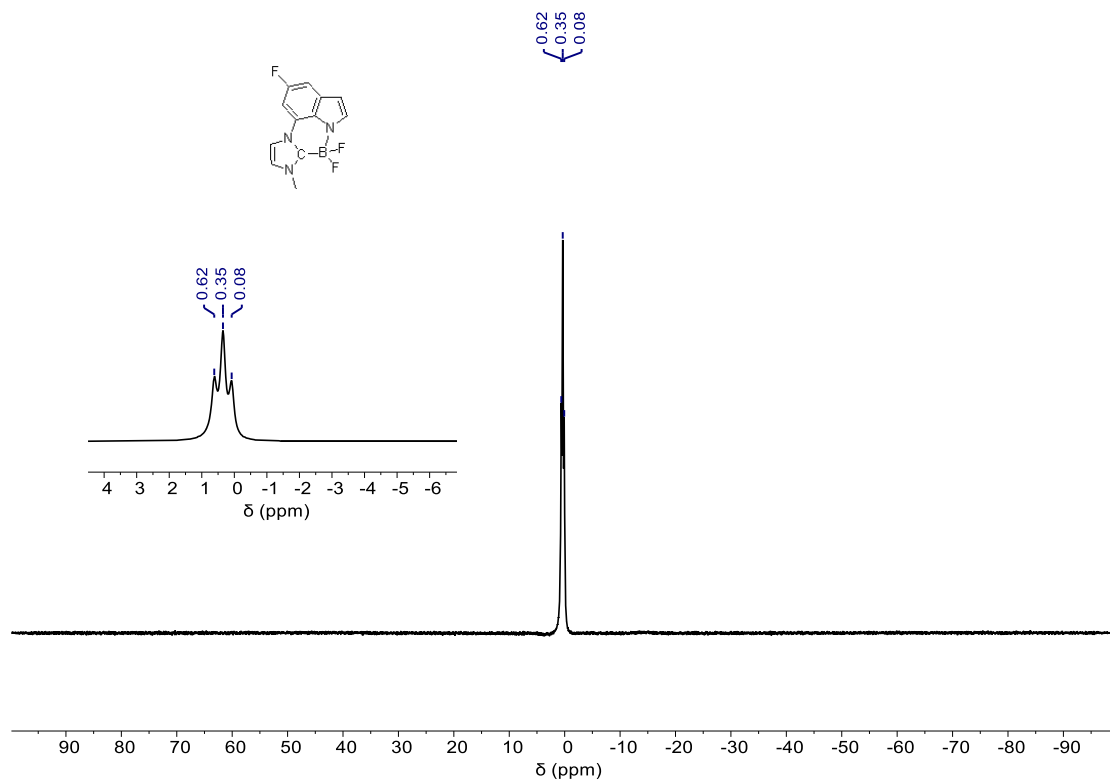


**Figure S20.**  $^{11}\text{B}\{^1\text{H}\}$  NMR spectra of **2** in  $\text{DMSO-}d_6$  at 160 MHz.

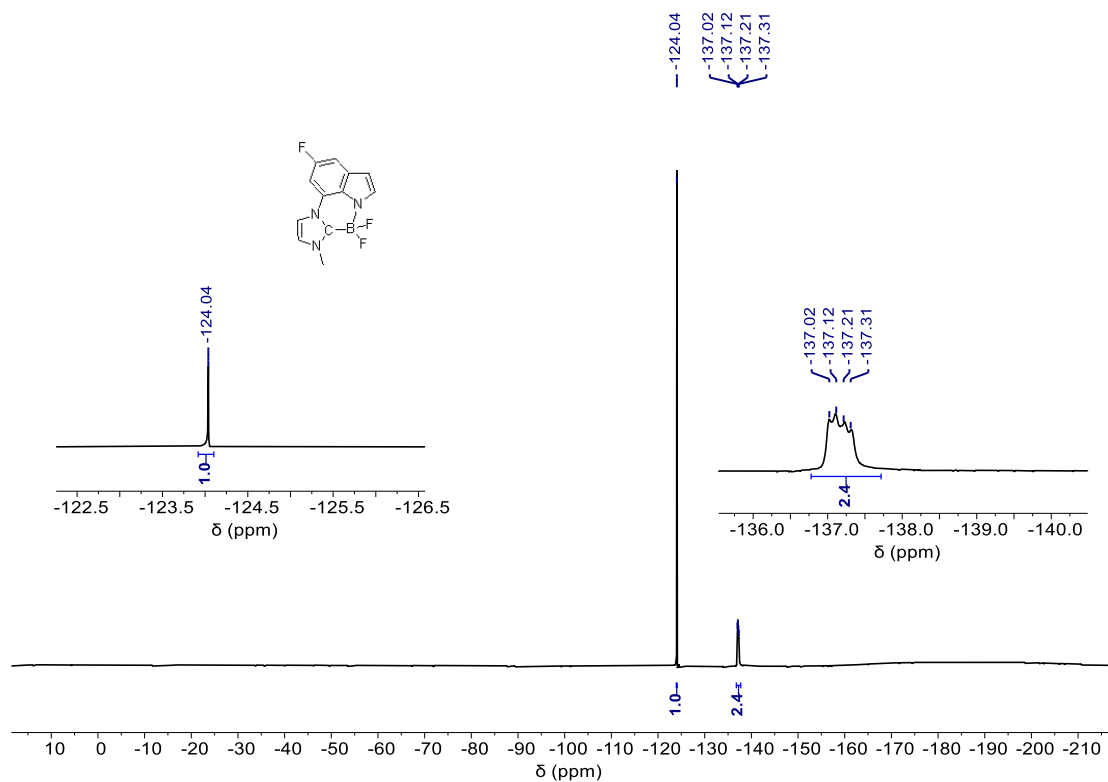


**Figure S21.**  $^{19}\text{F}\{^1\text{H}\}$  NMR spectra of **2** in  $\text{DMSO-}d_6$  at 376 MHz.

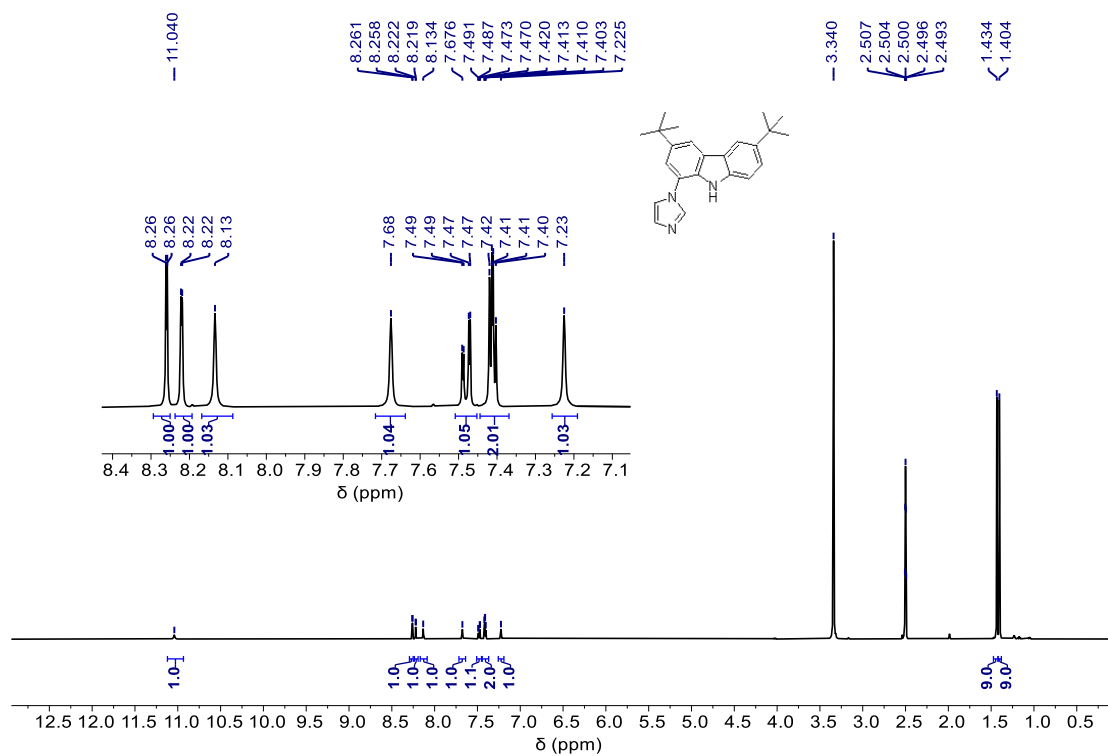


**Figure S22.**  $^1\text{H}$  NMR spectra of 3,6-di-*tert*-butyl-1-(1H-imidazol-1-yl)-9H-carbazole in  $\text{DMSO-}d_6$  at 500 MHz.

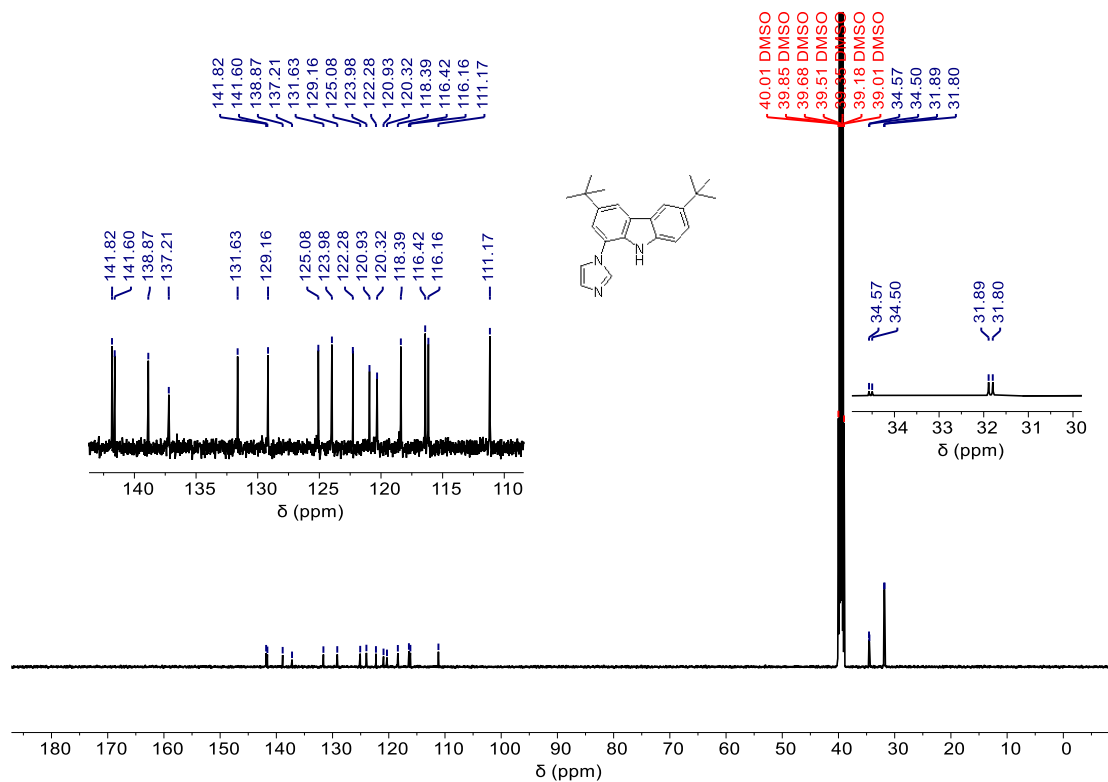


**Figure S23.**  $^{13}\text{C}\{^1\text{H}\}$  NMR spectra of 3,6-di-*tert*-butyl-1-(1*H*-imidazol-1-yl)-9*H*-carbazole in  $\text{DMSO-}d_6$  at 125 MHz.

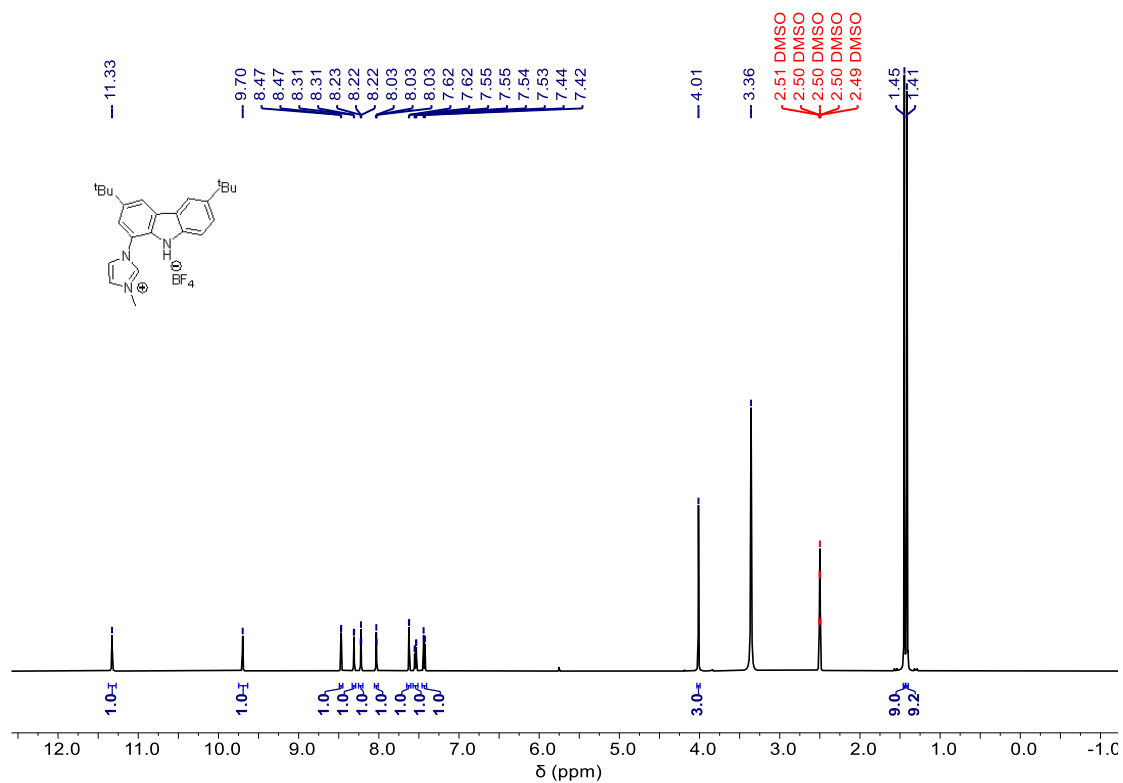


**Figure S24.**  $^1\text{H}$  NMR spectrum of 1-(3,6-di-*tert*-butyl-9*H*-carbazol-1-yl)-3-methyl-1*H*-imidazol-3-ium tetrafluoroborate in  $\text{DMSO-}d_6$  at 500 MHz.

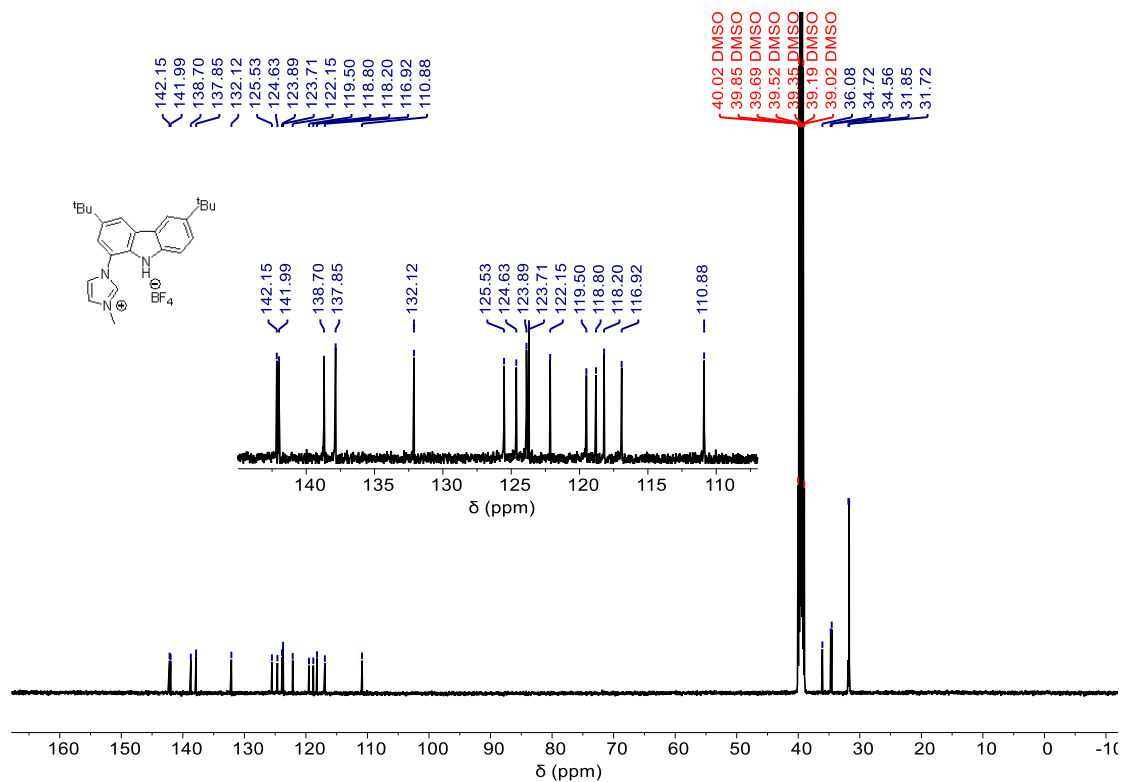


**Figure S25.**  $^{13}\text{C}\{^1\text{H}\}$  NMR spectra of 1-(3,6-di-*tert*-butyl-9*H*-carbazol-1-yl)-3-methyl-1*H*-imidazol-3-ium tetrafluoroborate in  $\text{DMSO-}d_6$  at 125 MHz.



**Figure S26.**  $^{11}\text{B}\{^1\text{H}\}$  NMR spectrum of 1-(3,6-di-*tert*-butyl-9*H*-carbazol-1-yl)-3-methyl-1*H*-imidazol-3-ium tetrafluoroborate in  $\text{DMSO-}d_6$  at 160 MHz.

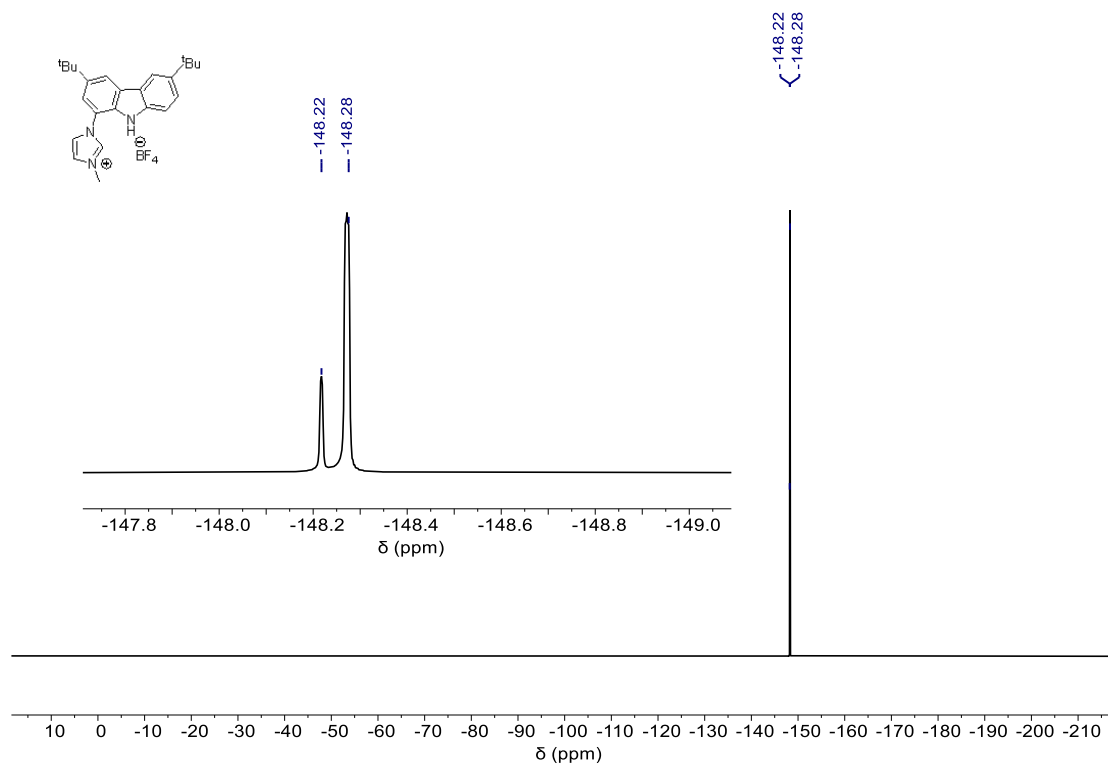


**Figure S27.**  $^{19}\text{F}\{^1\text{H}\}$  NMR spectra of 1-(3,6-di-*tert*-butyl-9*H*-carbazol-1-yl)-3-methyl-1*H*-imidazol-3-ium tetrafluoroborate in  $\text{DMSO-}d_6$  at 376 MHz.

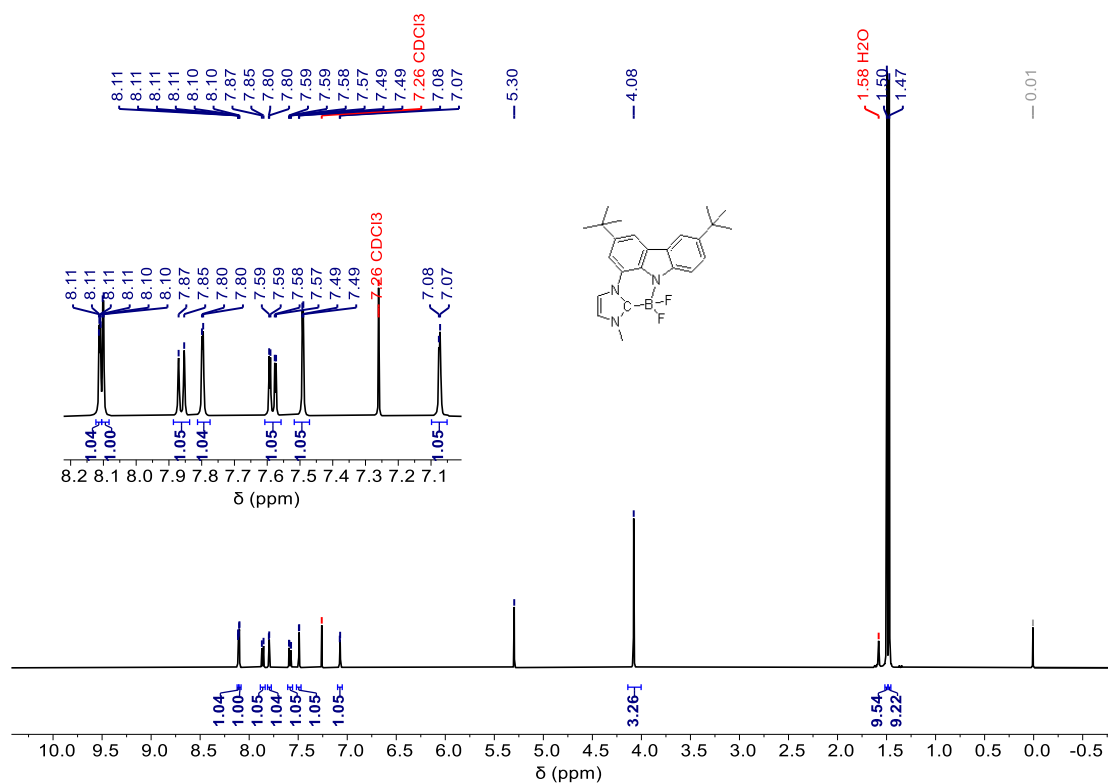


**Figure S28.**  $^1\text{H}$  NMR spectra of **3** in  $\text{CDCl}_3$  at 500 MHz.

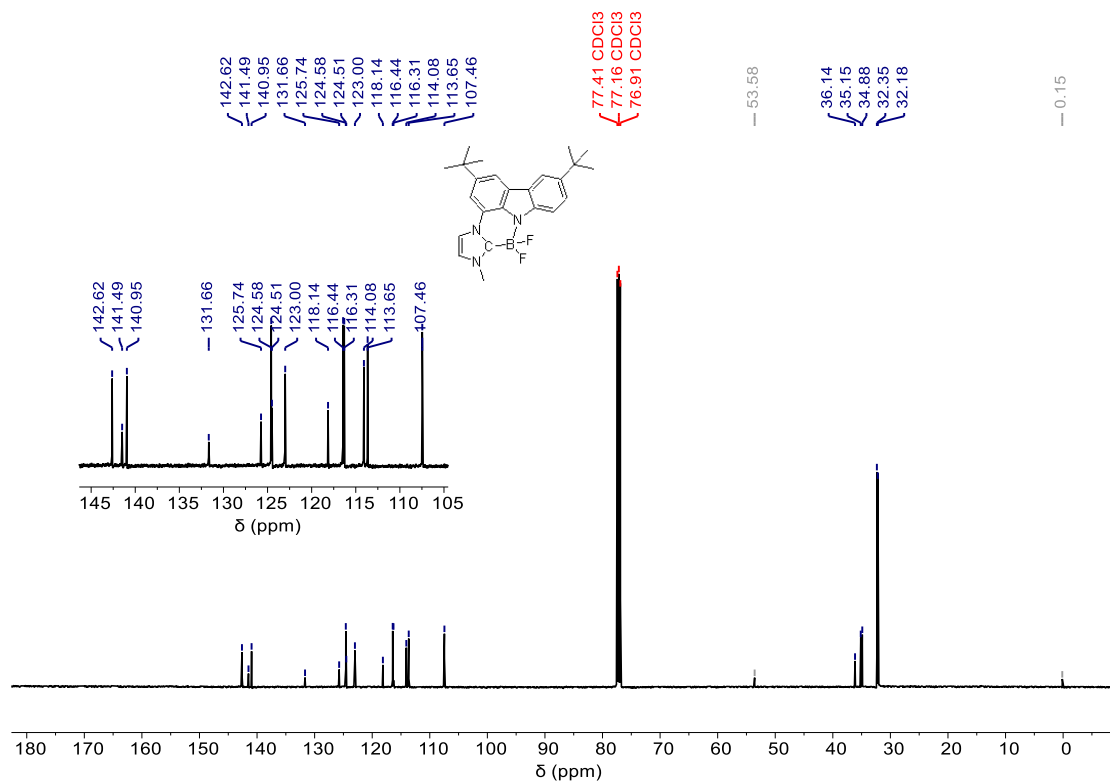


**Figure S29.**  $^{13}\text{C}\{^1\text{H}\}$  NMR spectra of **3** in  $\text{CDCl}_3$  at 125 MHz.

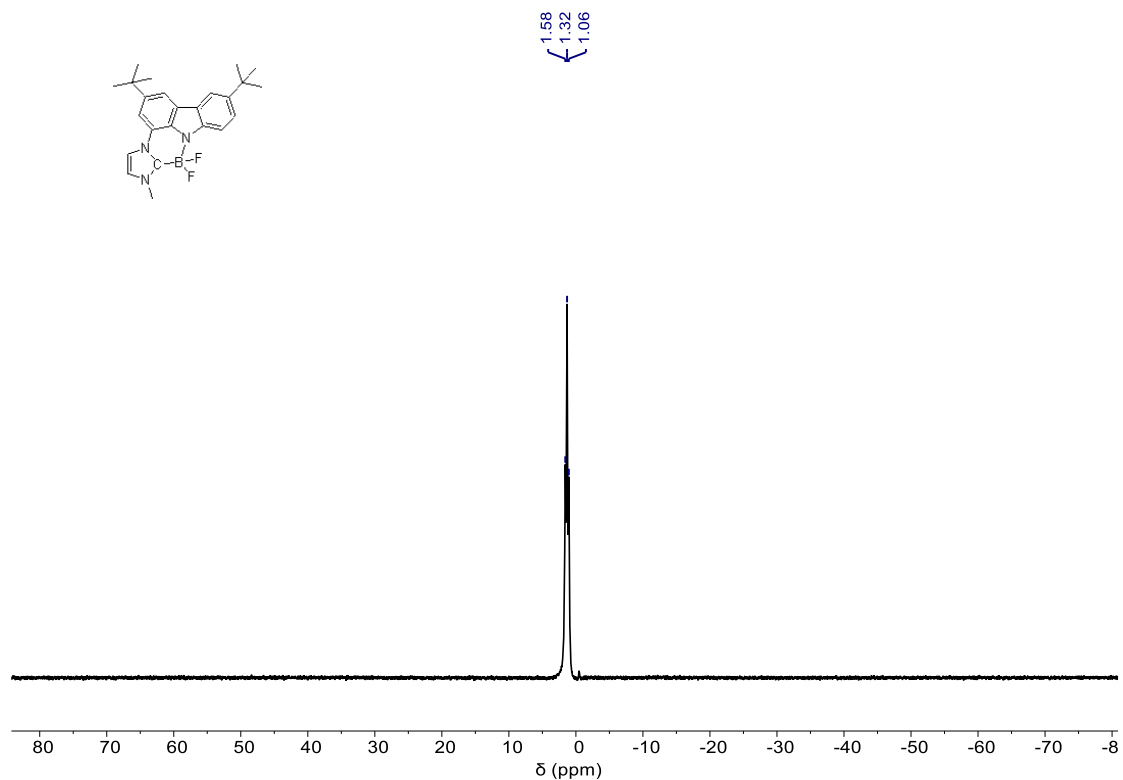


**Figure S30.**  $^{11}\text{B}\{^1\text{H}\}$  NMR spectra of **3** in  $\text{CDCl}_3$  at 160 MHz.

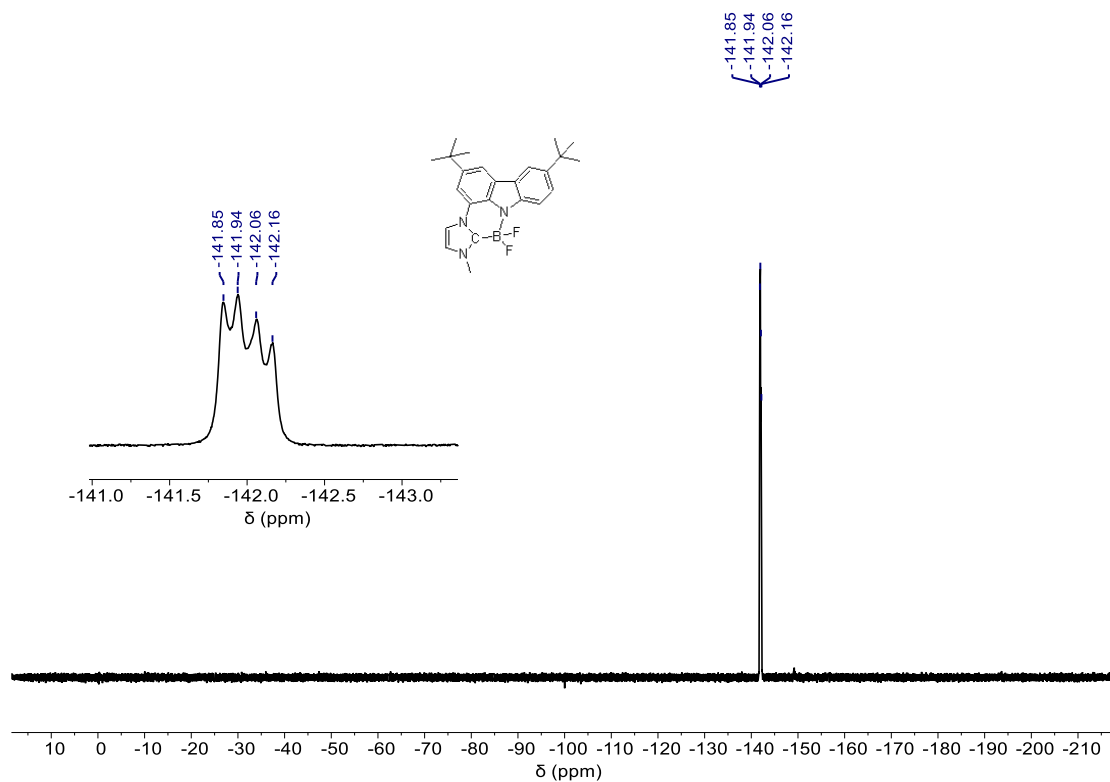


Figure S31.  $^{19}\text{F}\{^1\text{H}\}$  NMR spectra of **3** in  $\text{CDCl}_3$  at 376 MHz.

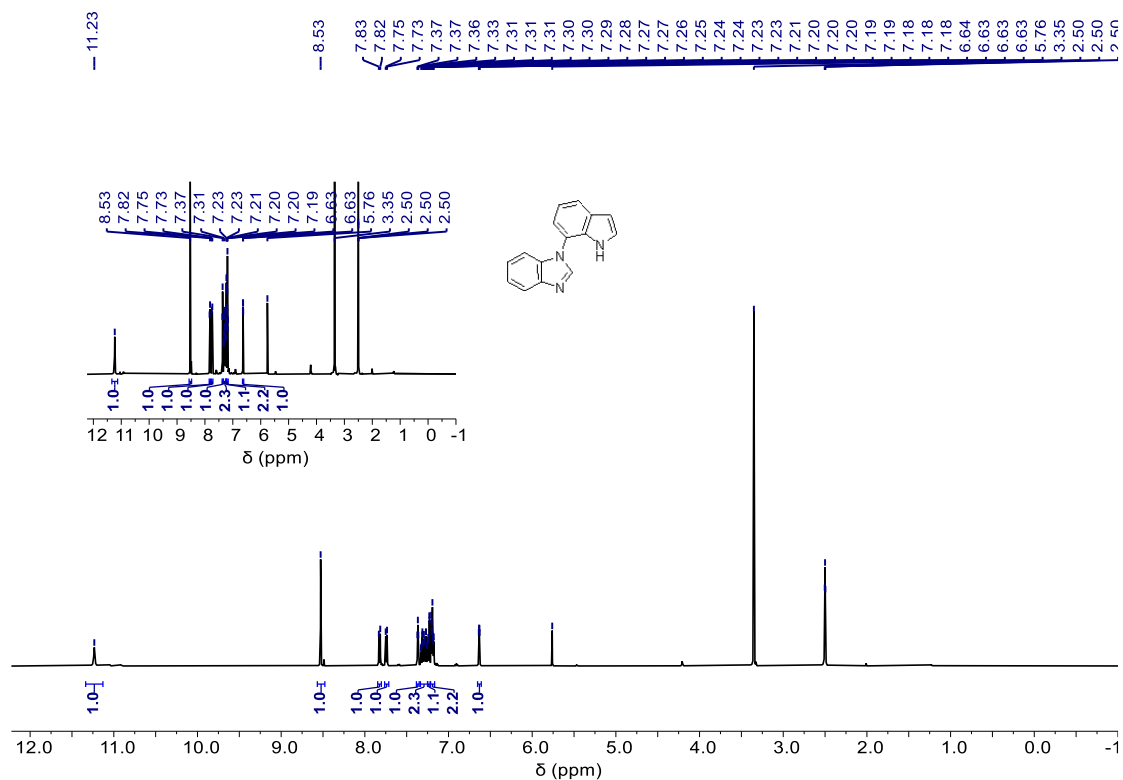
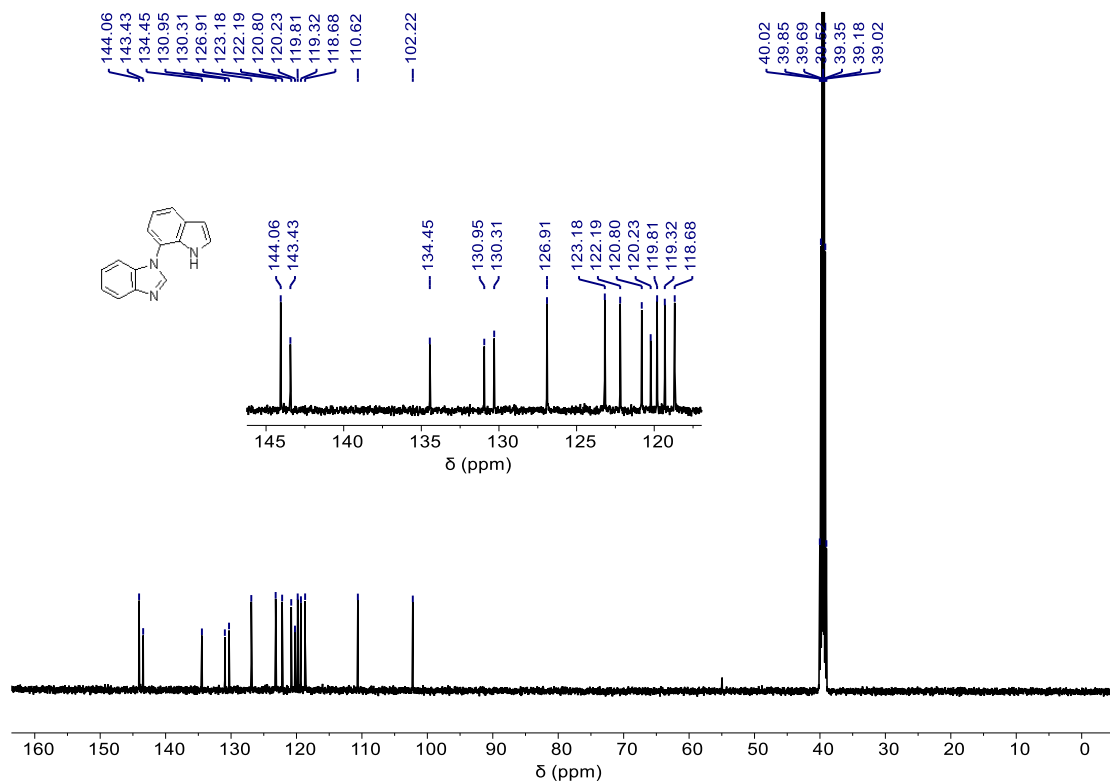
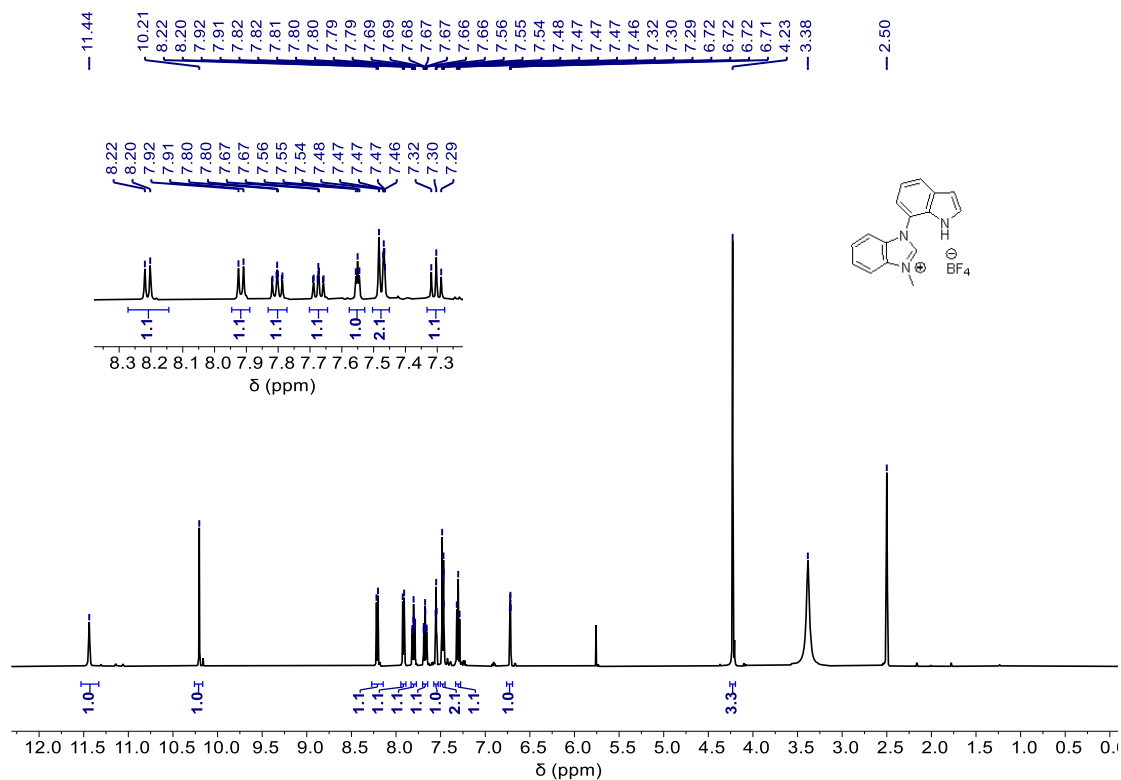


Figure S32.  $^1\text{H}$  NMR spectra of 1-(1H-indol-7-yl)-1H-benzo[d]imidazole in  $\text{DMSO}-d_6$  at 500 MHz.



**Figure S33.**  $^{13}\text{C}\{^1\text{H}\}$  NMR spectra of 1-(1*H*-indol-7-yl)-1*H*-benzo[*d*]imidazole in  $\text{DMSO-}d_6$  at 125 MHz.



**Figure S34.**  $^1\text{H}$  NMR spectra of 1-(1*H*-indol-7-yl)-3-methyl-1*H*-benzo[*d*]imidazol-3-ium tetrafluoroborate in  $\text{DMSO-}d_6$  at 500 MHz.



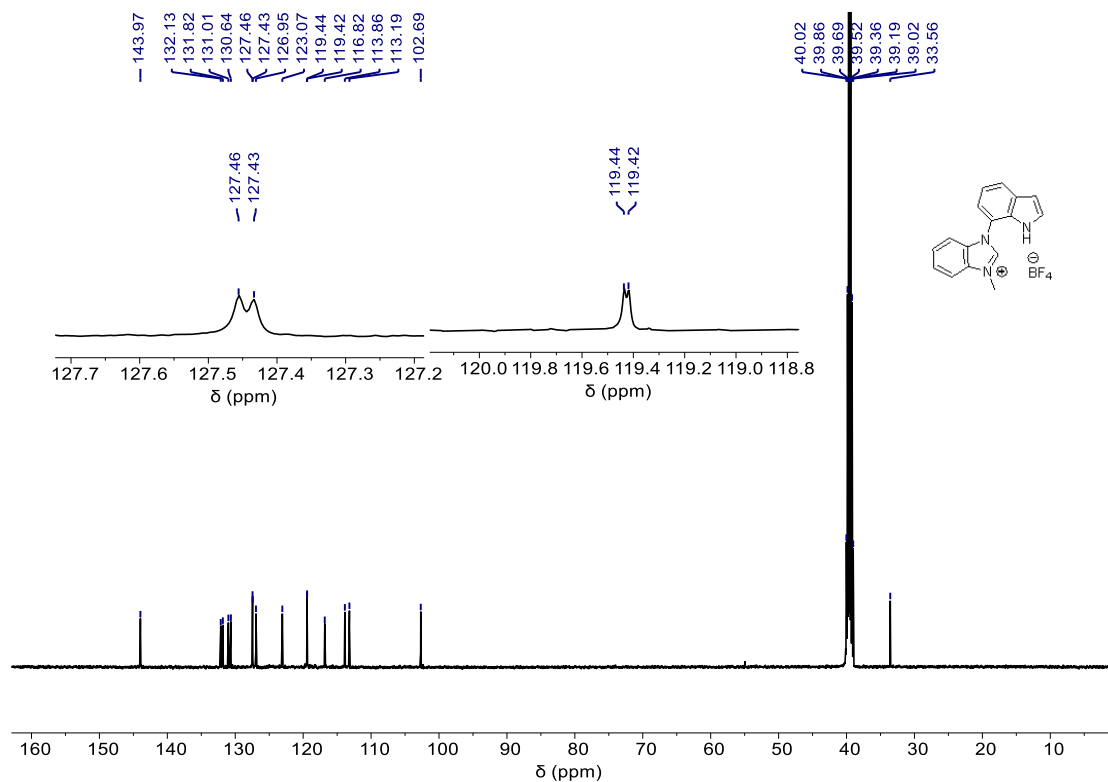


**Figure S35.**  $^{13}\text{C}\{^1\text{H}\}$  NMR spectra of 1-(1*H*-indol-7-yl)-3-methyl-1*H*-benzo[*d*]imidazol-3-ium tetrafluoroborate in  $\text{DMSO-}d_6$  at 125 MHz.

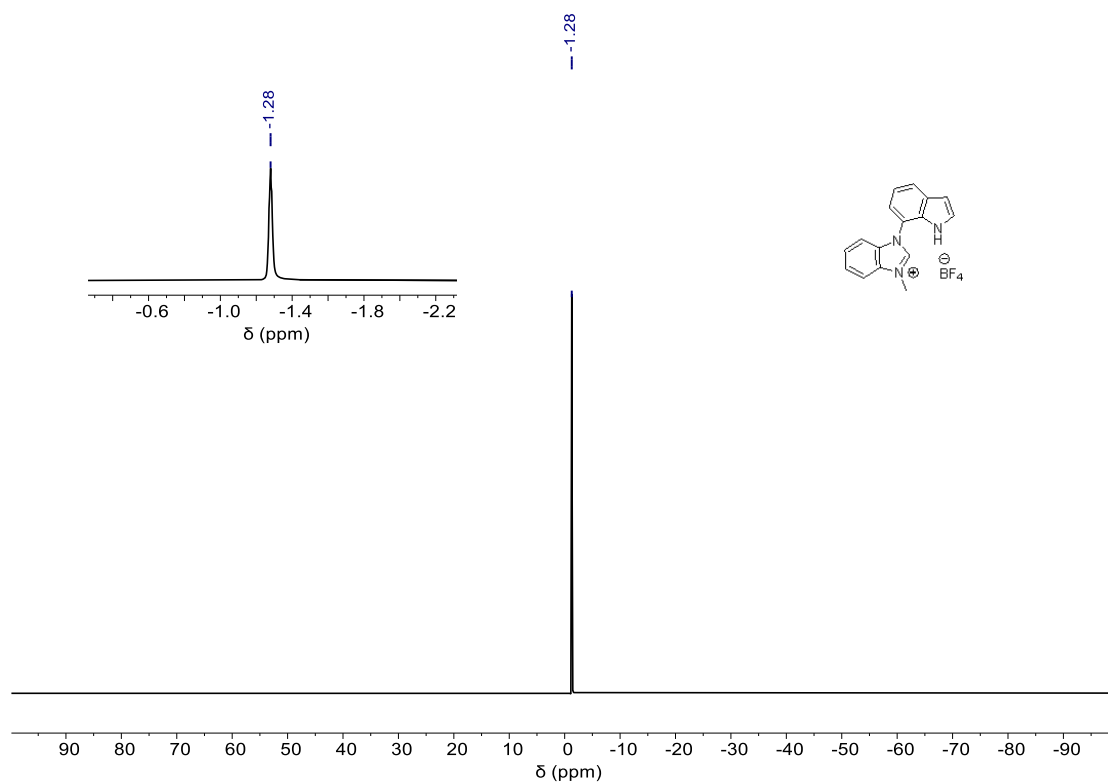


**Figure S36.**  $^{11}\text{B}\{^1\text{H}\}$  NMR spectra of 1-(1*H*-indol-7-yl)-3-methyl-1*H*-benzo[*d*]imidazol-3-ium tetrafluoroborate in  $\text{DMSO-}d_6$  at 160 MHz.

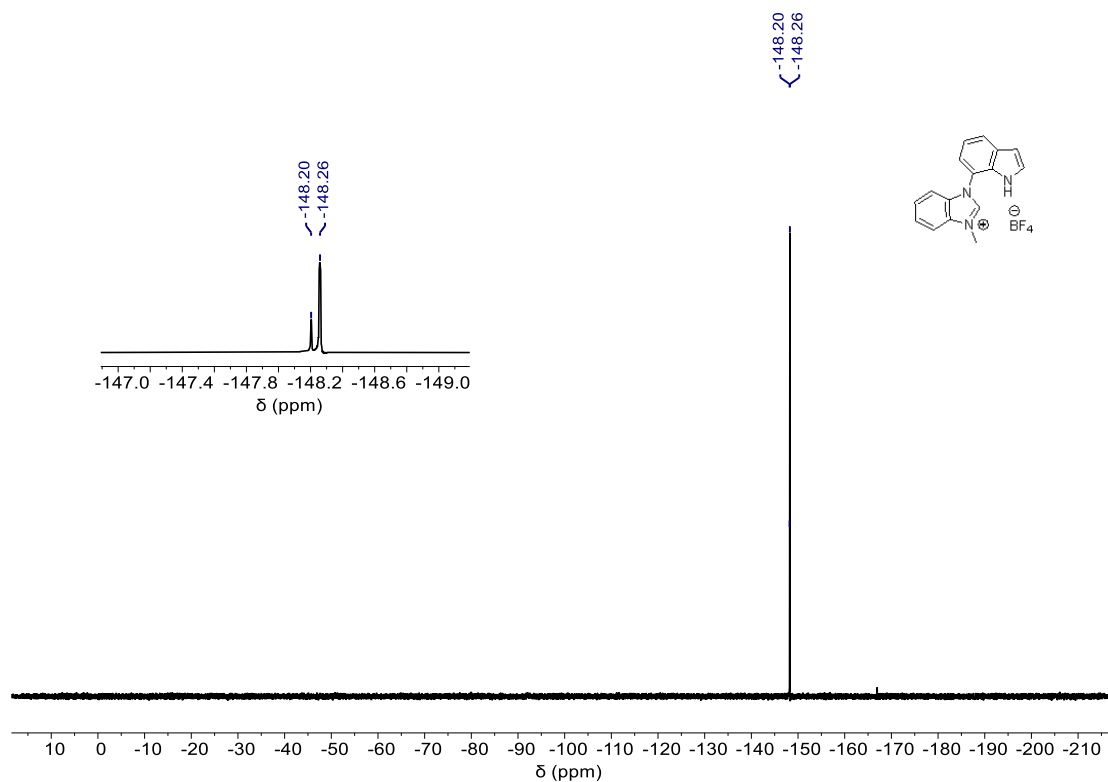


**Figure S37.**  $^{19}\text{F}\{^1\text{H}\}$  NMR spectra of 1-(1*H*-indol-7-yl)-3-methyl-1*H*-benzo[*d*]imidazol-3-ium tetrafluoroborate in  $\text{DMSO-}d_6$  at 376 MHz.

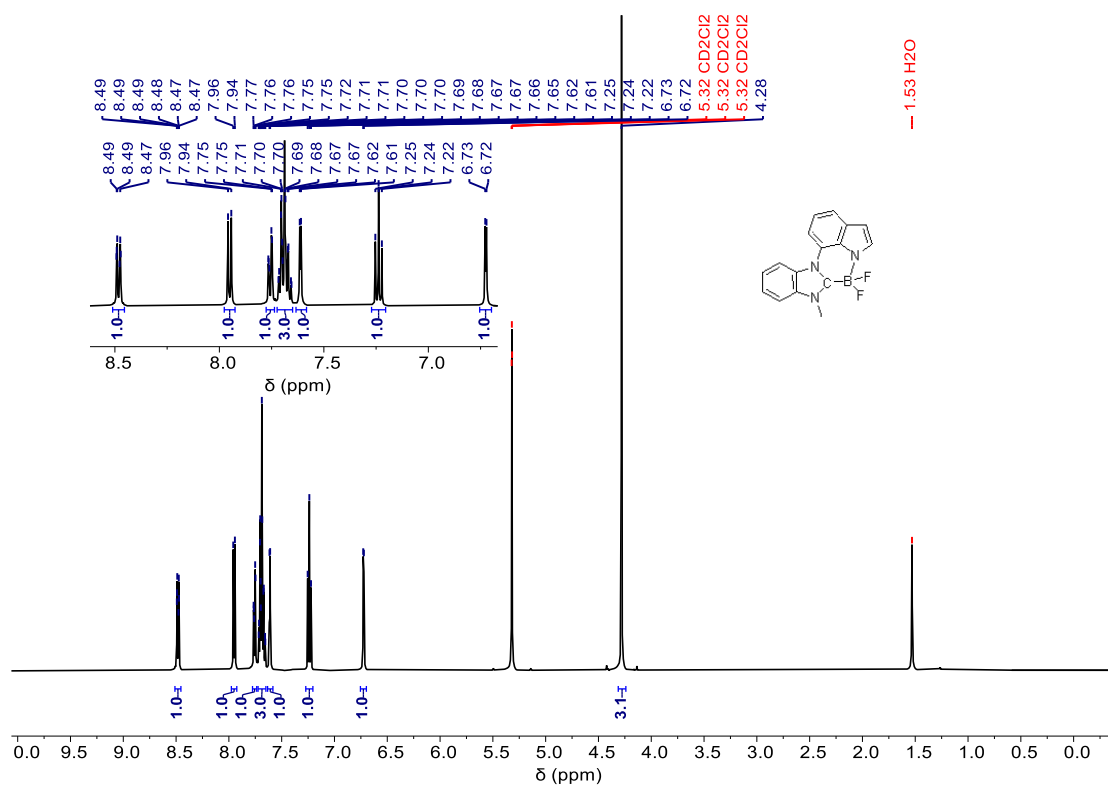


**Figure S38.**  $^1\text{H}$  NMR spectra of **4** in  $\text{CD}_2\text{Cl}_2$  at 500 MHz.

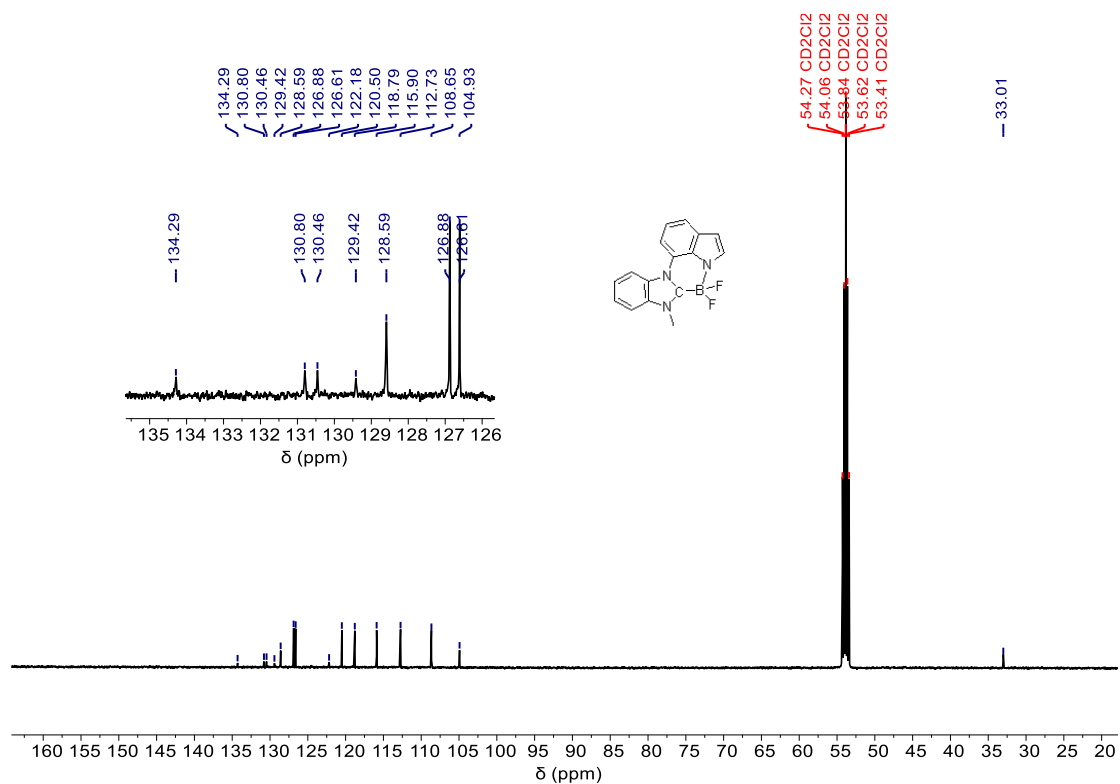


**Figure S39.**  $^{13}\text{C}\{^1\text{H}\}$  NMR spectra of **4** in  $\text{CD}_2\text{Cl}_2$  at 125 MHz.

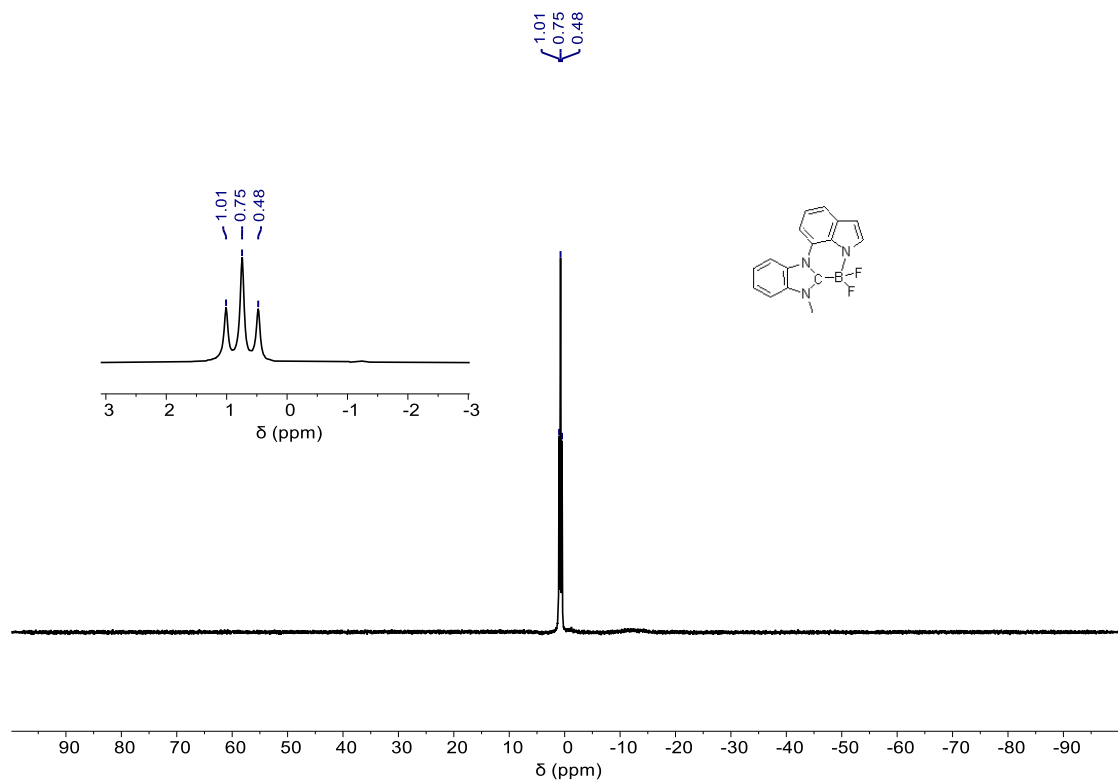


**Figure S40.**  $^{11}\text{B}\{^1\text{H}\}$  NMR spectra of **4** in  $\text{CD}_2\text{Cl}_2$  at 160 MHz.

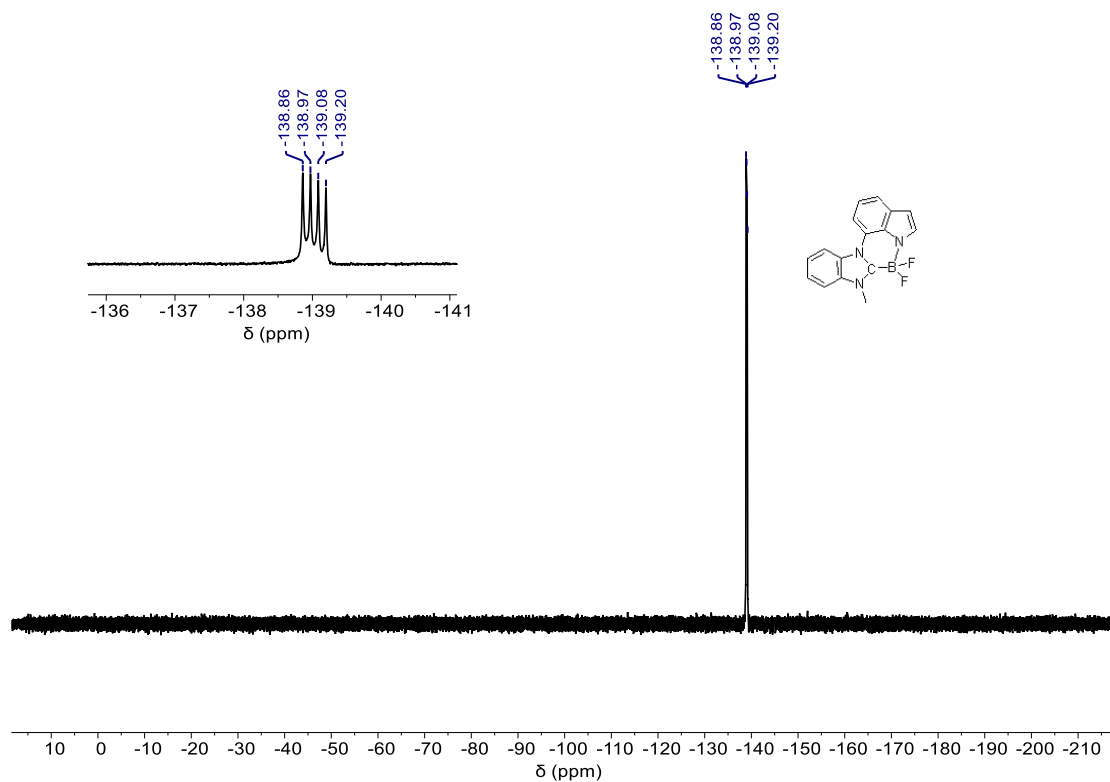


Figure S41.  $^{19}\text{F}\{^1\text{H}\}$  NMR spectra of **4** in  $\text{CD}_2\text{Cl}_2$  at 376 MHz.

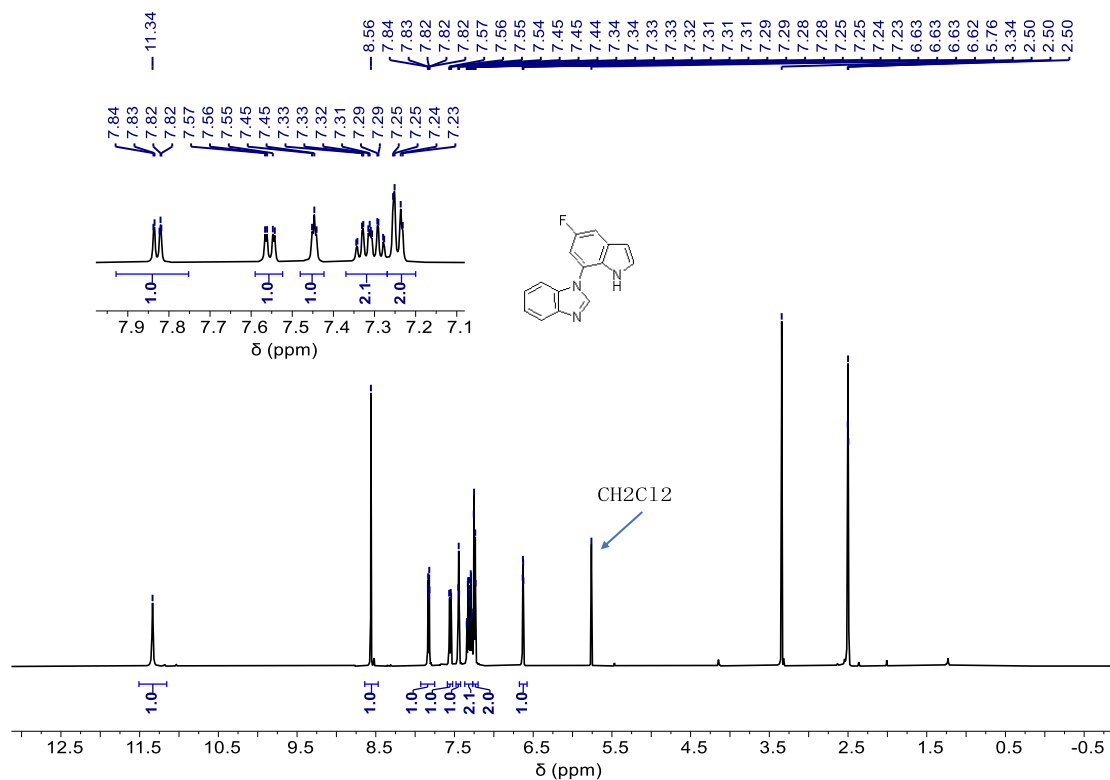
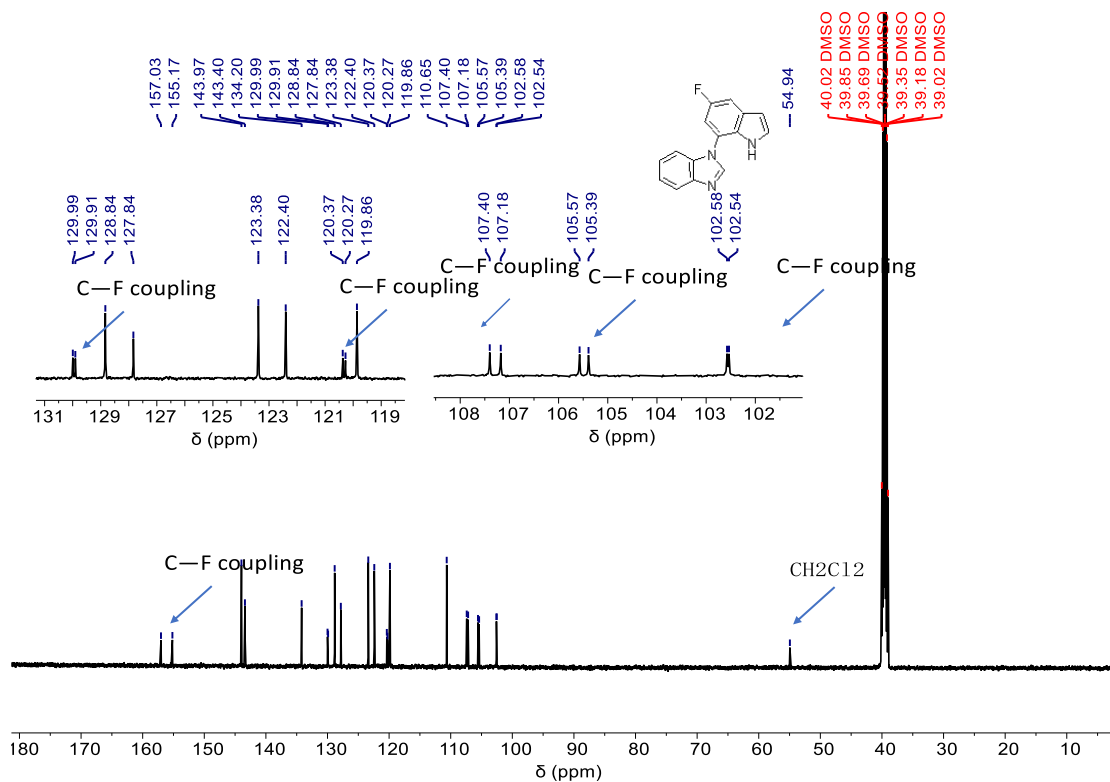
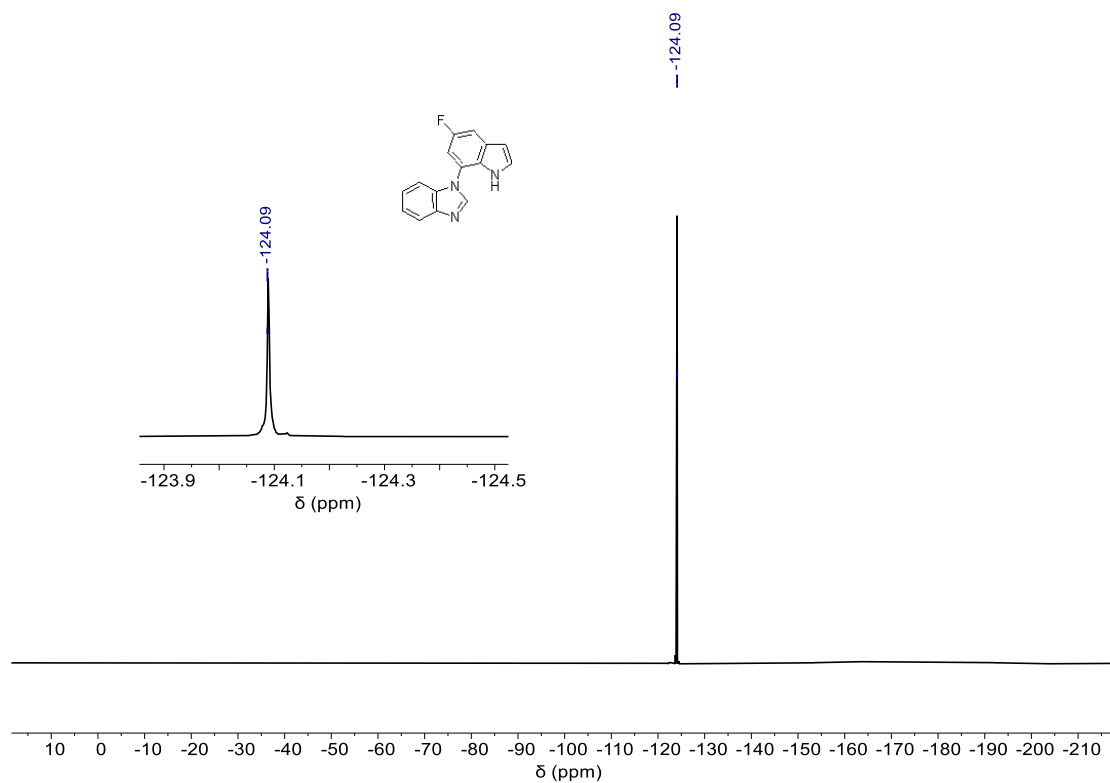


Figure S42.  $^1\text{H}$  NMR spectra of 1-(5-fluoro-1H-indol-7-yl)-1H-benzo[d]imidazole in  $\text{DMSO}-d_6$  at 500 MHz.



**Figure S43.**  $^{13}\text{C}\{^1\text{H}\}$  NMR spectra of 1-(5-fluoro-1*H*-indol-7-yl)-1*H*-benzo[*d*]imidazole in  $\text{DMSO-}d_6$  at 125 MHz.



**Figure S44.**  $^{19}\text{F}\{^1\text{H}\}$  NMR spectra of 1-(5-fluoro-1*H*-indol-7-yl)-1*H*-benzo[*d*]imidazole in  $\text{DMSO-}d_6$  at 376 MHz.

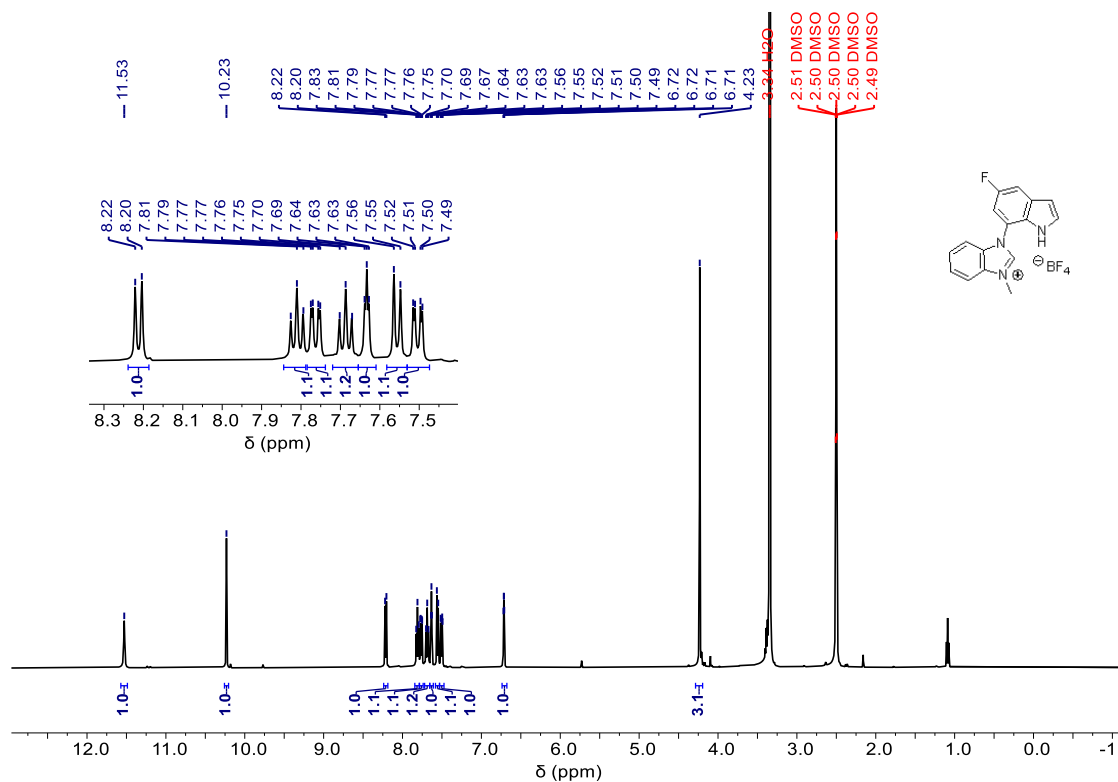


**Figure S45.** <sup>1</sup>H NMR spectra of 1-(5-fluoro-1*H*-indol-7-yl)-3-methyl-1*H*-benzo[*d*]imidazol-3-ium tetrafluoroborate in DMSO-*d*<sub>6</sub> at 500 MHz.

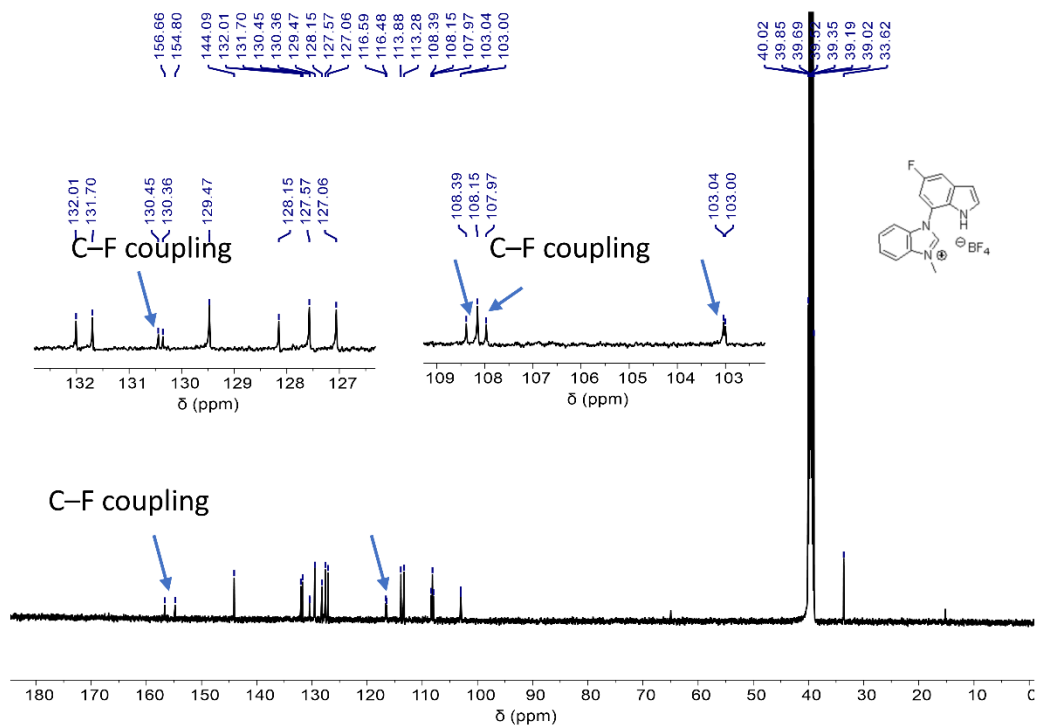


**Figure S46.** <sup>13</sup>C{<sup>1</sup>H} NMR spectra of 1-(5-fluoro-1*H*-indol-7-yl)-3-methyl-1*H*-benzo[*d*]imidazol-3-ium tetrafluoroborate in DMSO-*d*<sub>6</sub> at 125 MHz.

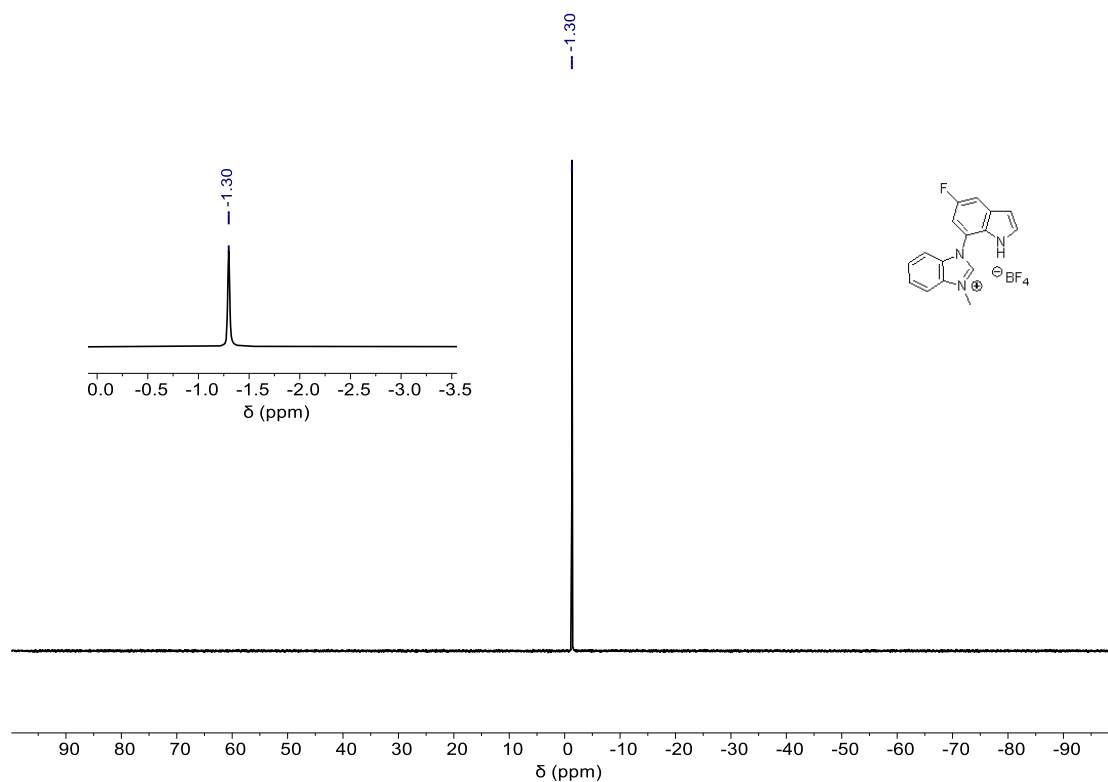


**Figure S47.**  $^{11}\text{B}\{^1\text{H}\}$  NMR spectra of 1-(5-fluoro-1*H*-indol-7-yl)-3-methyl-1*H*-benzo[*d*]imidazol-3-ium tetrafluoroborate in  $\text{DMSO-}d_6$  at 160 MHz.

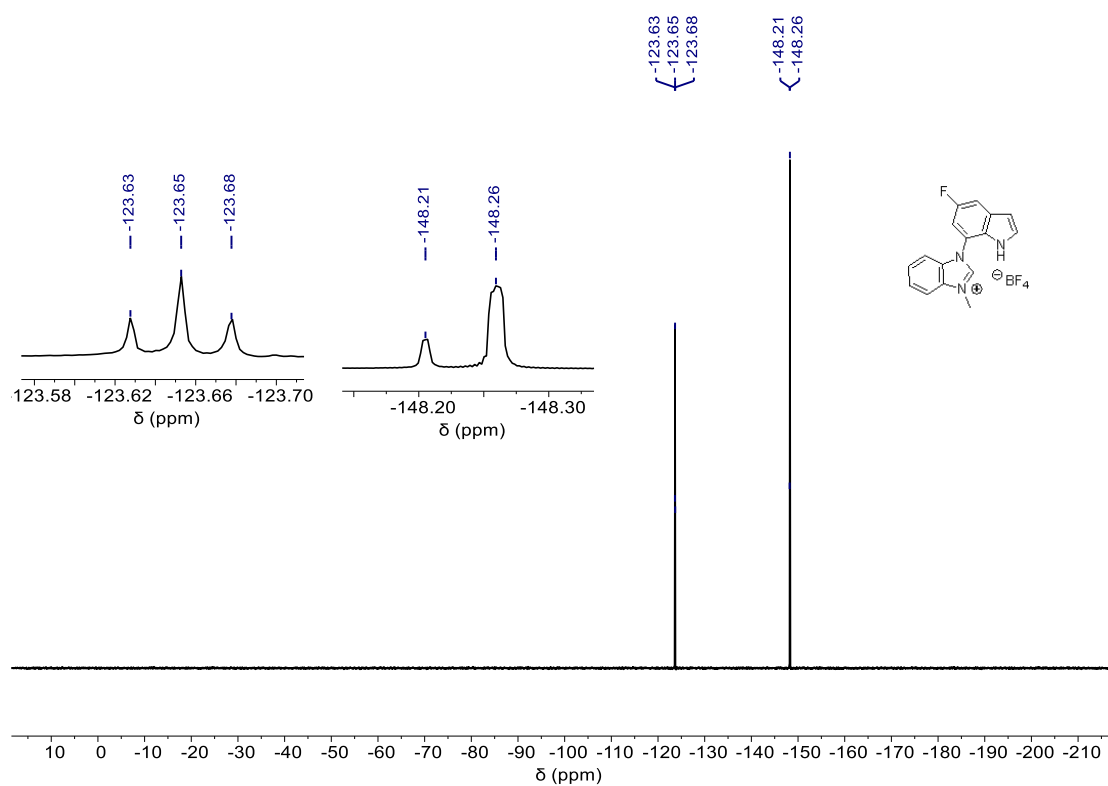


**Figure S48.**  $^{19}\text{F}\{^1\text{H}\}$  NMR spectra of 1-(5-fluoro-1*H*-indol-7-yl)-3-methyl-1*H*-benzo[*d*]imidazol-3-ium tetrafluoroborate in  $\text{DMSO-}d_6$  at 376 MHz.

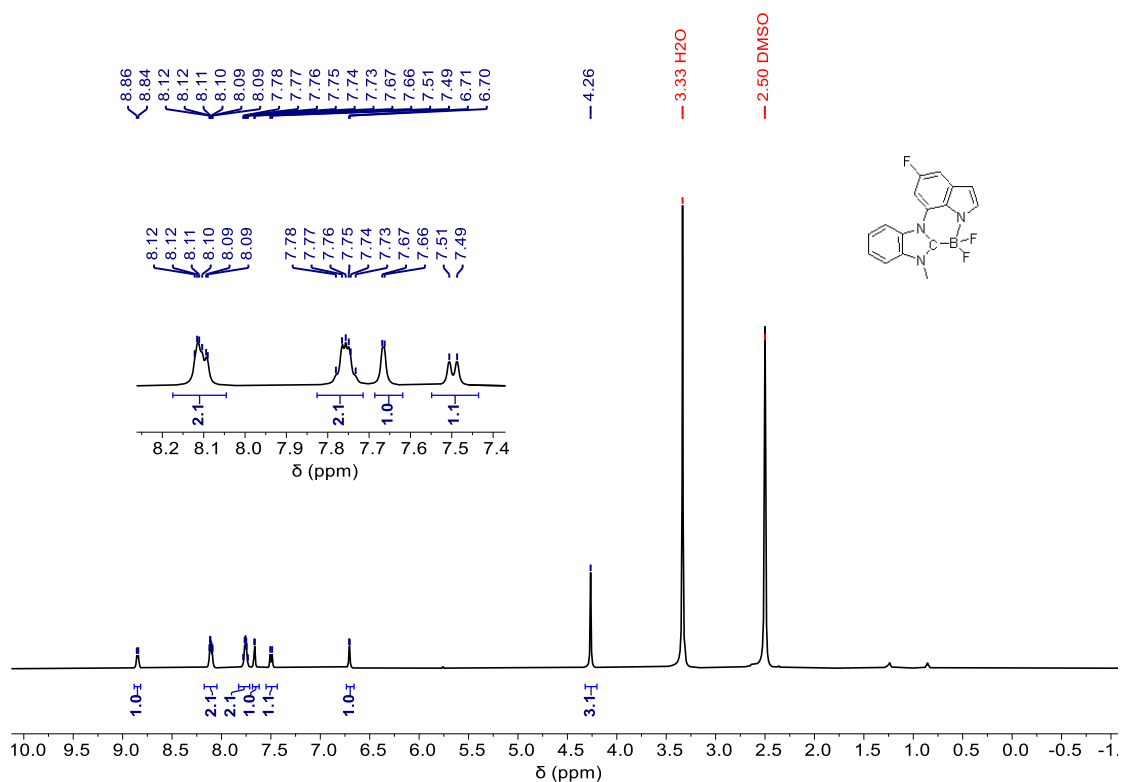


Figure S49. <sup>1</sup>H NMR spectra of 5 in DMSO-*d*<sub>6</sub> at 500 MHz.

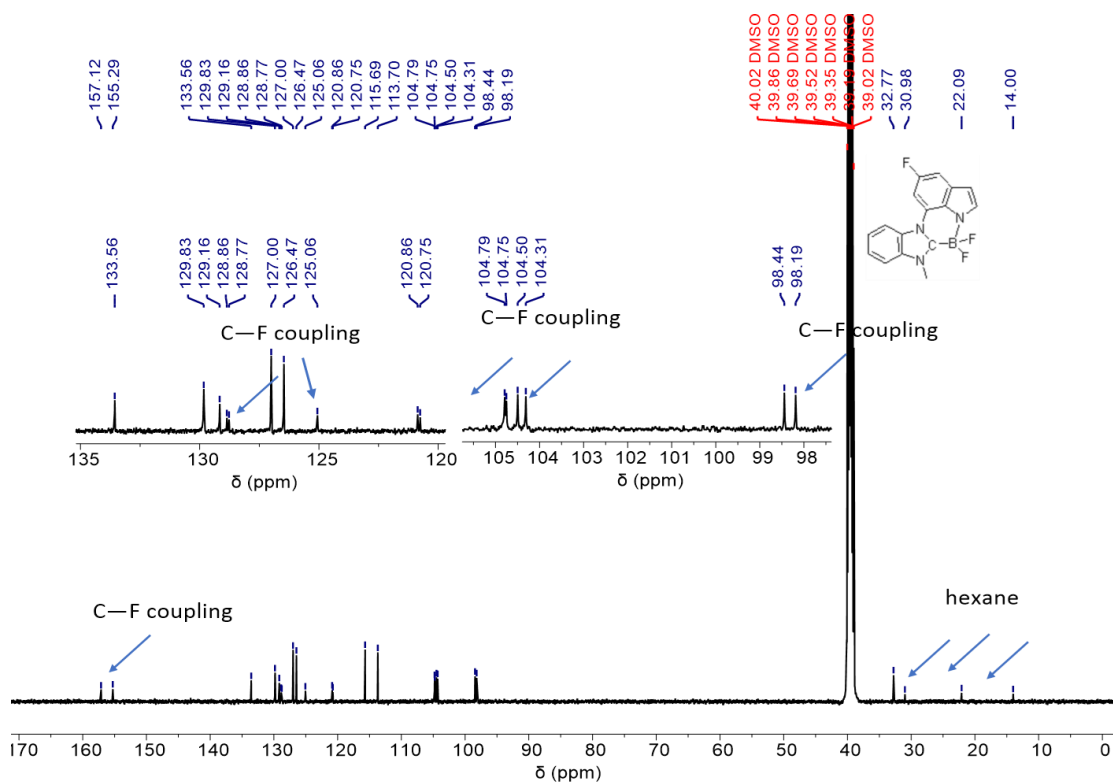


Figure S50. <sup>13</sup>C{<sup>1</sup>H} NMR spectra of 5 in DMSO-*d*<sub>6</sub> at 125 MHz.



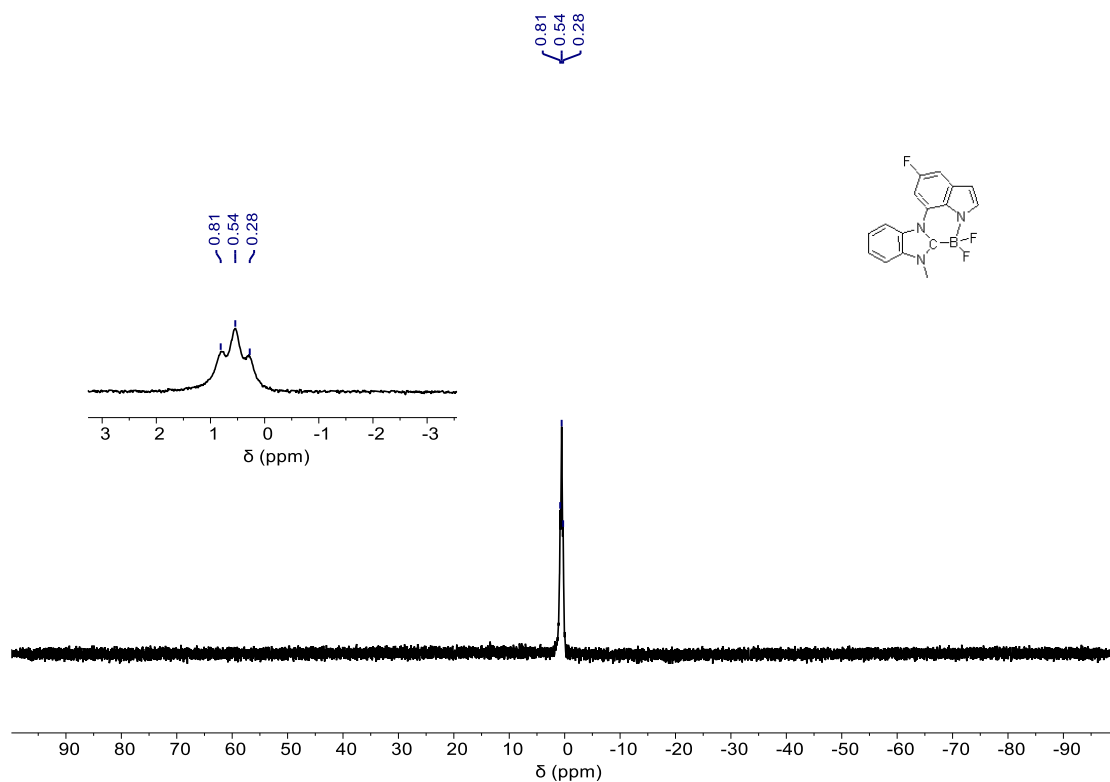


Figure S51.  $^{11}\text{B}\{^1\text{H}\}$  NMR spectra of **5** in  $\text{DMSO-}d_6$  at 160 MHz.

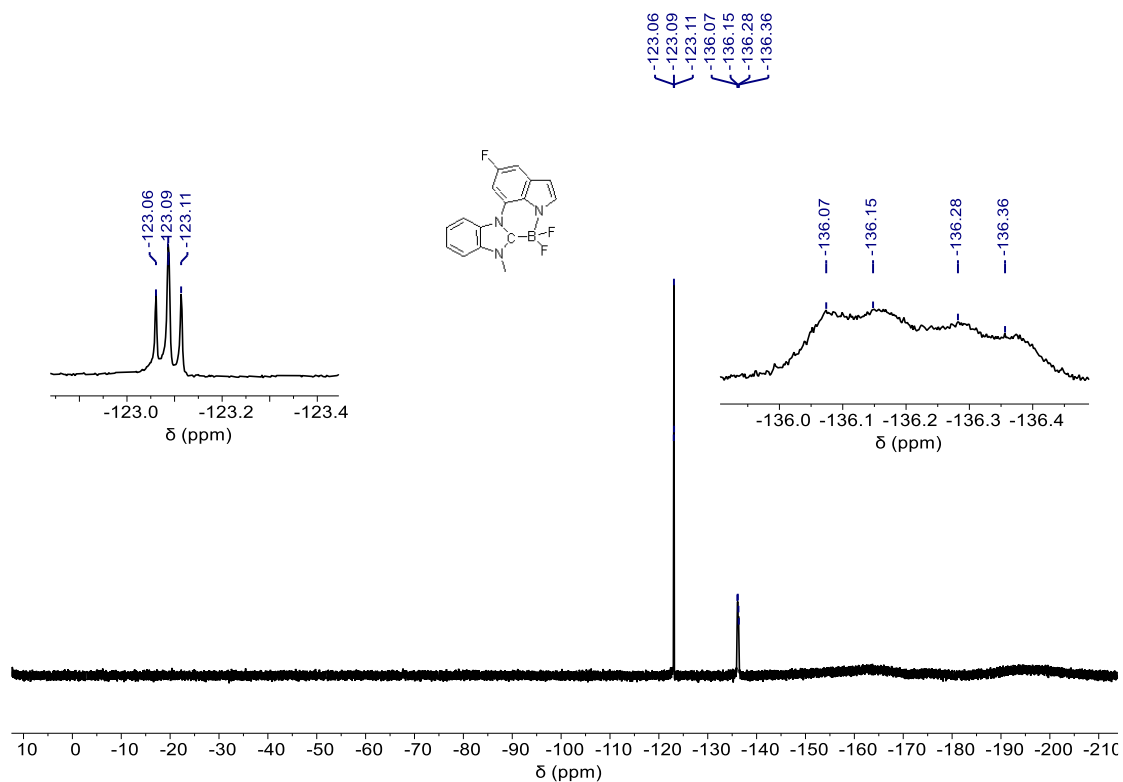
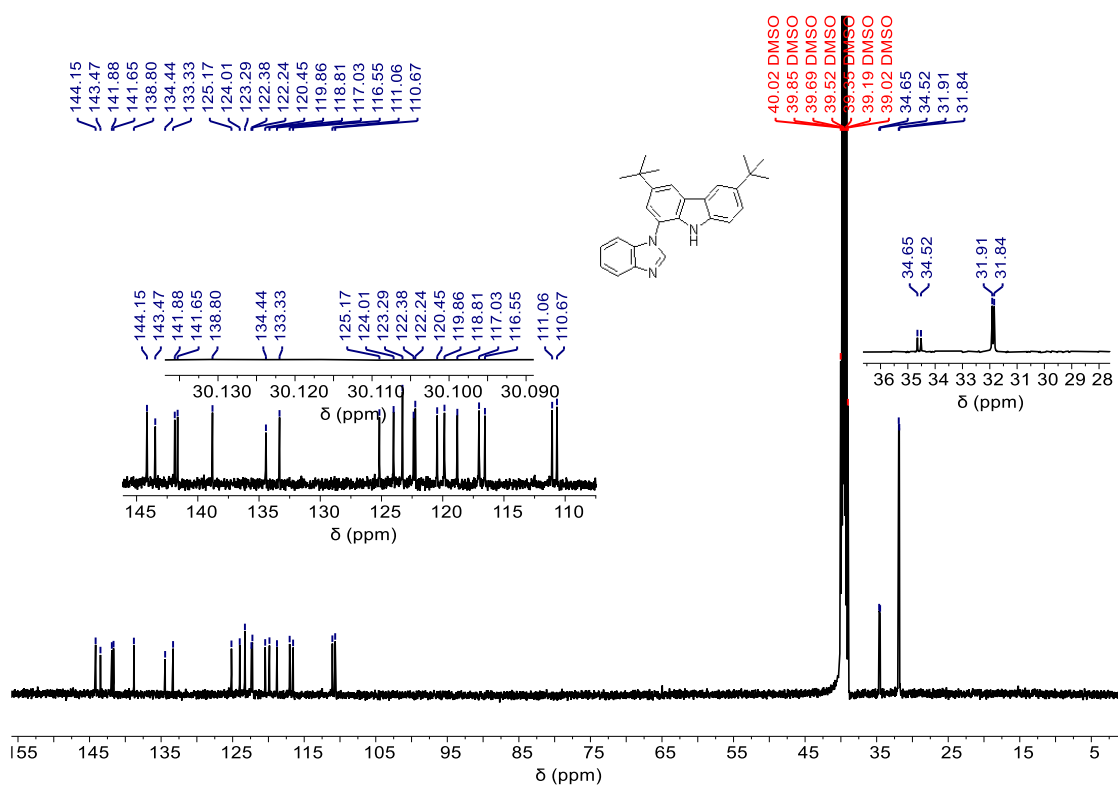
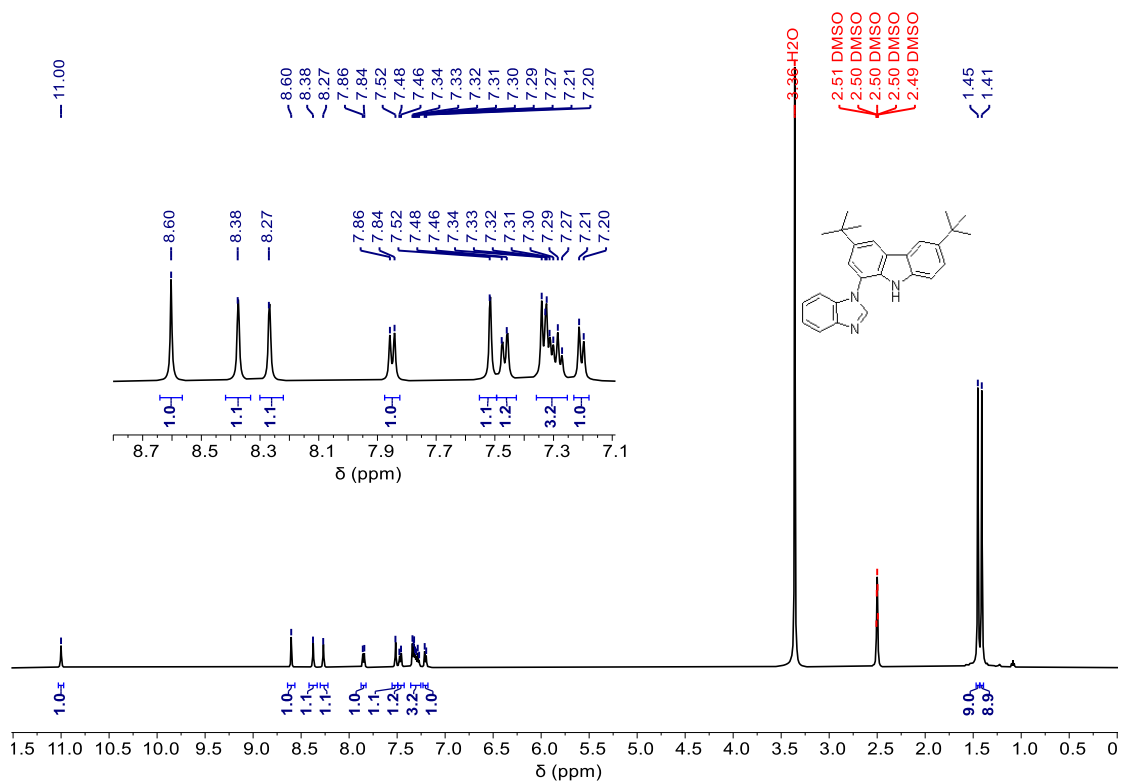
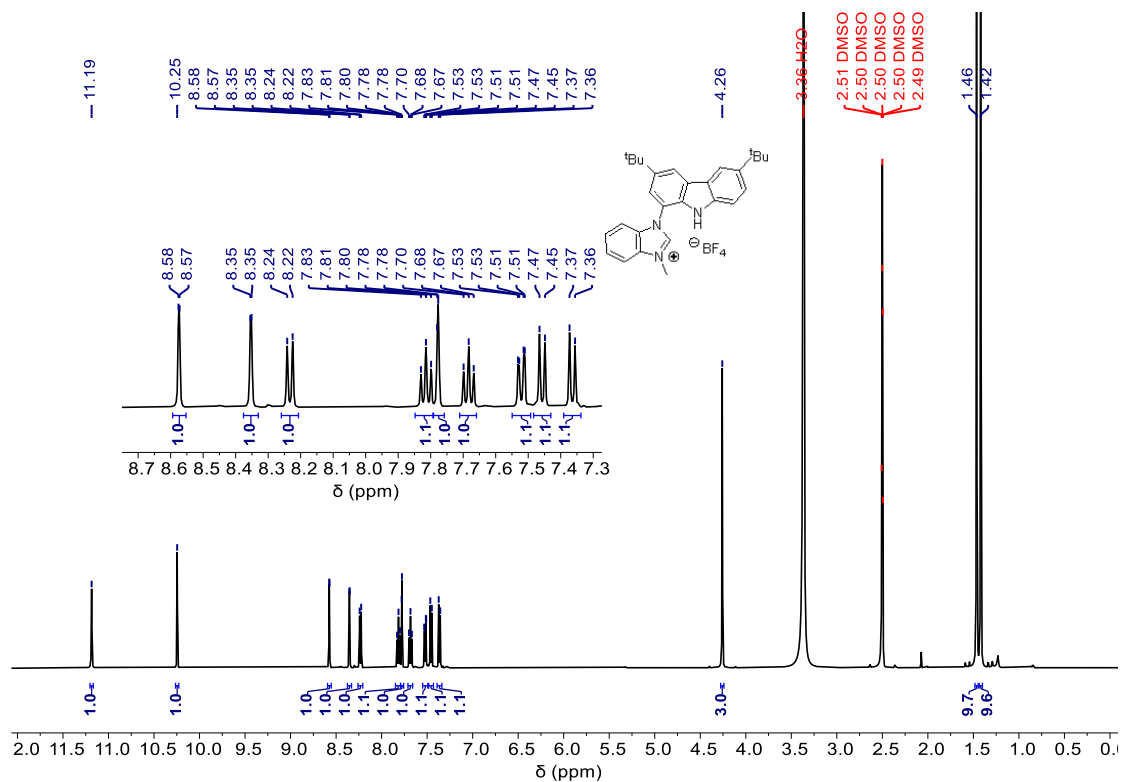
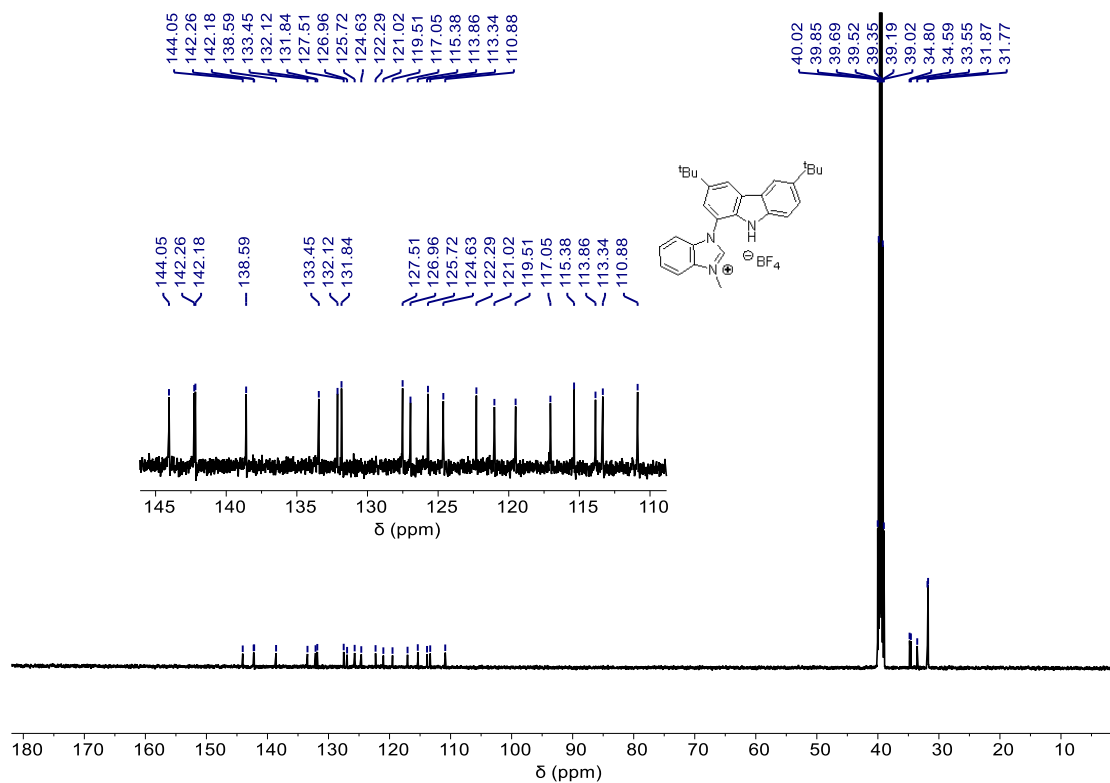


Figure S52.  $^{19}\text{F}\{^1\text{H}\}$  NMR spectra of **5** in  $\text{DMSO-}d_6$  at 376 MHz.





**Figure S55.** <sup>1</sup>H NMR spectra of 1-(3,6-di-*tert*-butyl-9*H*-carbazol-1-yl)-3-methyl-1*H*-benzo[*d*]imidazol-3-ium tetrafluoroborate in DMSO-*d*<sub>6</sub> at 500 MHz.



**Figure S56.** <sup>13</sup>C{<sup>1</sup>H} NMR spectra of 1-(3,6-di-*tert*-butyl-9*H*-carbazol-1-yl)-3-methyl-1*H*-benzo[*d*]imidazol-3-ium tetrafluoroborate in DMSO-*d*<sub>6</sub> at 125 MHz.

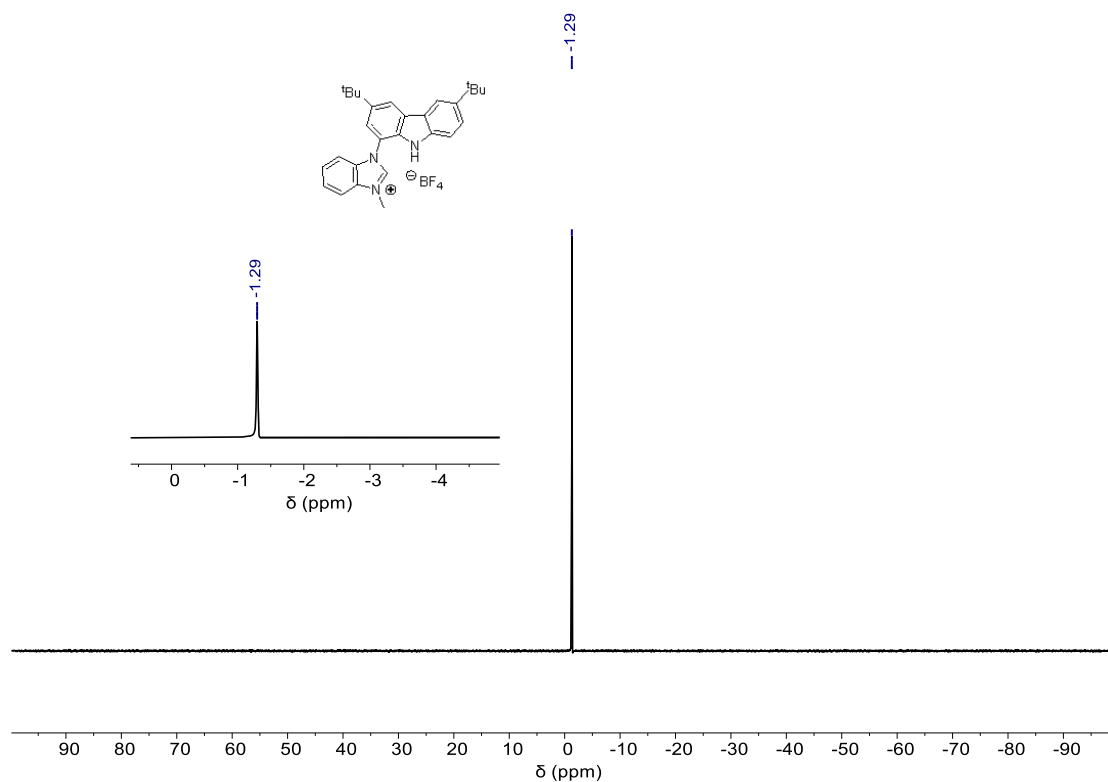


**Figure S57.**  $^{11}\text{B}\{^1\text{H}\}$  NMR spectra of 1-(3,6-di-*tert*-butyl-9*H*-carbazol-1-yl)-3-methyl-1*H*-benzo[*d*]imidazol-3-ium tetrafluoroborate in  $\text{DMSO-}d_6$  at 160 MHz.

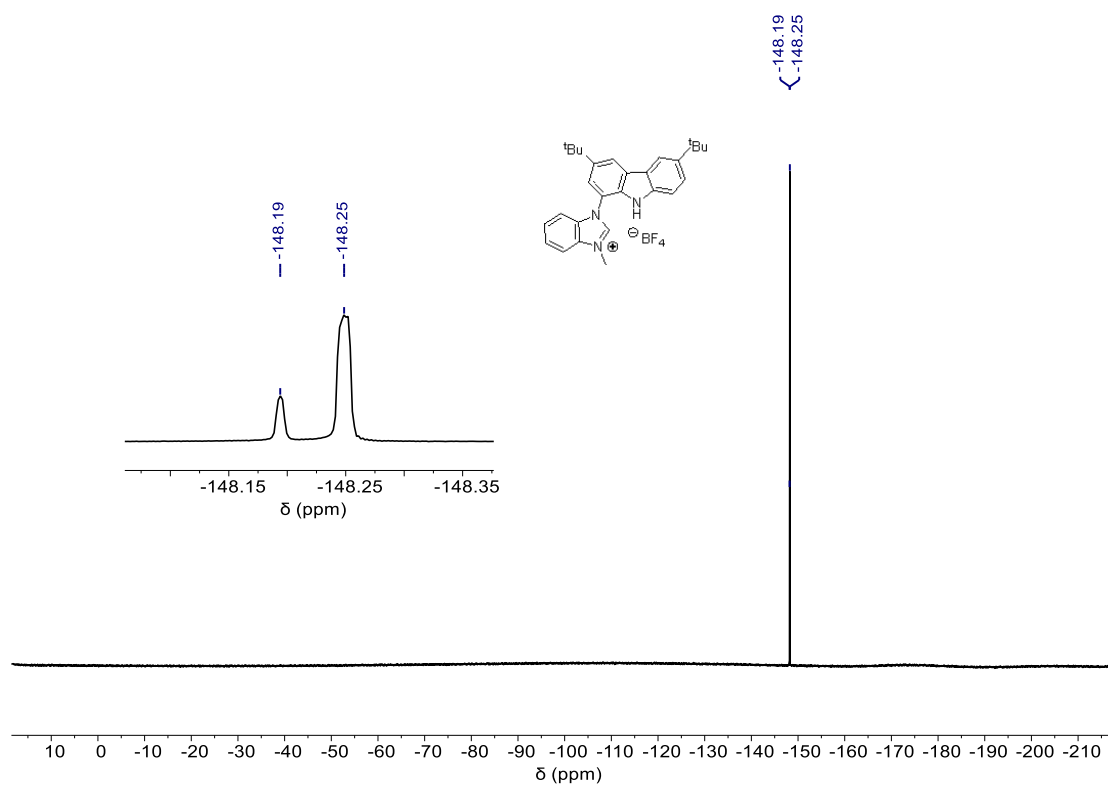


**Figure S58.**  $^{19}\text{F}\{^1\text{H}\}$  NMR spectra of 1-(3,6-di-*tert*-butyl-9*H*-carbazol-1-yl)-3-methyl-1*H*-benzo[*d*]imidazol-3-ium tetrafluoroborate in  $\text{DMSO-}d_6$  at 376 MHz.

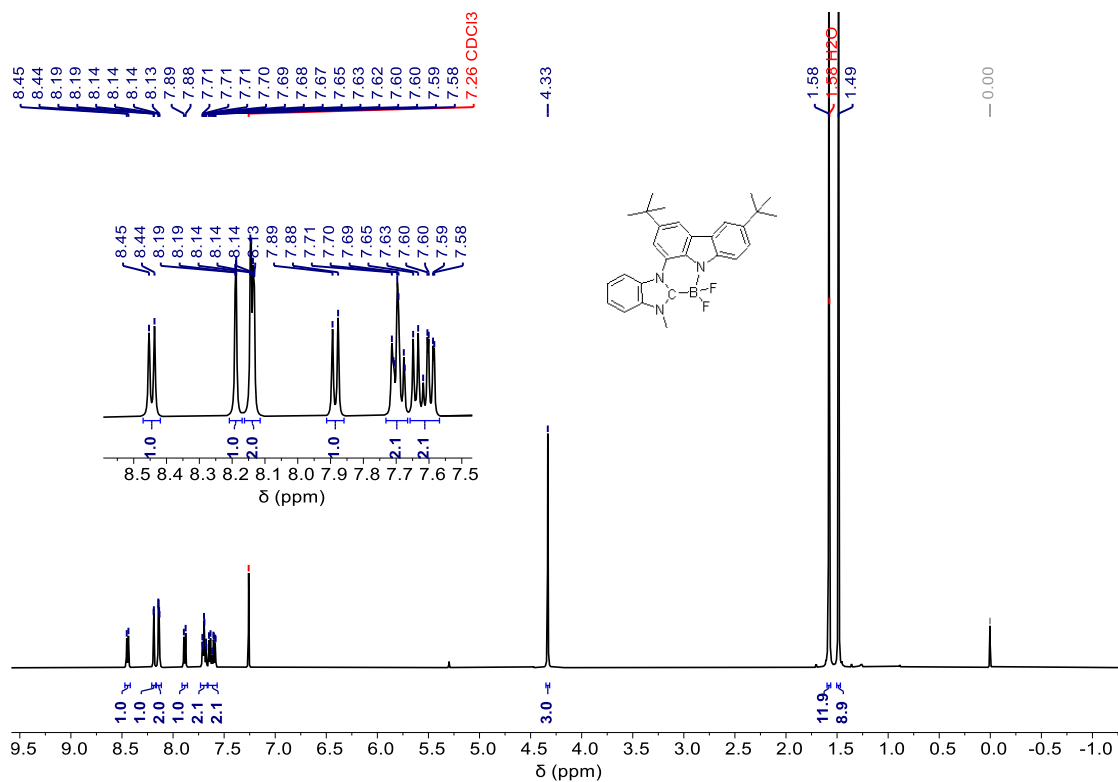


**Figure S59.**  $^1\text{H}$  NMR spectra of **6** in  $\text{CDCl}_3$  at 500 MHz.

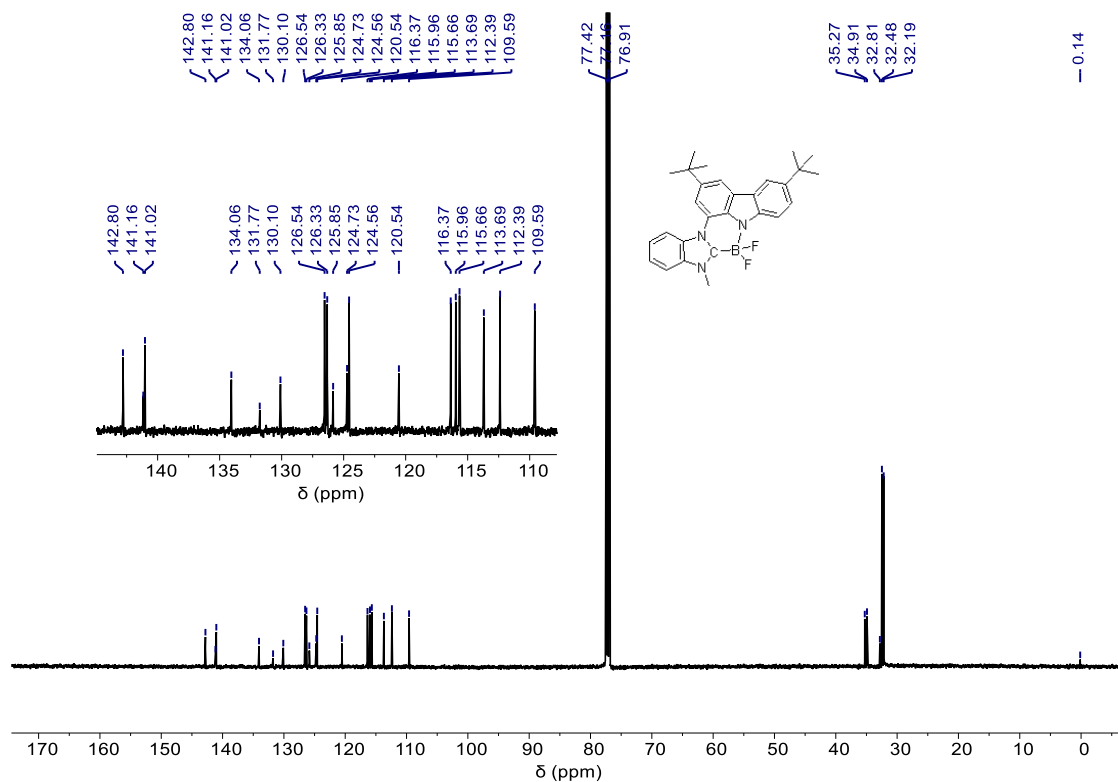


**Figure S60.**  $^{13}\text{C}\{^1\text{H}\}$  NMR spectra of **6** in  $\text{CDCl}_3$  at 125 MHz.

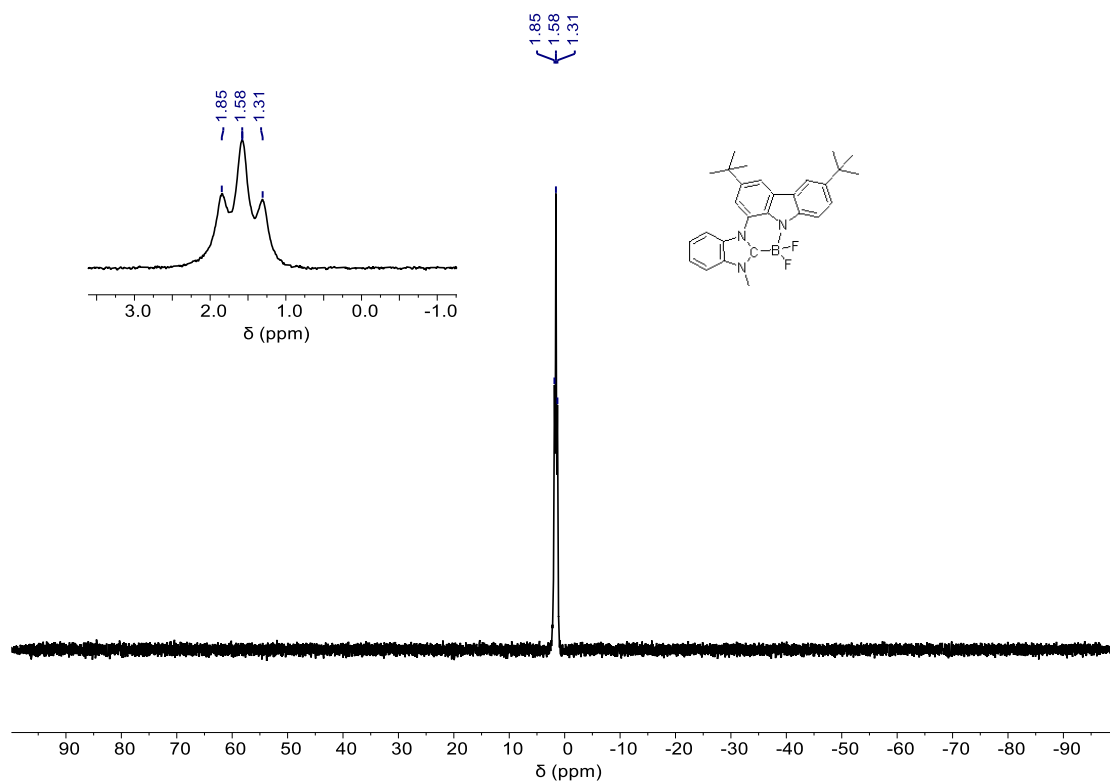


Figure S61.  $^{11}\text{B}\{^1\text{H}\}$  NMR spectra of **6** in  $\text{CDCl}_3$  at 160 MHz.

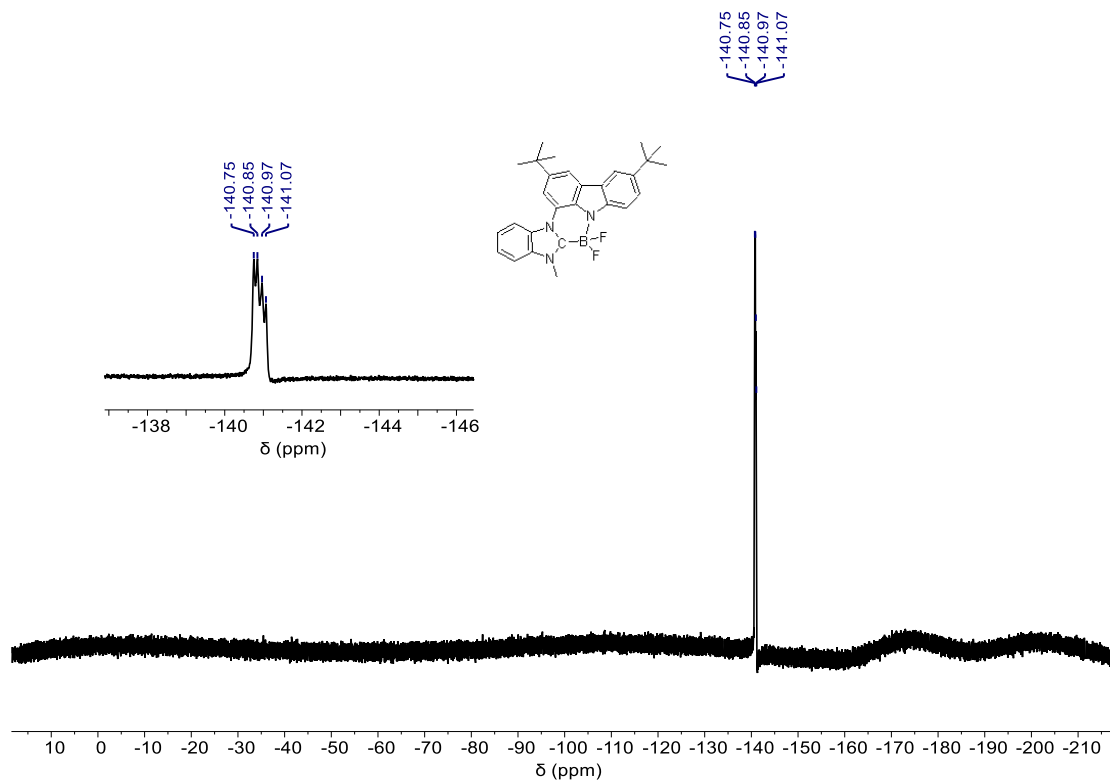
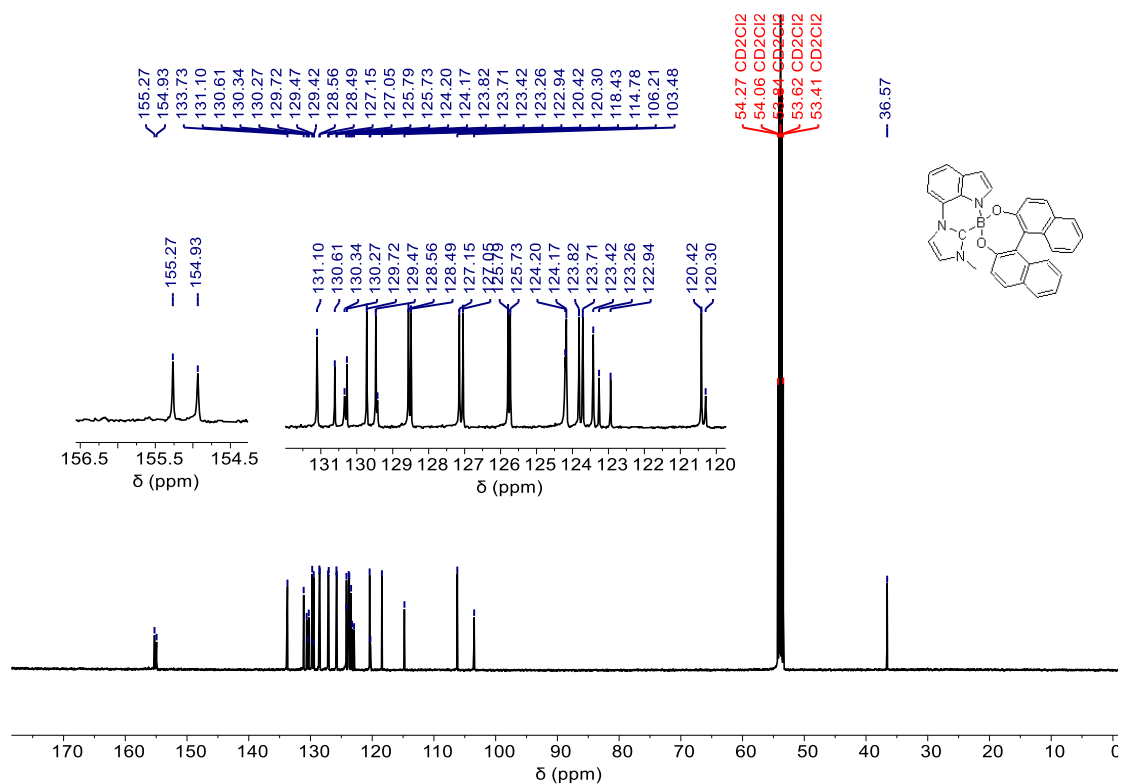
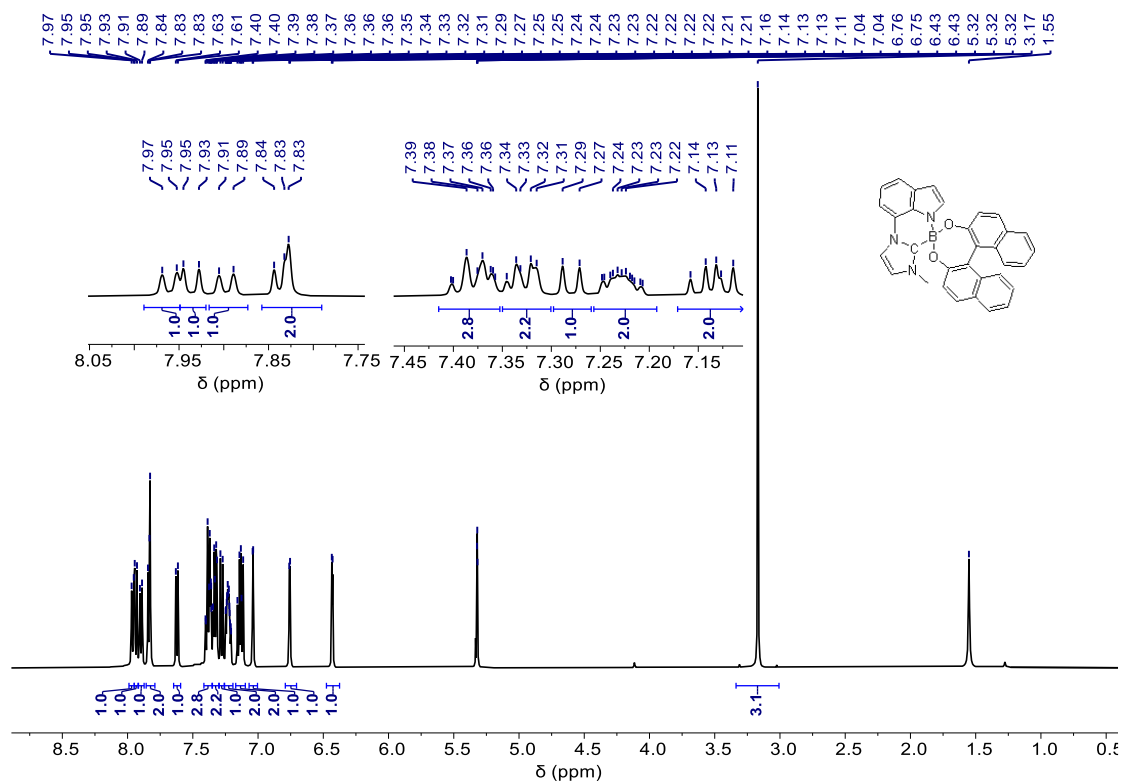
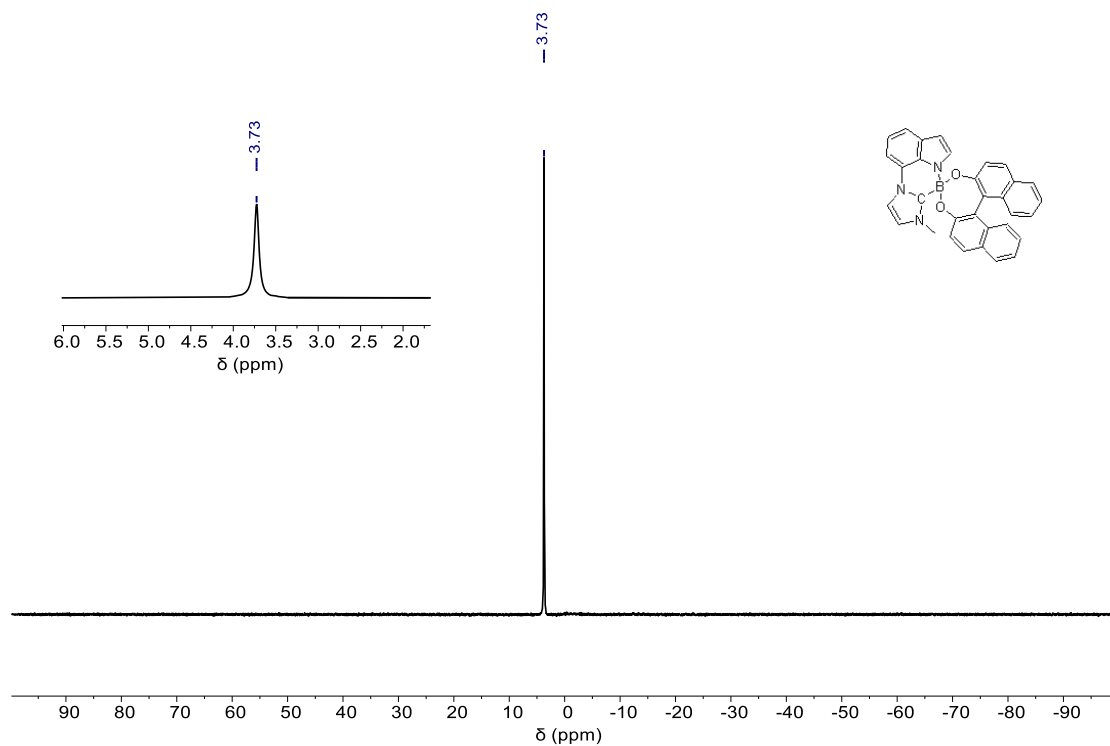


Figure S62.  $^{19}\text{F}\{^1\text{H}\}$  NMR spectra of **6** in  $\text{CDCl}_3$  at 376 MHz.





**Figure S65.**  $^{11}\text{B}\{^1\text{H}\}$  NMR spectra of **7** in  $\text{CD}_2\text{Cl}_2$  at 160 MHz.



## Thermal stabilities

Thermogravimetric analysis (TGA) was undertaken using SHIMADZU TGA-50 Instrument at a heating rate of 10 °C/min under a nitrogen environment. The decomposition temperatures ( $T_d$ ) were determined by the recorded temperature at 5% weight loss.

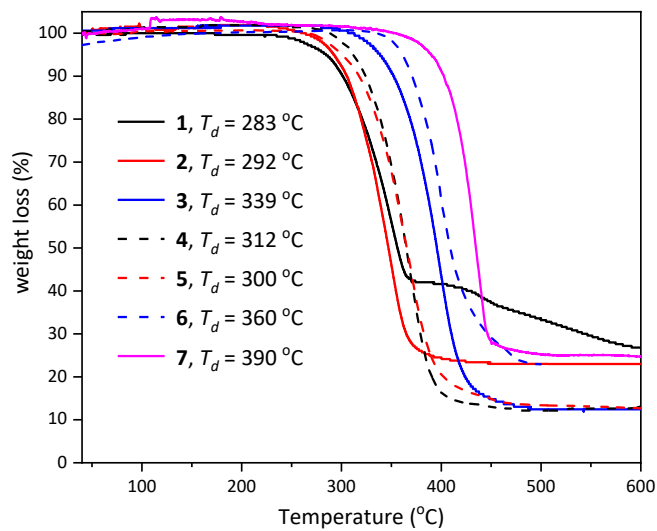


**Figure S66.** Thermal gravimetric analysis (TGA) curves of **1-7**.

## Single-crystal X-ray diffraction

**Table S1.** Single-crystal X-ray diffraction data and structure refinements of **1**, **3**, **4** and **6**.

	<b>1</b>	<b>3</b>	<b>4</b>	<b>6</b>
formula	C <sub>12</sub> H <sub>10</sub> BF <sub>2</sub> N <sub>3</sub>	C <sub>24</sub> H <sub>28</sub> BF <sub>2</sub> N <sub>3</sub>	C <sub>16</sub> H <sub>12</sub> BF <sub>2</sub> N <sub>3</sub>	C <sub>28</sub> H <sub>30</sub> BF <sub>2</sub> N <sub>3</sub>
fw	245.04	407.30	295.10	457.36
Tem., K	100.0(2)	298.0(2)	100.0(2)	100.0(2)
color	colorless	colorless	colorless	colorless
crystal size	0.25 x 0.22 x 0.19	0.32 x 0.26 x 0.24	0.21 x 0.19 x 0.18	0.26 x 0.18 x 0.16
crystal system	monoclinic	tetragonal	monoclinic	monoclinic
space group	<i>P</i> 2 <sub>1</sub> / <i>c</i>	<i>P</i> $\bar{4}$ 2 <sub>1</sub> <i>c</i>	<i>P</i> 2 <sub>1</sub> / <i>c</i>	<i>P</i> 2 <sub>1</sub> / <i>c</i>
<i>a</i> , Å	7.7848(5)	18.6377(13)	6.8997(5)	13.6165(5)
<i>b</i> , Å	18.2595(10)	18.6377(13)	9.3476(7)	14.8008(5)
<i>c</i> , Å	7.9179(5)	27.574(3)	20.3994(15)	12.2884(4)
$\alpha$ , deg	90	90	90	90
$\beta$ , deg	108.873(4)	90	99.599(2)	108.416(2)
$\gamma$ , deg	90	90	90	90
<i>V</i> , Å <sup>3</sup>	1064.99(11)	9578.2(17)	1297.25(17)	2349.71(14)
<i>Z</i>	4	16	4	4
<i>D</i> <sub>c</sub> , g cm <sup>-3</sup>	1.528	1.130	1.511	1.293
$\mu$ , mm <sup>-1</sup>	0.632	0.397	0.590	0.444
<i>F</i> (000)	504.0	3456	608.0	968.0
2 $\theta$ range, deg	8.426–115.38	4.978–114.038	3.822–134.348	7.902–126.834
no. reflections	11825	118624	48053	49353
no. independent reflections	2154 [ <i>R</i> (int) = 0.0634]	9819 [ <i>R</i> (int) = 0.0948]	3555 [ <i>R</i> (int) = 0.0803]	5822 [ <i>R</i> (int) = 0.0373]
Data/restraints/parameters	2154/0/165	9819/0/557	3555/0/201	5822/0/314
<i>GOF</i> on <i>F</i> <sup>2</sup>	1.061	1.022	1.151	1.047
<i>R</i> <sub>1</sub> <sup>a</sup>	0.0431	0.0348	0.0625	0.0364
<i>wR</i> <sub>2</sub> <sup>b</sup>	0.1129	0.0938	0.1713	0.0987
residual $\rho$ , eÅ <sup>-3</sup>	0.35/–0.31	0.12/–0.13	0.31/–0.32	0.36/–0.21

$$^a R = \sum ||F_o| - |F_c|| / \sum |F_o|. \quad ^b RW = \{ \sum [w(F_o^2 - F_c^2)^2] / \sum [w(F_o^2)^2] \}^{1/2}$$

Crystals growing method:

The solid of **1**, **4** and **6** was dissolved in a small amount of CH<sub>2</sub>Cl<sub>2</sub>, respectively and then hexane was added to the solution slowly. The resulting solution was left at –20 °C in a freezer overnight and single crystals of **1** was obtained as colorless crystals. For **3**, it was dissolved in a small amount of THF and then hexane was added to the solution slowly. The resulting solution was left at r.t. overnight and single crystals of **3** was obtained as colorless crystals.

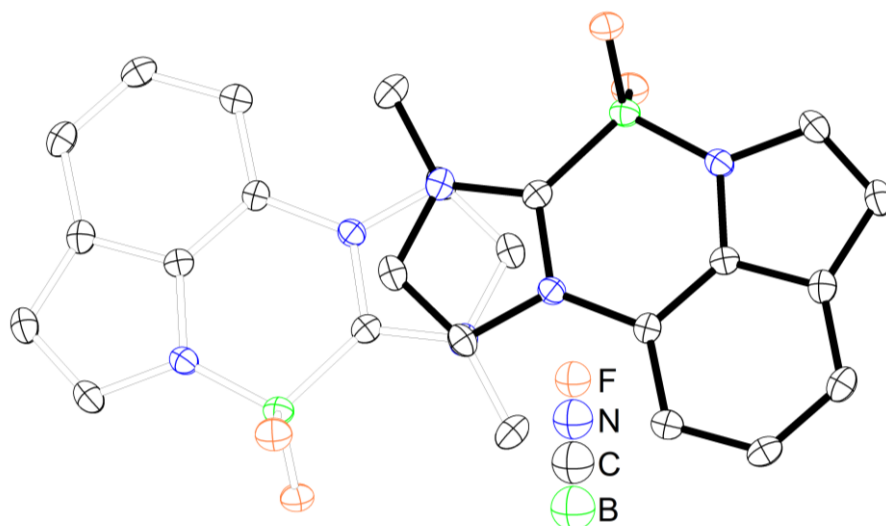


**Figure S67.** The crystal packing of **1** determined by single-crystal X-ray diffraction at 100 K. All ellipsoids are drawn at the 50% probability level, and H atoms are omitted for clarity.

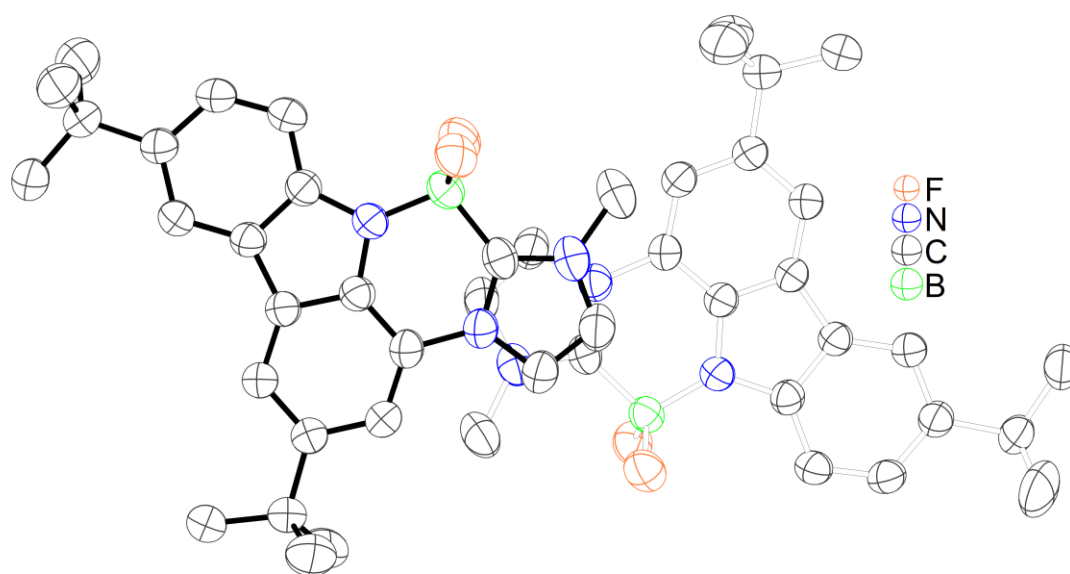


**Figure S68.** The crystal packing of **3** determined by single-crystal X-ray diffraction at 100 K. All ellipsoids are drawn at the 50% probability level, and H atoms are omitted for clarity.

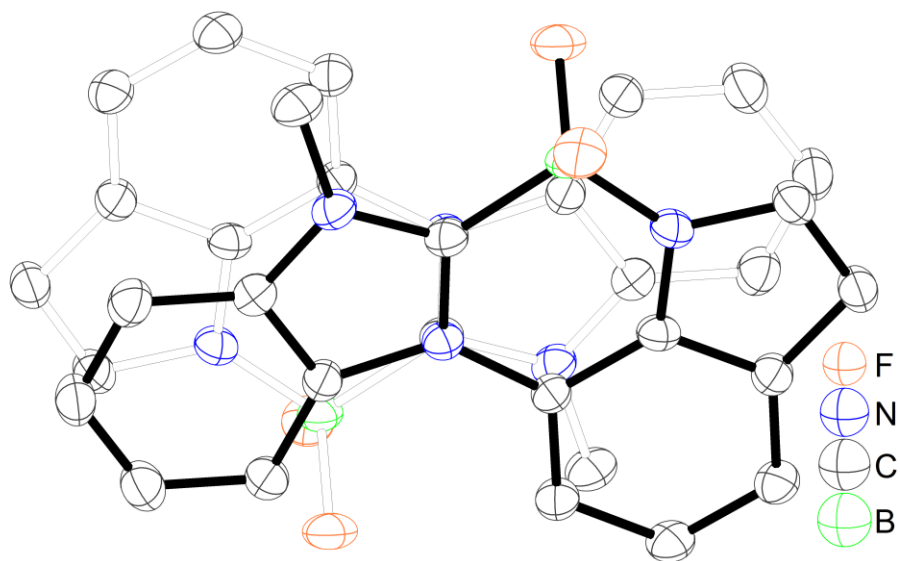


**Figure S69.** The crystal packing of **4** determined by single-crystal X-ray diffraction at 100 K. All ellipsoids are drawn at the 50% probability level, and H atoms are omitted for clarity.

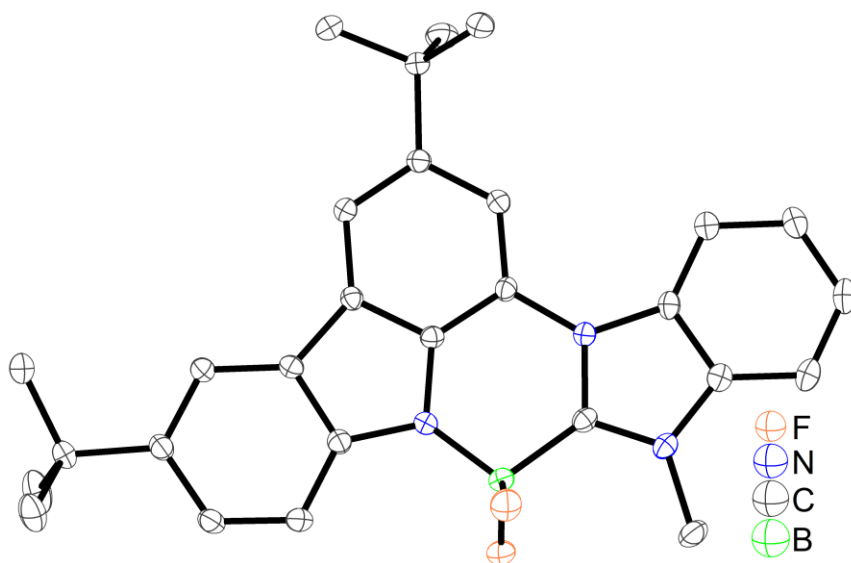


**Figure S70.** The crystal structure of **6** determined by single-crystal X-ray diffraction at 100 K. All ellipsoids are drawn at the 50% probability level, and H atoms are omitted for clarity.

## Photophysical properties

**Table S2.** Photophysical data for **1–7** in solutions and the solid states at 298 K.

		$\lambda_{\text{abs}}$ (nm) ( $\epsilon \times 10^4 \text{ cm}^{-1} \text{ M}^{-1}$ )	$\lambda_{\text{em}}$ (nm)	$\phi$	$\tau_{\text{F}}$ (ns)	Stokes shift ( $\text{cm}^{-1}$ )
<b>1</b>	CH <sub>2</sub> Cl <sub>2</sub>	314 (1.1)	384	0.583	5.9	5808
	THF	315 (1.2)	384	0.562	6.2	5704
	MeOH	313 (1.1)	385	0.511	6.1	5974
	DMSO	312 (1.1)	391	0.234	11.9	6475
	solid		361 <sup>sh</sup> ; 374;	0.427	5.3	
<b>2</b>	CH <sub>2</sub> Cl <sub>2</sub>	323 (1.0)	380	0.266	4.0	4643
	MeOH	320 (0.7)	380	0.291	6.1	4934
	DMSO	320 (0.7)	393	0.153	10.4	5804
	solid		374 <sup>sh</sup> ; 413 <sup>sh</sup> ; 440	0.519	5.3	
<b>3</b>	CH <sub>2</sub> Cl <sub>2</sub>	369 (0.9)	385 <sup>sh</sup> ; 392	0.472	4.3	1126
	THF	369 (0.8)	382 <sup>sh</sup> ; 391	0.449	6.5	853
	MeOH	364 (0.7)	381 <sup>sh</sup> ; 391	0.562	6.6	1226
	DMSO	365 (0.8)	392	0.228	6.0	1887
	solid		406	0.071	4.5	
<b>4</b>	CH <sub>2</sub> Cl <sub>2</sub>	329 (1.0)	444	0.732	10.3	7872
	THF	328 (1.1)	449	0.552	9.4	8216
	MeOH	327 (1.2)	453	0.140	2.9	8505
	DMSO	324 (1.2)	467	0.259	4.3	9450
	solid		441	0.558	11.3	
<b>5</b>	CH <sub>2</sub> Cl <sub>2</sub>	336 (1.2)	436	0.551	6.4	6826
	THF	334 (0.3)	436	0.529	7.1	7004
	MeOH	332 (1.1)	441	0.222	3.7	7444
	DMSO	331 (1.3)	445	0.173	3.6	7739
	solid		459	0.449	8.5	
<b>6</b>	CH <sub>2</sub> Cl <sub>2</sub>	371 (1.3)	453	0.777	7.6	4879
	THF	370 (1.3)	455	0.697	7.4	5049
	MeOH	366 (1.2)	456	0.661	7.4	5392
	DMSO	370 (1.1)	458	0.392	8.3	5193
	solid		421	0.669	5.6	
<b>7</b>	CH <sub>2</sub> Cl <sub>2</sub>	324 (1.7)	386	0.022	5.2	4957
	THF	325 (1.5)	384	0.040	0.6	4728
	MeOH	318(1.5)	382	0.036	1.0	5268
	DMSO	<sup>a</sup>	391	0.051	1.6	/
	solid		390	0.243	4.5	

<sup>a</sup>The peak can't be determined due to the broad lowest energy absorption. <sup>b</sup>Depending on the absorbance, the photophysical measurements were performed at concentrations in a range of 0.5~1.0×10<sup>-5</sup> mol L<sup>-1</sup>.

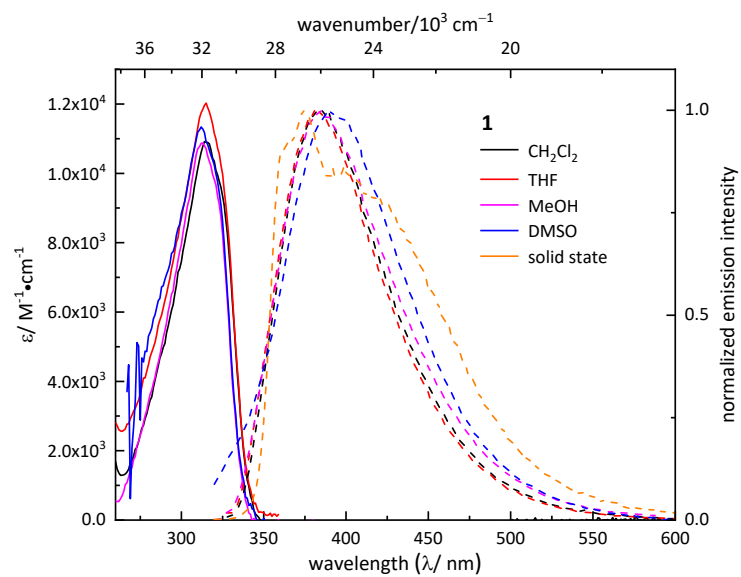


**Figure S71.** UV-vis absorption spectra (solid lines) and emission spectra (dash lines) of **1** in different solvents and the solid state at 298 K.

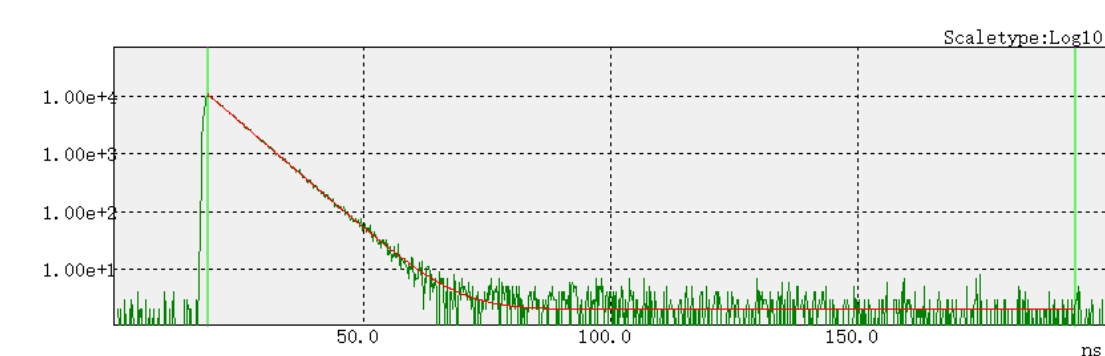


**Figure S72.** Lifetime decay of **1** in  $\text{CH}_2\text{Cl}_2$  at 298 K, the red line is the fitting line.

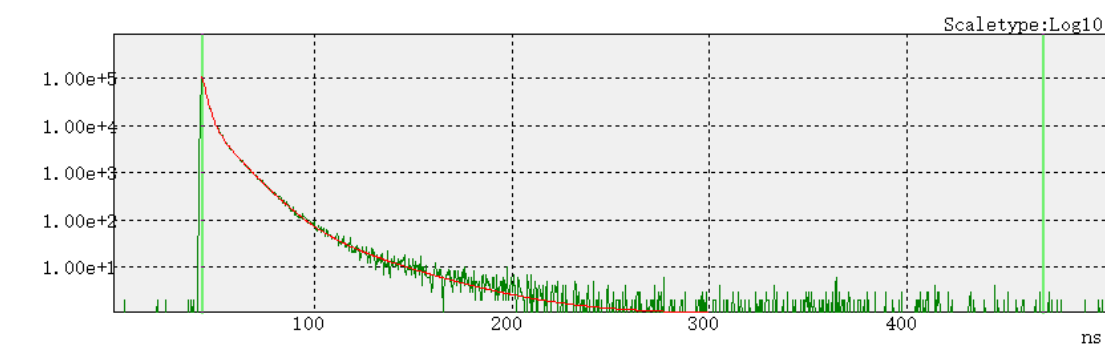


**Figure S73.** Lifetime decay of **1** in the solid state at 298 K, the red line is the fitting line.

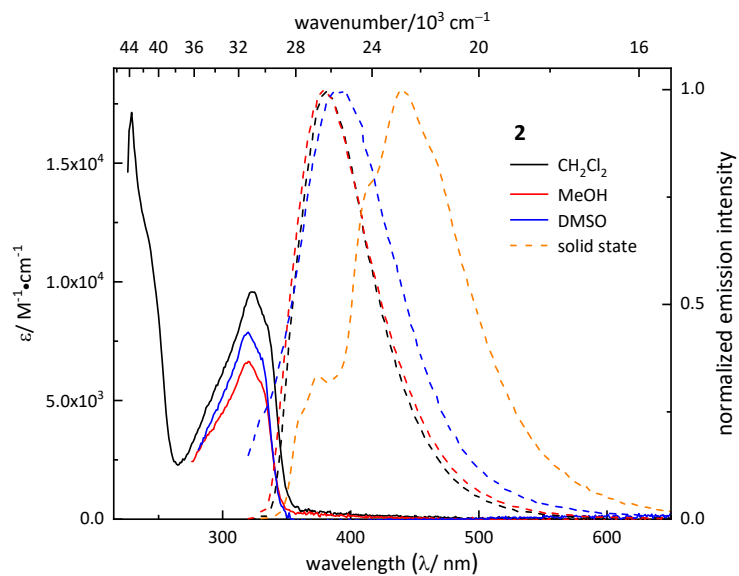


**Figure S74.** UV-vis absorption spectra (solid lines) and emission spectra (dash lines) of **2** in different solvents and the solid state at 298 K.

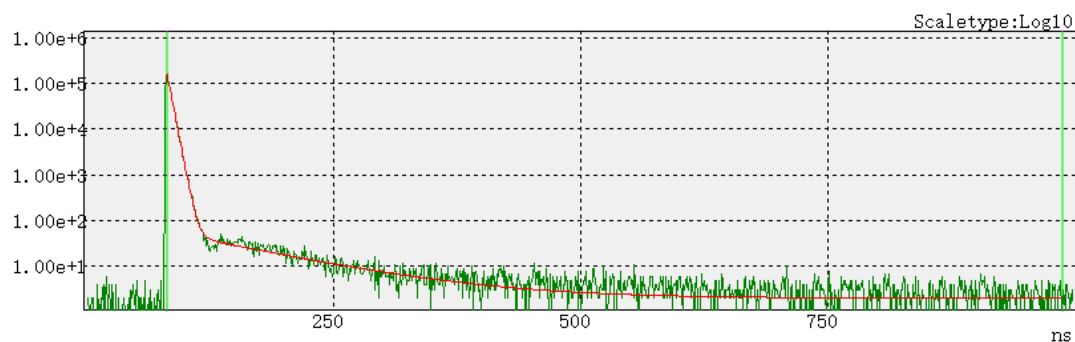


**Figure S75.** Lifetime decay of **2** in  $\text{CH}_2\text{Cl}_2$  at 298 K, the red line is the fitting line.

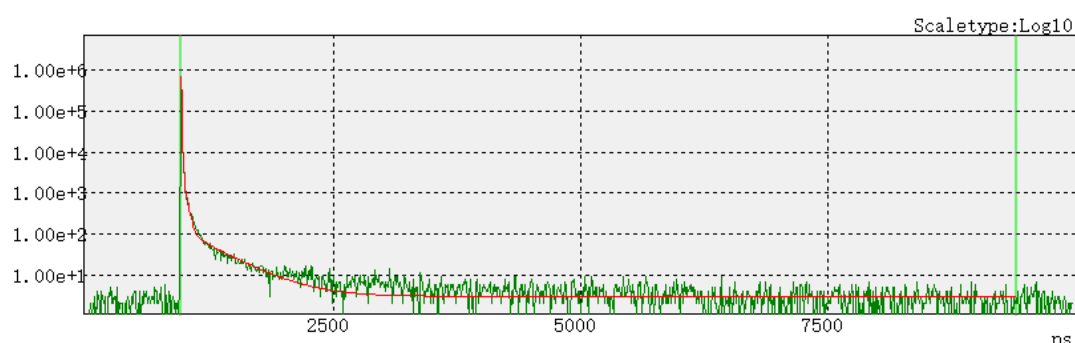


**Figure S76.** Lifetime decay of **2** in the solid state at 298 K, the red line is the fitting line.

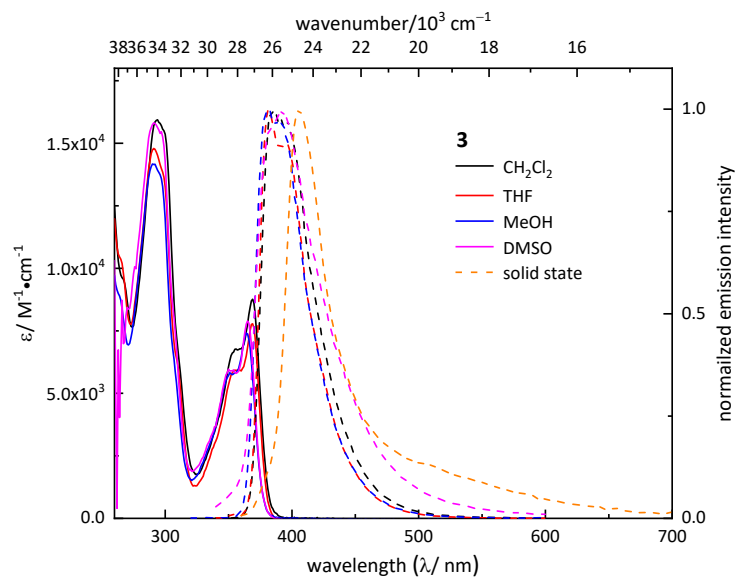


**Figure S77.** UV-vis absorption spectra (solid lines) and emission spectra (dash lines) of **3** in different solvents and the solid state at 298 K.

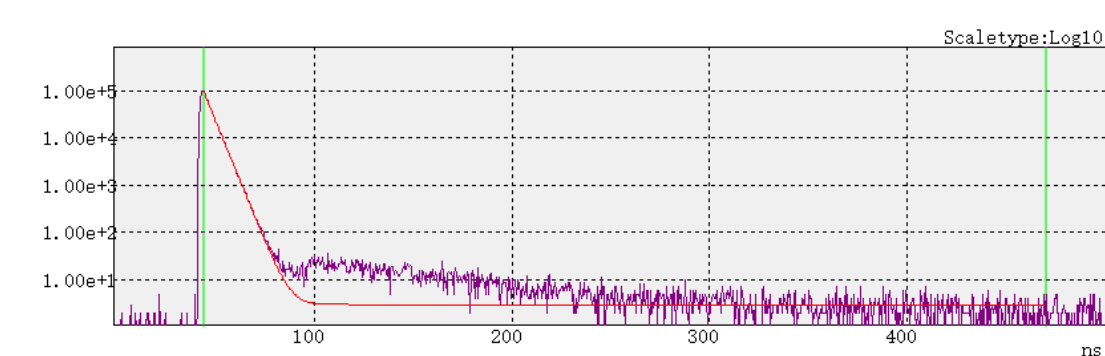


**Figure S78.** Lifetime decay of **3** in  $\text{CH}_2\text{Cl}_2$  at 298 K, the red line is the fitting line.

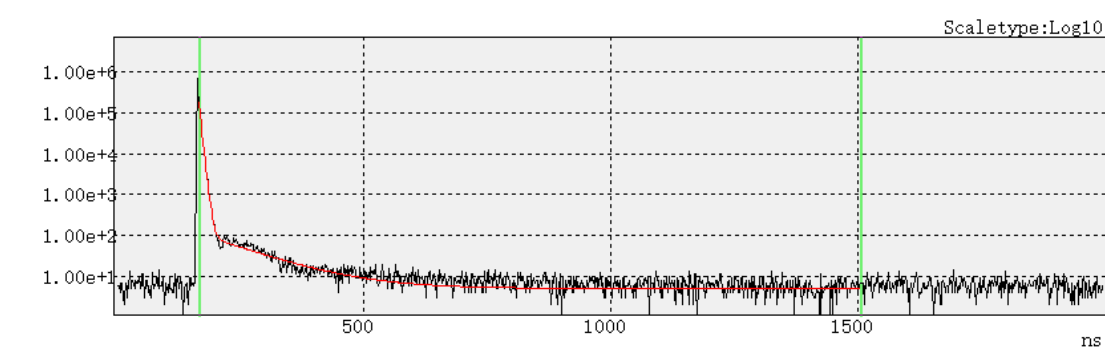


**Figure S79.** Lifetime decay of **3** in the solid state at 298 K, the red line is the fitting line.



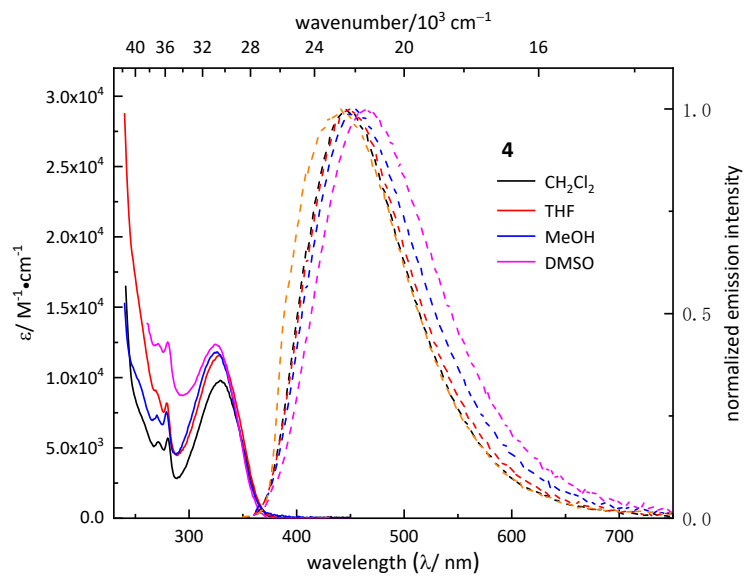


**Figure S80.** UV-vis absorption spectra (solid lines) and emission spectra (dash lines) of **4** in different solvents and the solid state at 298 K.

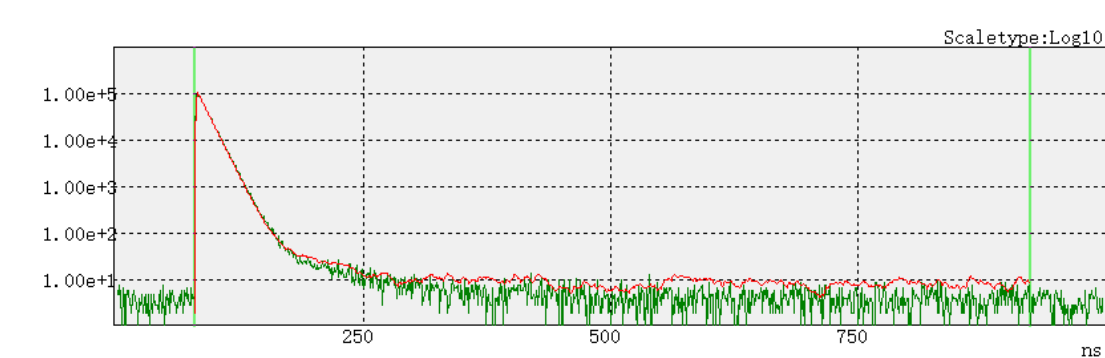


**Figure S81.** Lifetime decay of **4** in  $\text{CH}_2\text{Cl}_2$  at 298 K, the red line is the fitting line.

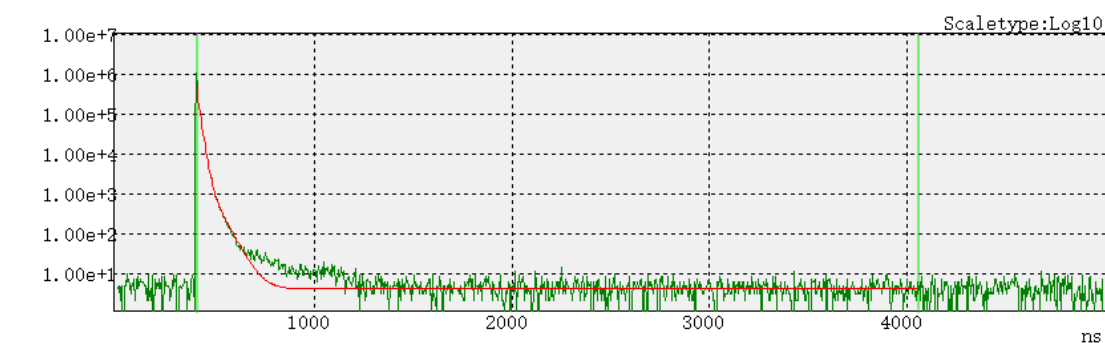


**Figure S82.** Lifetime decay of **4** in the solid state at 298 K, the red line is the fitting line.

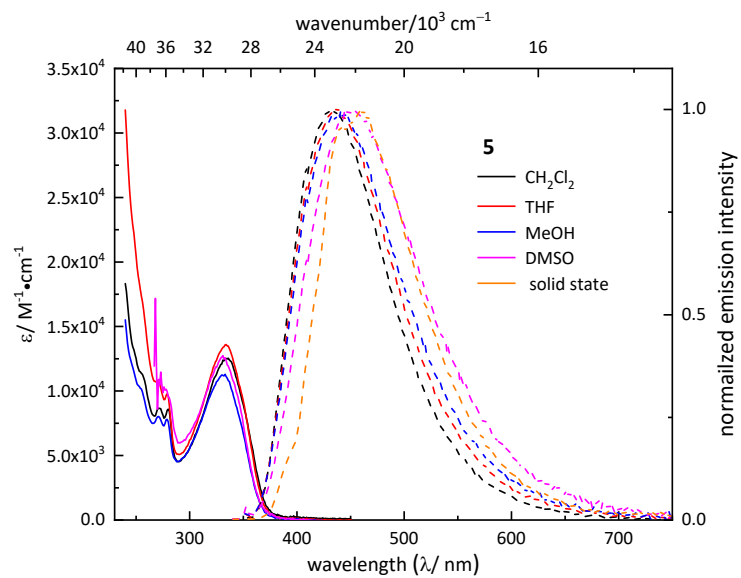


**Figure S83.** UV-vis absorption spectra (solid lines) and emission spectra (dash lines) of **5** in different solvents and the solid state at 298 K.

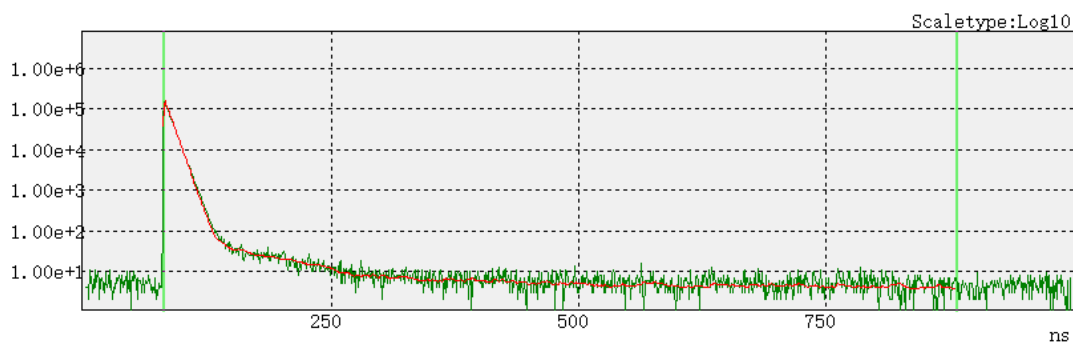


**Figure S84.** Lifetime decay of **5** in  $\text{CH}_2\text{Cl}_2$  at 298 K, the red line is the fitting line.

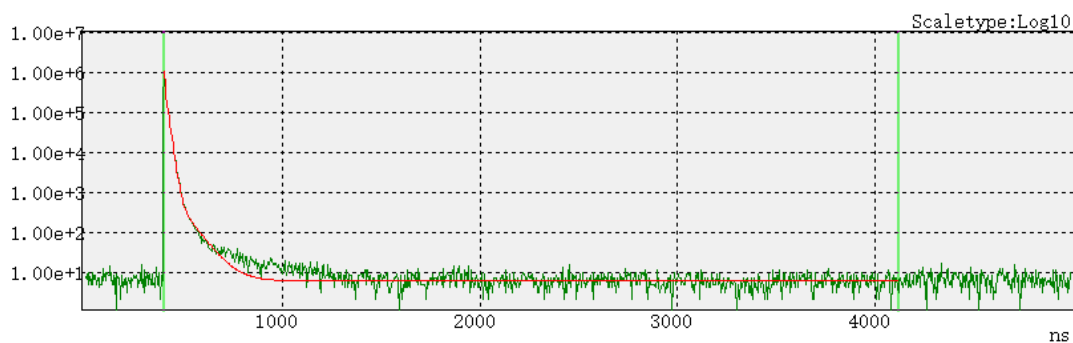


**Figure S85.** Lifetime decay of **5** in the solid state at 298 K, the red line is the fitting line.

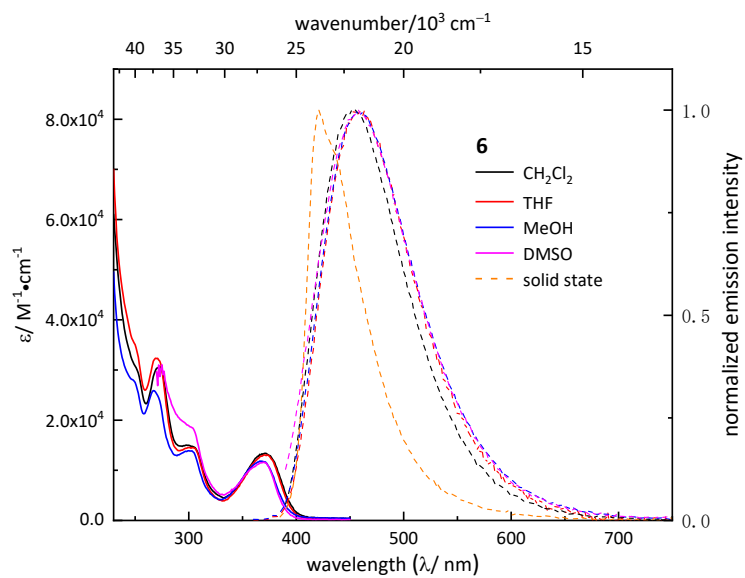


**Figure S86.** UV-vis absorption spectra (solid lines) and emission spectra (dash lines) of **6** in different solvents and the solid state at 298 K.

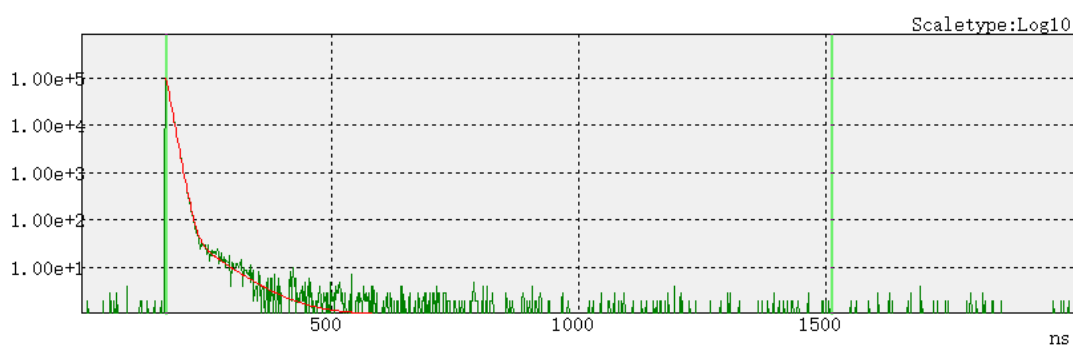


**Figure S87.** Lifetime decay of **6** in  $\text{CH}_2\text{Cl}_2$  at 298 K, the red line is the fitting line.

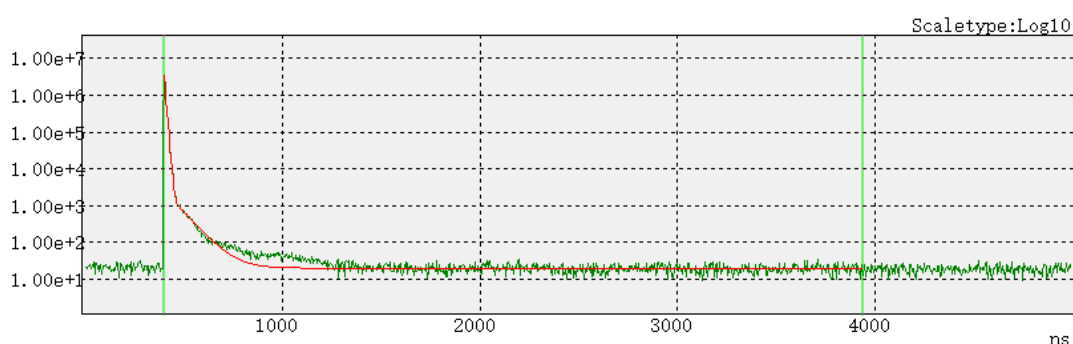


**Figure S88.** Lifetime decay of **6** in the solid state at 298 K, the red line is the fitting line.

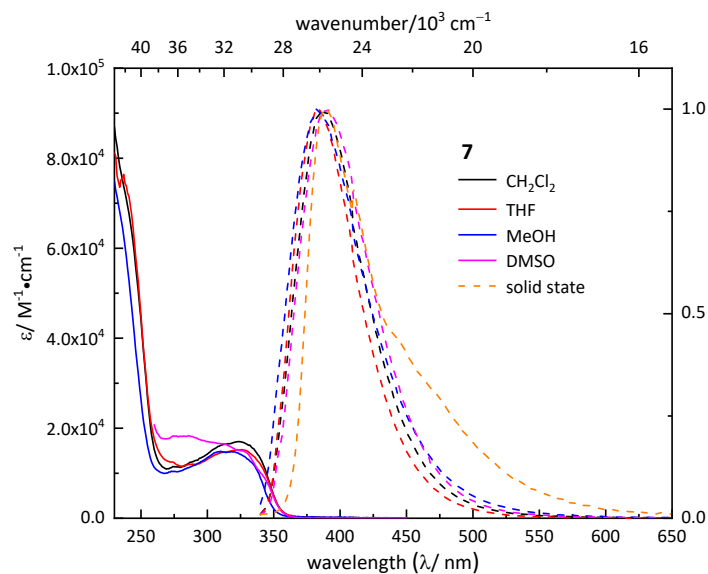


**Figure S89.** UV-vis absorption spectra (solid lines) and emission spectra (dash lines) of **7** in different solvents and the solid state at 298 K.

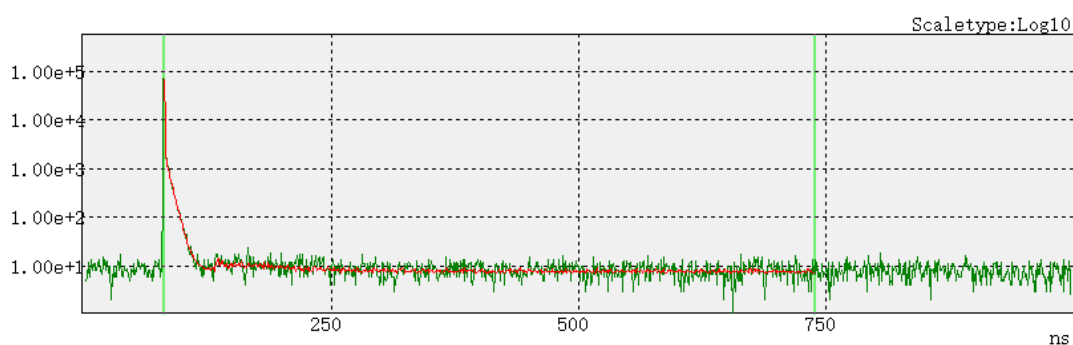


**Figure S90.** Lifetime decay of **7** in  $\text{CH}_2\text{Cl}_2$  at 298 K, the red line is the fitting line.

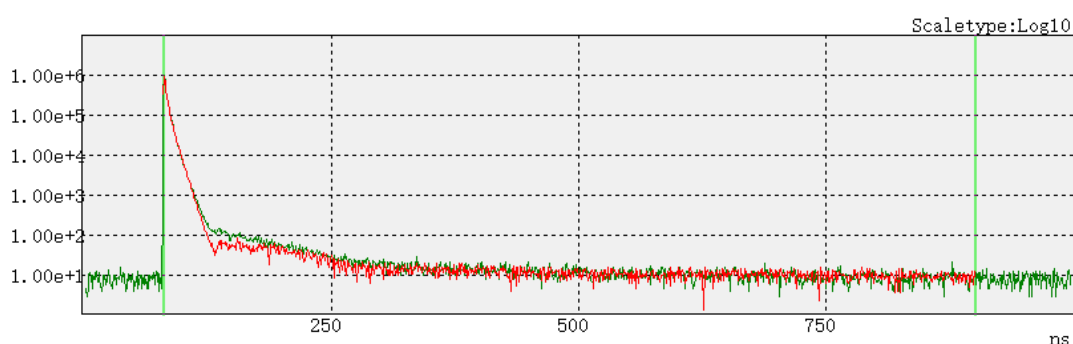


**Figure S91.** Lifetime decay of **7** in the solid state at 298 K, the red line is the fitting line.

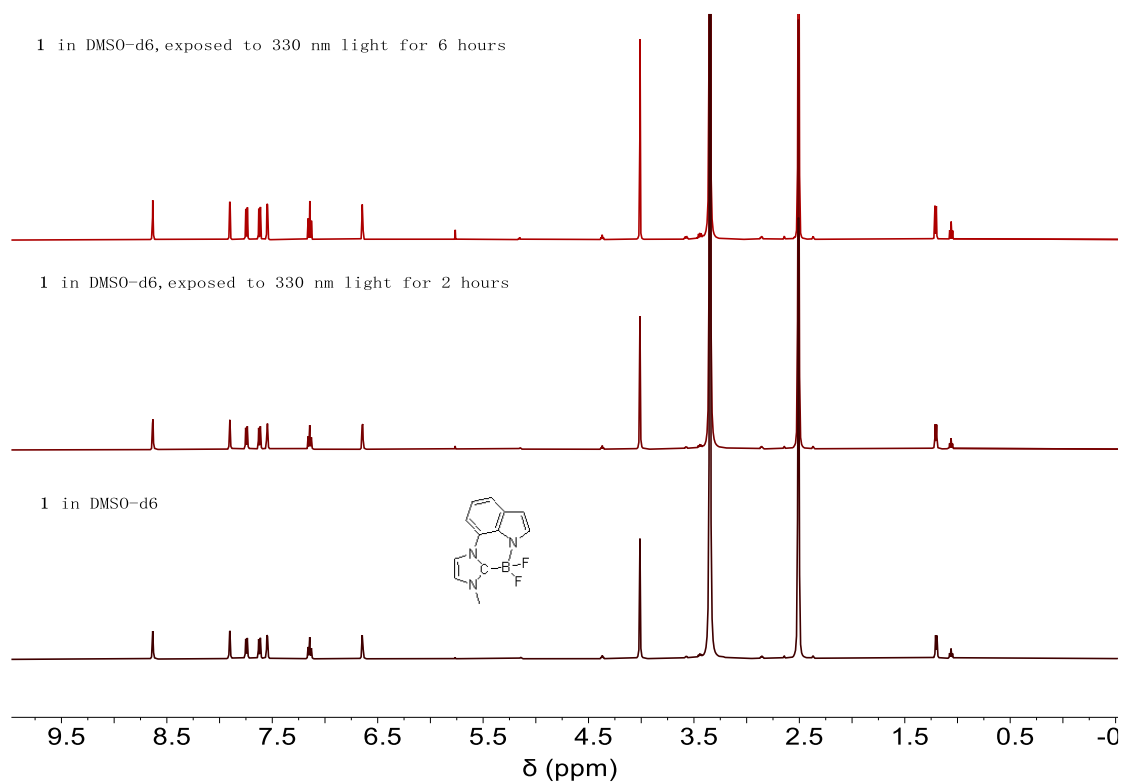


**Figure S92.** <sup>1</sup>H NMR spectra of **1** in DMSO-*d*<sub>6</sub> at 500 MHz, the optical power density is ca. 7 mW cm<sup>-2</sup>.

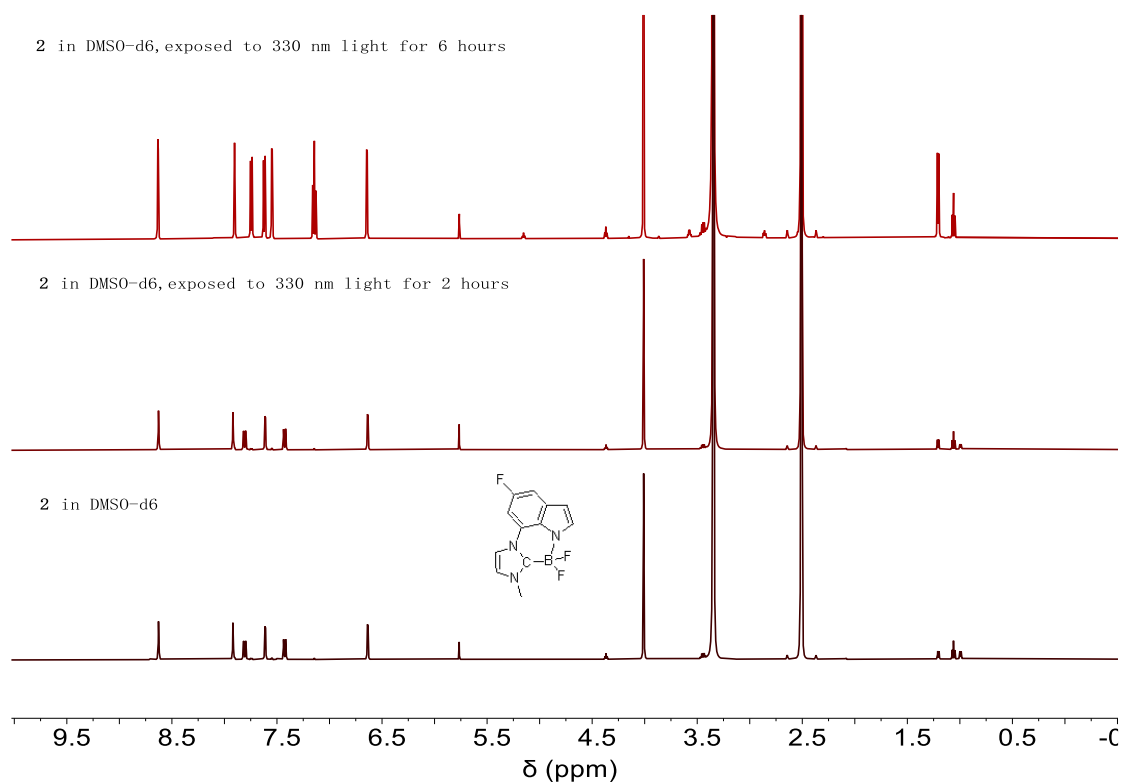


**Figure S93.** <sup>1</sup>H NMR spectra of **2** in DMSO-*d*<sub>6</sub> at 500 MHz, the optical power density is ca. 7 mW cm<sup>-2</sup>.

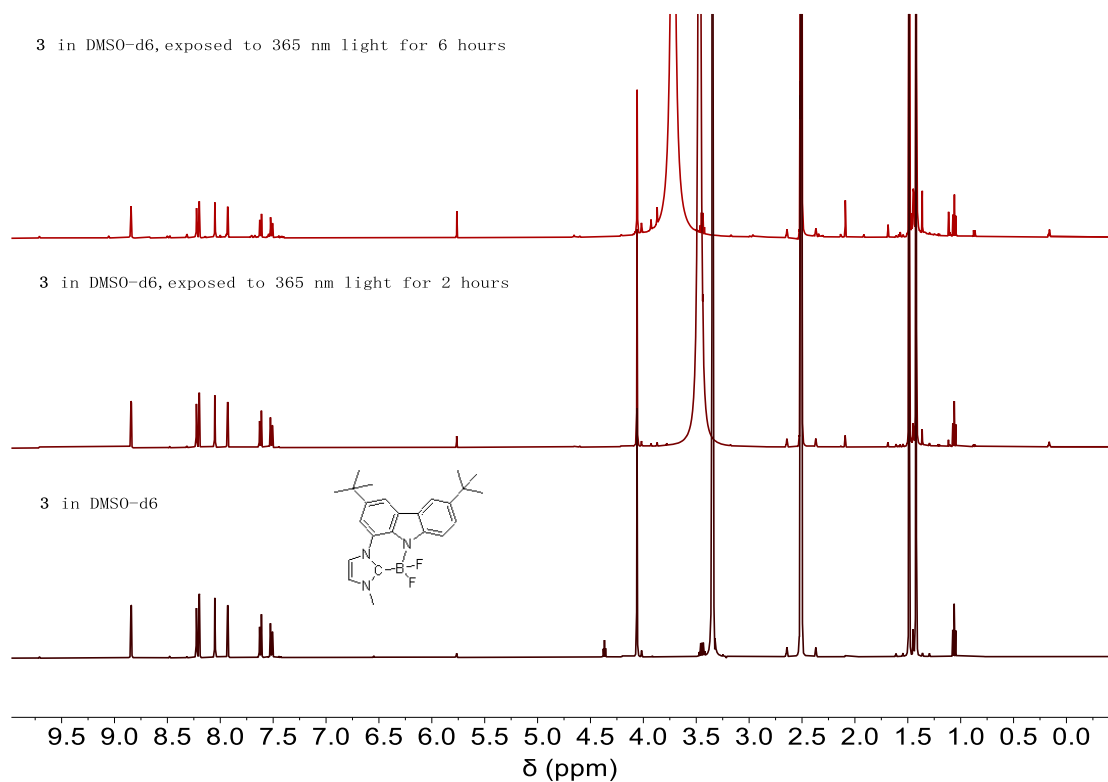


**Figure S94.** <sup>1</sup>H NMR spectra of **3** in DMSO-*d*<sub>6</sub> at 500 MHz, the optical power is 44.6 W.

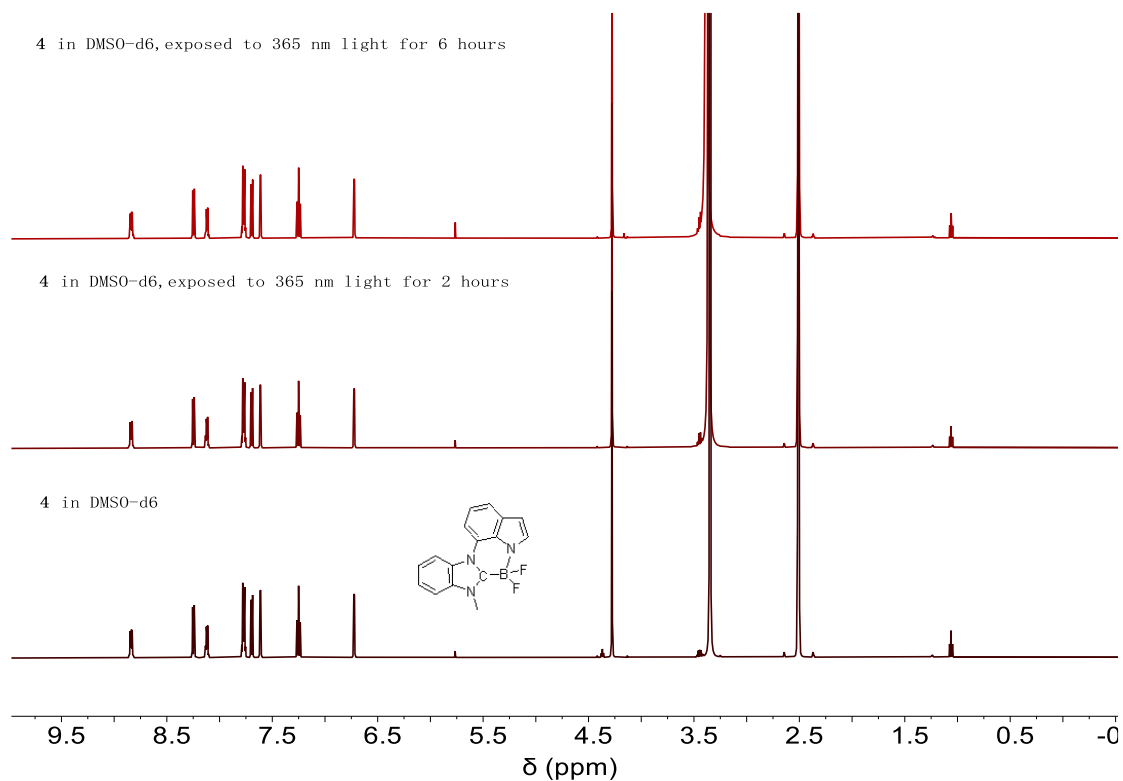


**Figure S95.** <sup>1</sup>H NMR spectra of **4** in DMSO-*d*<sub>6</sub> at 500 MHz, the optical power is 44.6 W.

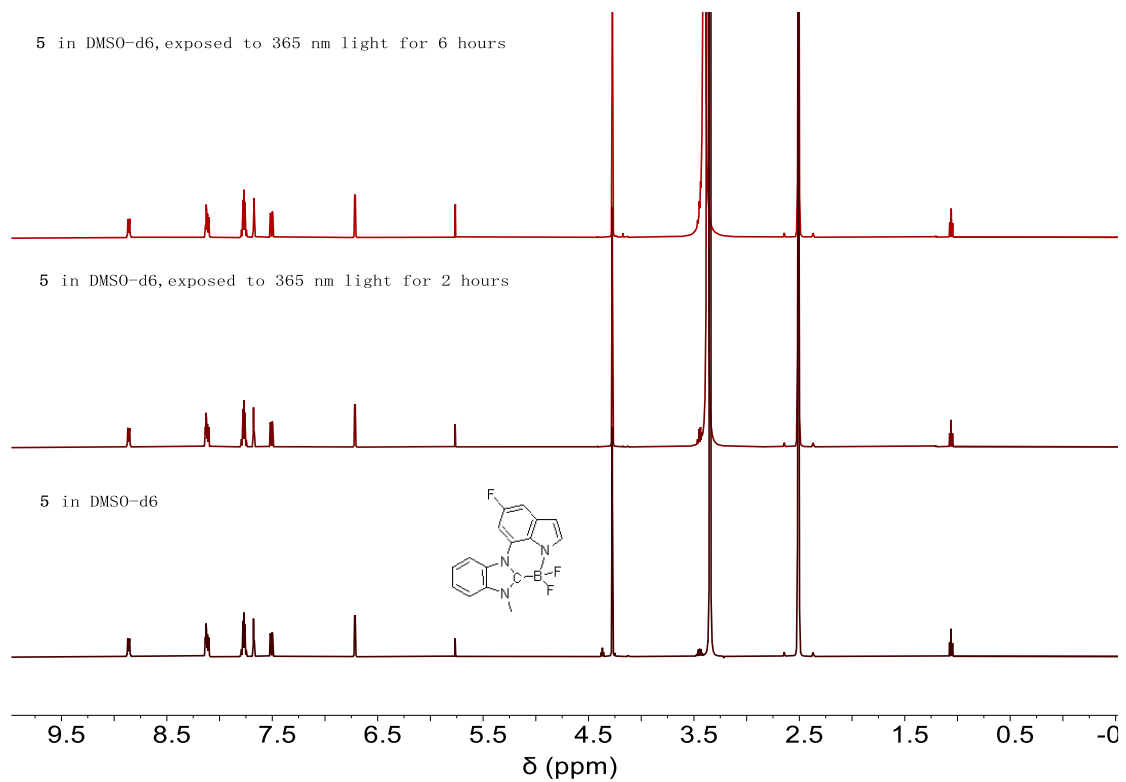


**Figure S96.** <sup>1</sup>H NMR spectra of **5** in DMSO-*d*<sub>6</sub> at 500 MHz, the optical power is 44.6 W.

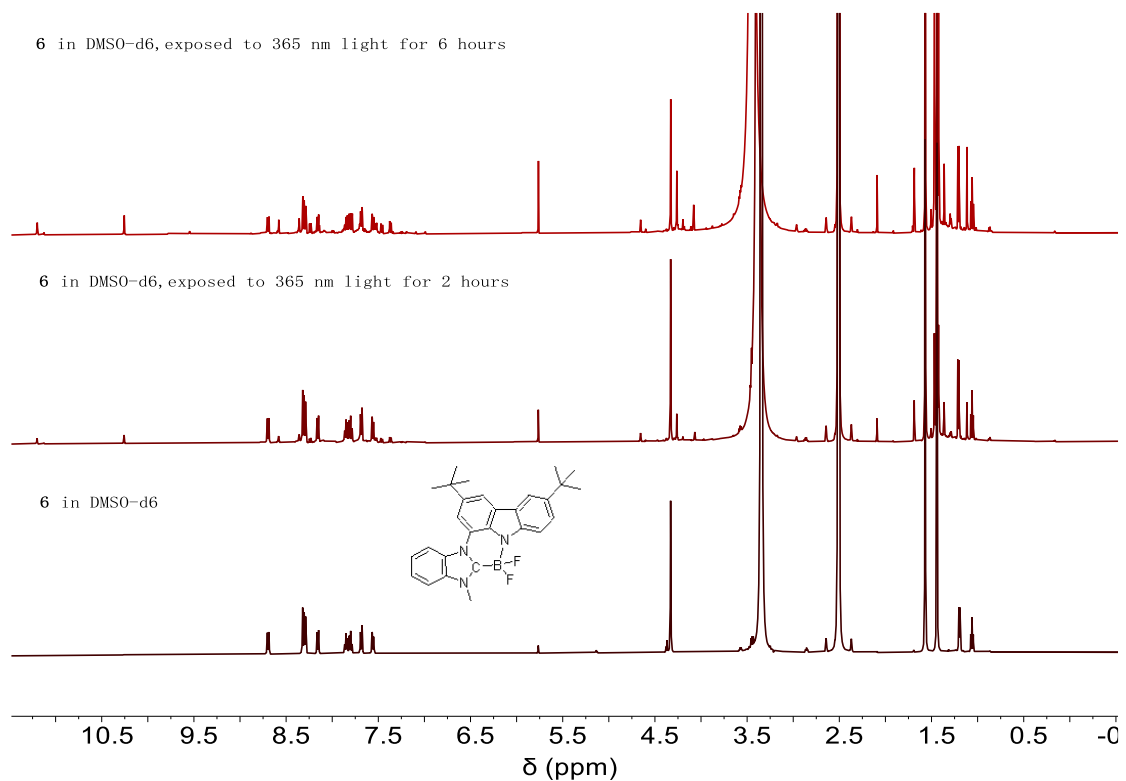


**Figure S97.** <sup>1</sup>H NMR spectra of **6** in DMSO-*d*<sub>6</sub> at 500 MHz, the optical power is 44.6 W.

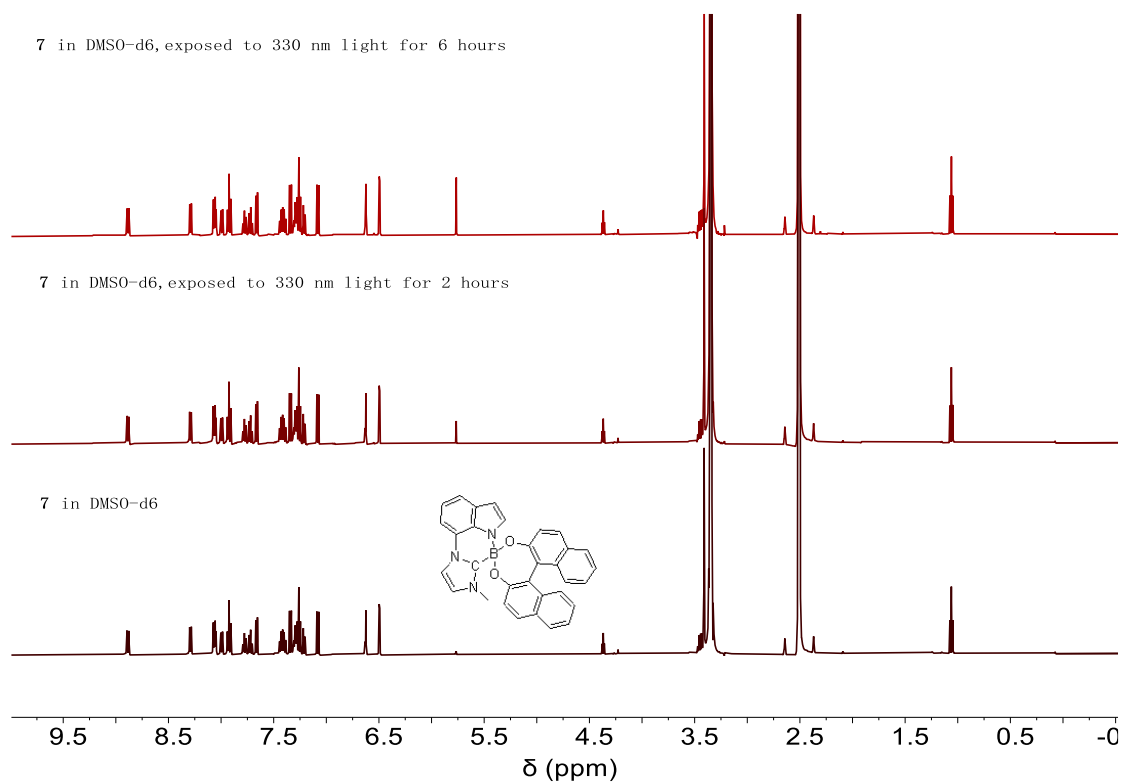
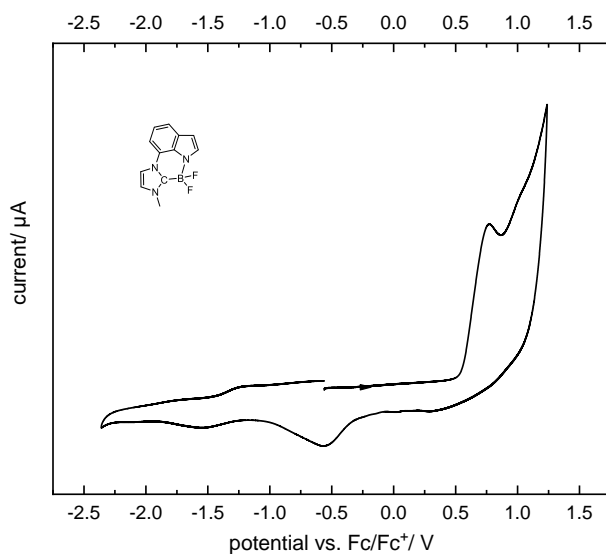


**Figure S98.**  $^1\text{H}$  NMR spectra of **7** in DMSO- $d_6$  at 500 MHz, the optical power density is ca.  $7 \text{ mW cm}^{-2}$ .

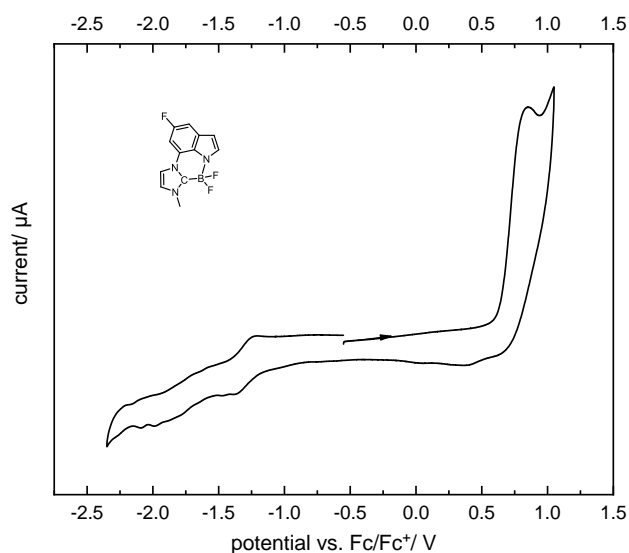


## Cyclic voltammetry

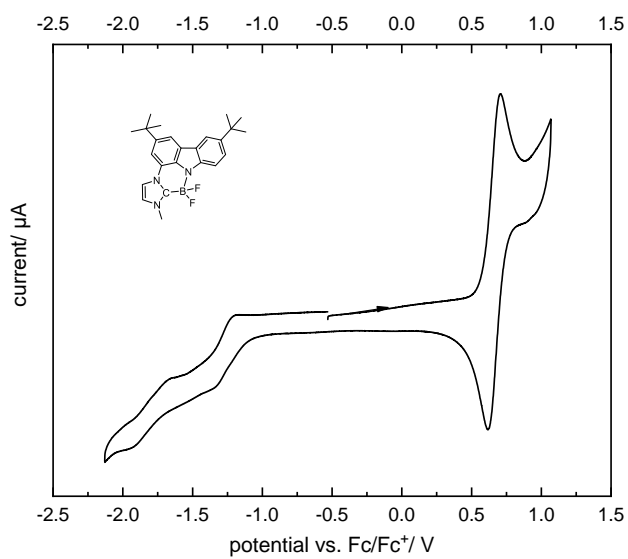
Cyclic voltammograms measured in  $\text{CH}_2\text{Cl}_2$  in the presence of  $\text{TBAPF}_6$  (0.1 M) as the electrolyte, scan rates of  $50 \text{ mV s}^{-1}$  with potentials given vs. the ferrocene/ferrocenium ( $\text{Fc}/\text{Fc}^+$ ) couple. The cyclic voltammograms were plotted according to IUPAC convention. All the measurements were performed with an initial potential of 0 V. The initial scan directions were marked by arrows in the Cyclic voltammograms.



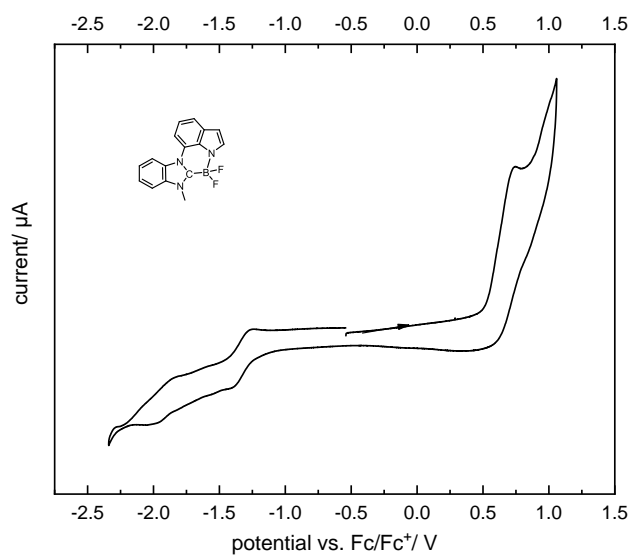
**Figure S99.** Cyclic voltammogram of **1** in  $\text{CH}_2\text{Cl}_2$ .



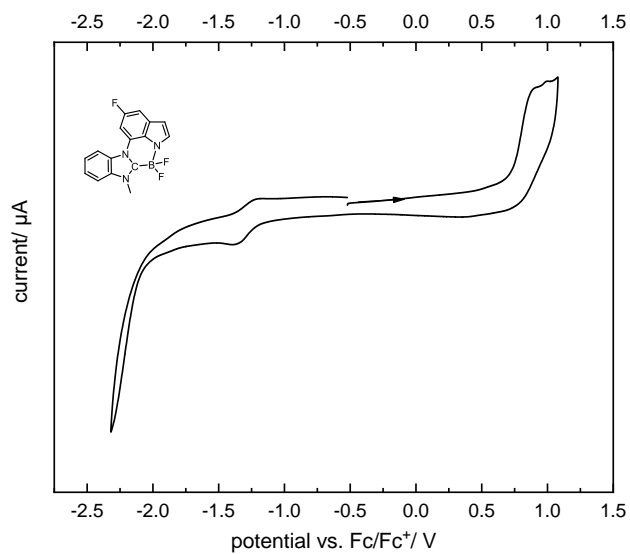
**Figure S100.** Cyclic voltammogram of **2** in  $\text{CH}_2\text{Cl}_2$ .



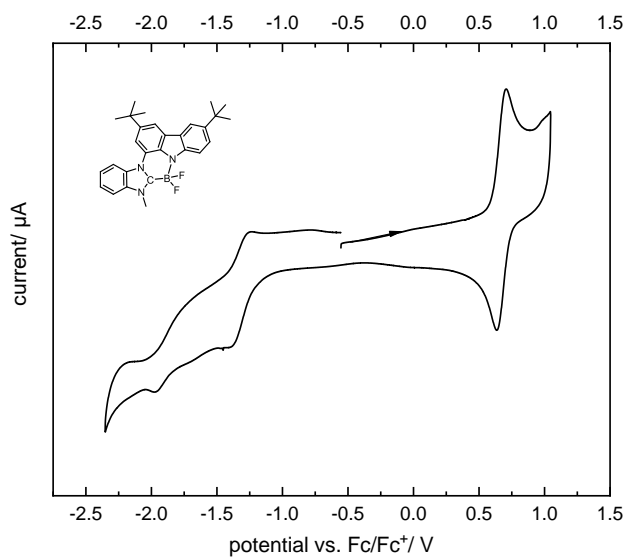
**Figure S101.** Cyclic voltammogram of **3** in CH<sub>2</sub>Cl<sub>2</sub>.



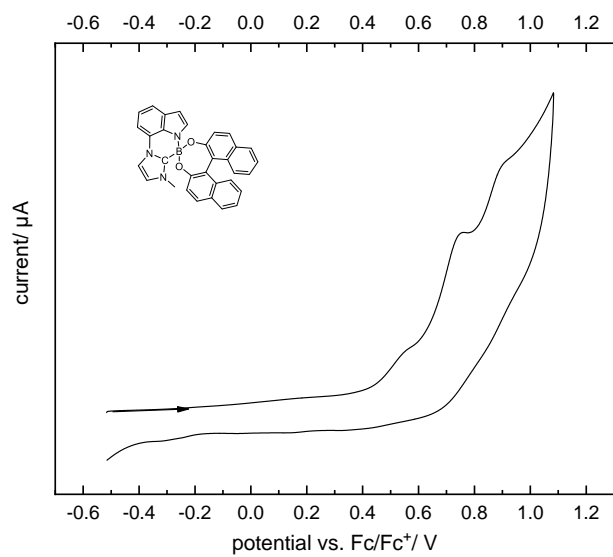
**Figure S102.** Cyclic voltammogram of **4** in CH<sub>2</sub>Cl<sub>2</sub>.



**Figure S103.** Cyclic voltammogram of **5** in  $\text{CH}_2\text{Cl}_2$ .



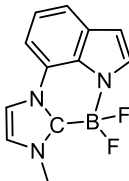
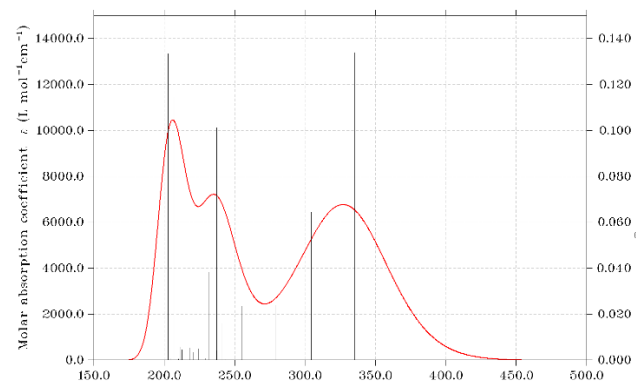
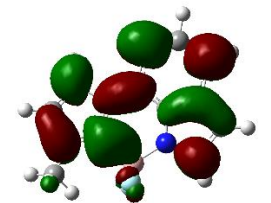
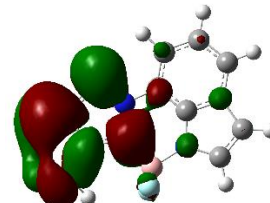
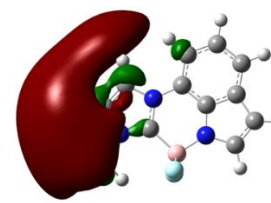
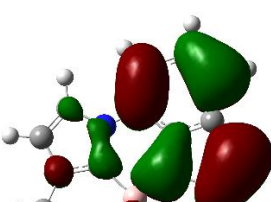
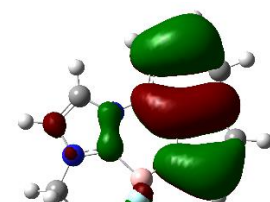
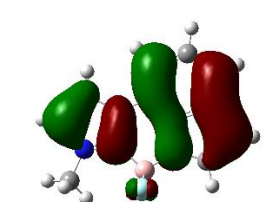
**Figure S104.** Cyclic voltammogram of **6** in  $\text{CH}_2\text{Cl}_2$ .



**Figure S105.** Cyclic voltammogram of **7** in  $\text{CH}_2\text{Cl}_2$ .

## TD-DFT calculations

**Table S3.** Calculated UV-vis absorption spectrum, orbitals and energies in gas phase of **1**.

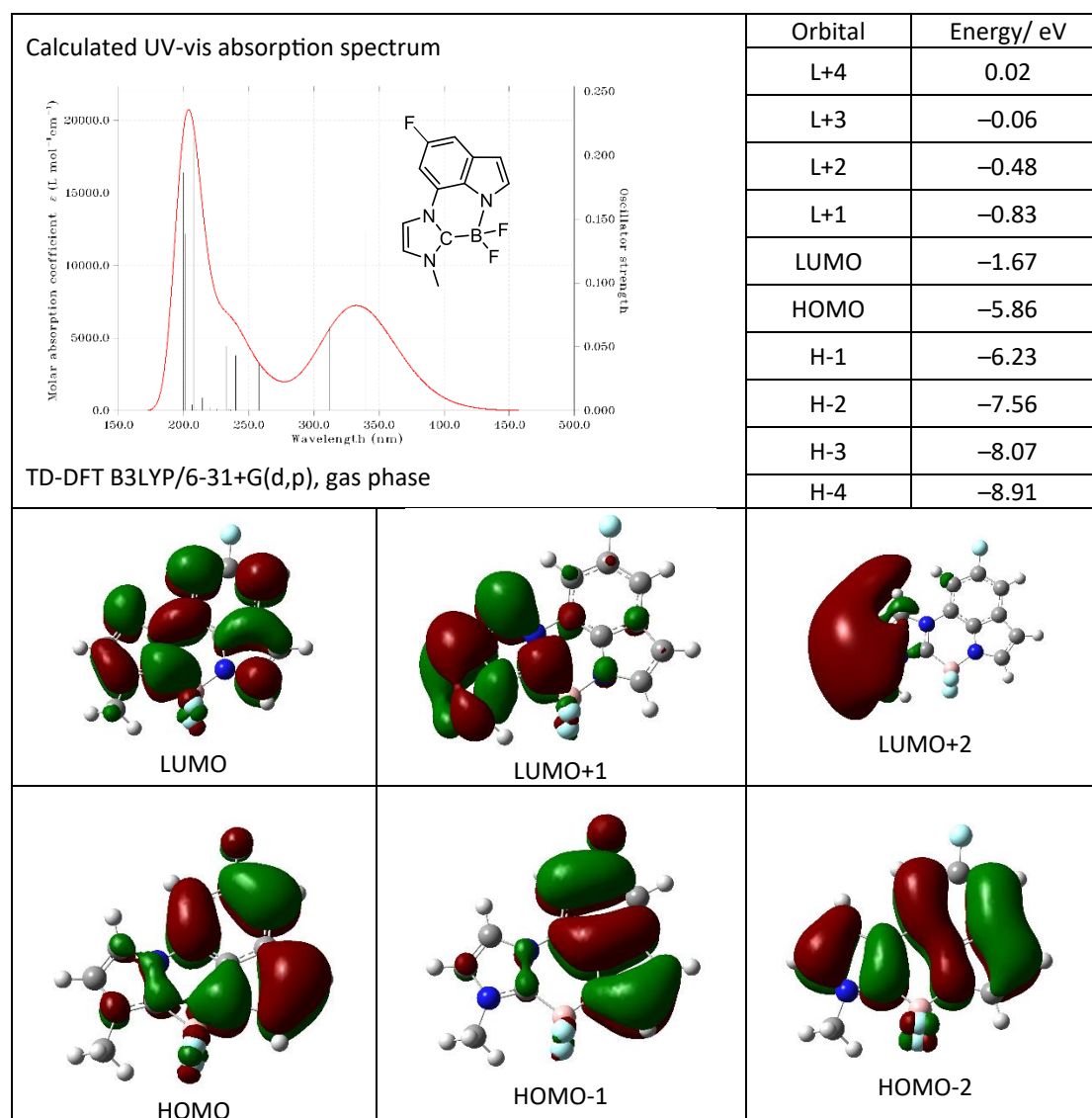
Calculated UV-vis absorption spectrum		Orbital	Energy/ eV
 		L+4	0.15
		L+3	-0.06
		L+2	-0.41
		L+1	-0.70
		LUMO	-1.45
		HOMO	-5.68
		H-1	-6.15
		H-2	-7.34
		H-3	-7.90
		H-4	-8.83
TD-DFT B3LYP/6-31+G(d,p), gas phase			
 LUMO		 LUMO+1	
 LUMO+2			
 HOMO		 HOMO-1	
		 HOMO-2	

**Table S4.** Transitions of **1** assigned by TD-DFT calculations.

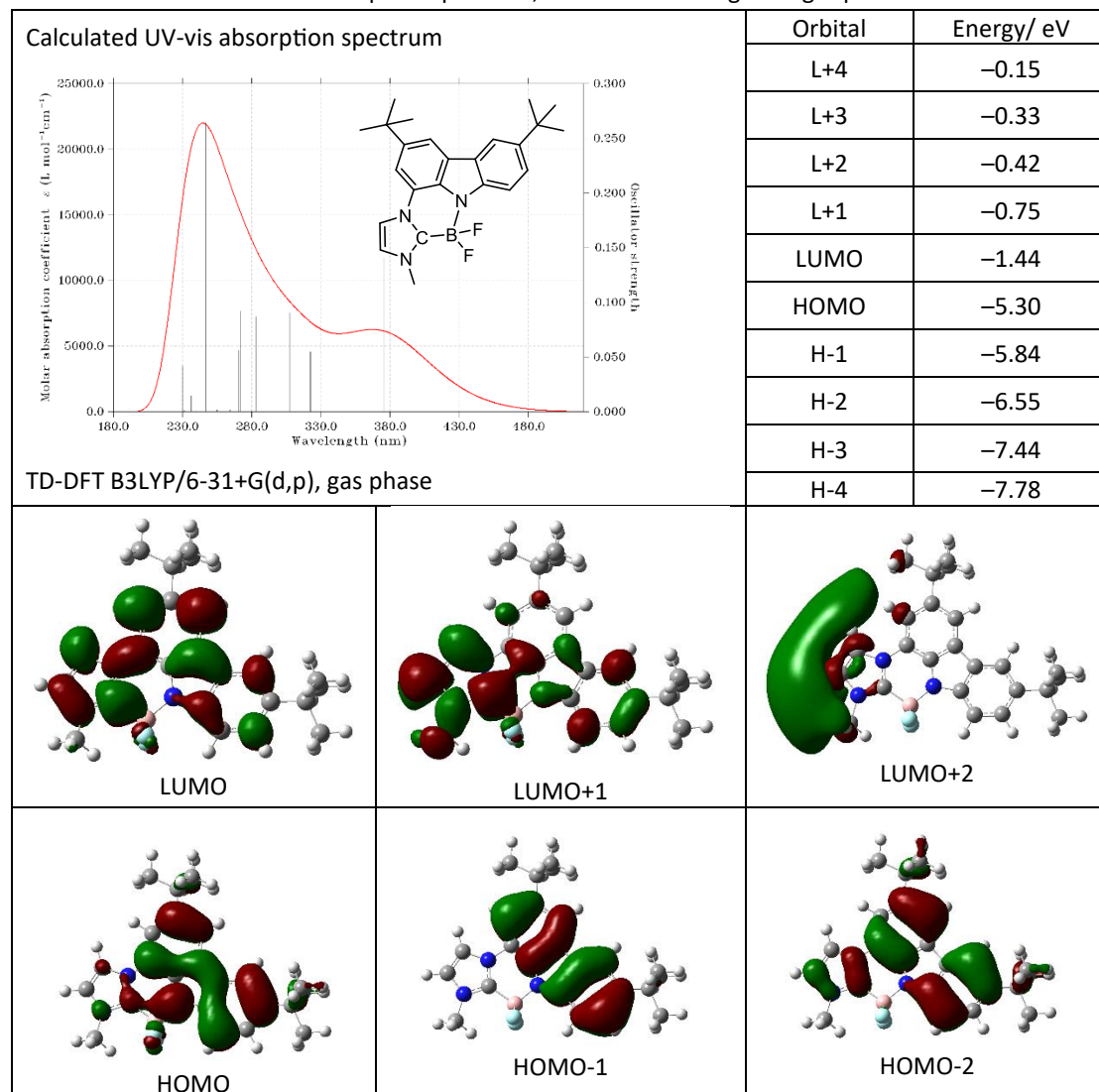
Excited State	E/eV	$\lambda$ /nm	major contributions	<i>f</i>
1	3.69	335	H→L	0.1339
2	4.07	304	H-1→L	0.0645
3	4.44	279	H→L+1	0.0240
4	4.79	259	H→L+2	0.0001
5	4.86	255	H-1→L+1	0.0236
6	5.09	243	H→L+3	0.0003
7	5.15	241	H-2→L (23%); H→L+4 (61%)	0.0158
8	5.22	237	H-2→L (30%); H-4→L (22%); H-4→L+1 (29%)	0.1013

9	5.23	237	H-1→L+2	0.0040
10	5.36	231	H-2→L (34%); H-1→L+4 (32%); H→L+5 (26%)	0.0382

---

**Table S5.** Calculated UV-vis absorption spectrum, orbitals and energies in gas phase of **2**.**Table S6.** Transitions of **2** assigned by TD-DFT calculations.

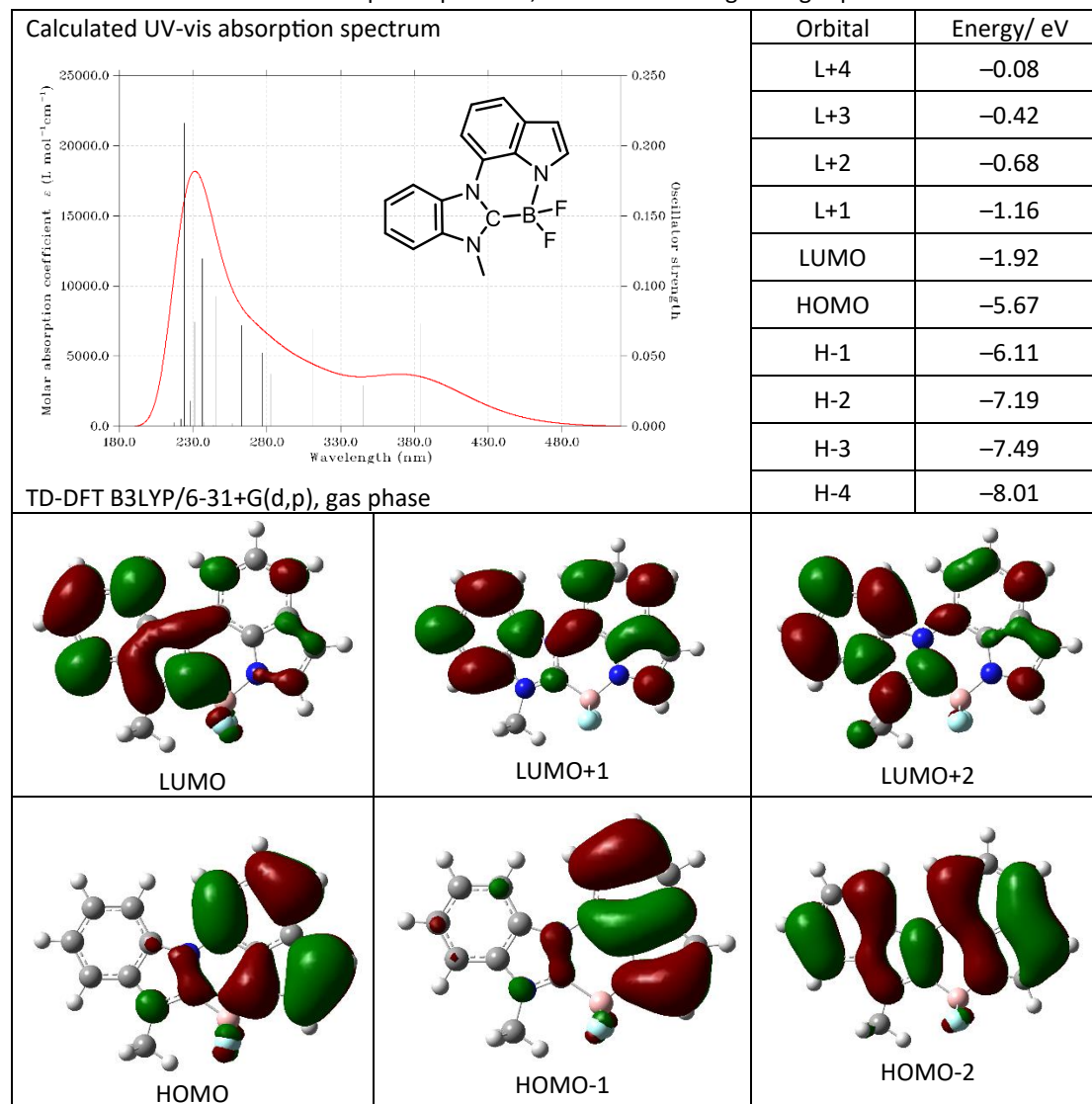
Excited State	E/eV	$\lambda$ /nm	major contributions	<i>f</i>
1	3.64	340	H→L	0.1400
2	3.97	312	H-1→L	0.0651
3	4.47	277	H→L+1	0.0132
4	4.81	258	H-1→L+1	0.0363
5	4.90	253	H→L+2	0.0001
6	5.16	240	H-2→L (33%); H→L+4 (60%)	0.0429
7	5.25	236	H-1→L+2	0.0005
8	5.28	235	H→L+3	0.0011
9	5.32	233	H-2→L (19%); H-1→L+4 (17%); H→L+4 (18%); H→L+5 (42%)	0.0505
10	5.36	231	H-2→L (36%); H-1→L+4 (30%); H→L+4 (15%)	0.0441

**Table S7.** Calculated UV-vis absorption spectrum, orbitals and energies in gas phase of **3**.**Table S8.** Transitions of **3** assigned by TD-DFT calculations.

Excited State	E/eV	$\lambda$ /nm	major contributions	<i>f</i>
1	3.30	376	H→L	0.1409
2	3.85	322	H-1→L (77%); H→L+1 (16%)	0.0548
3	4.04	307	H-1→L (14%); H→L+1 (81%)	0.0904
4	4.38	283	H→L+3	0.0870
5	4.42	280	H→L+2	0.0010
6	4.56	272	H-1→L+1	0.0921
7	4.58	271	H-2→L	0.0561
8	4.69	264	H→L+4	0.0015
9	4.85	256	H-1→L+3 (34%); H→L+6 (51%)	0.0984
10	5.36	231	H→L+5	0.0016

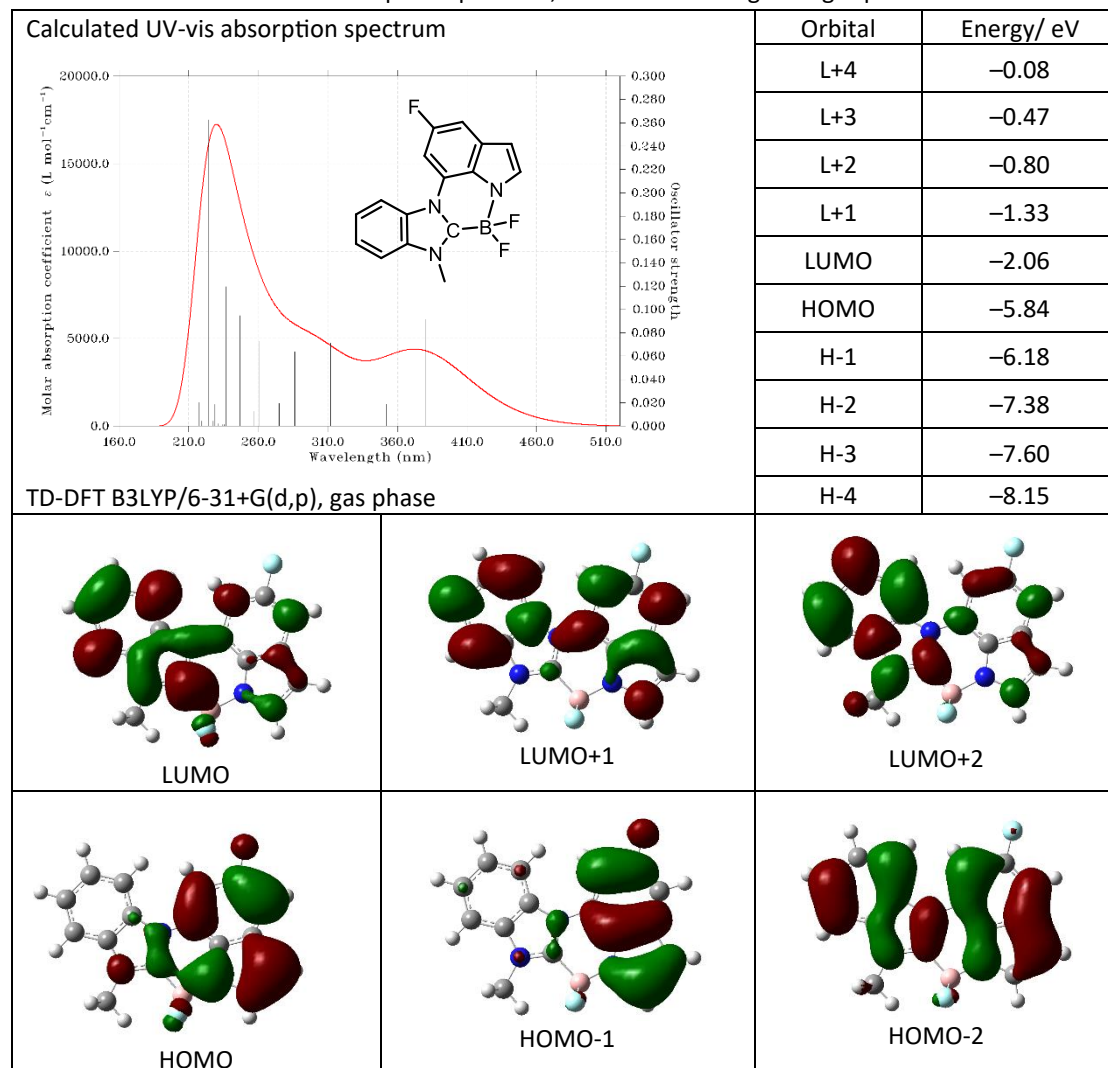


**Table S9.** Calculated UV-vis absorption spectrum, orbitals and energies in gas phase of **4**.

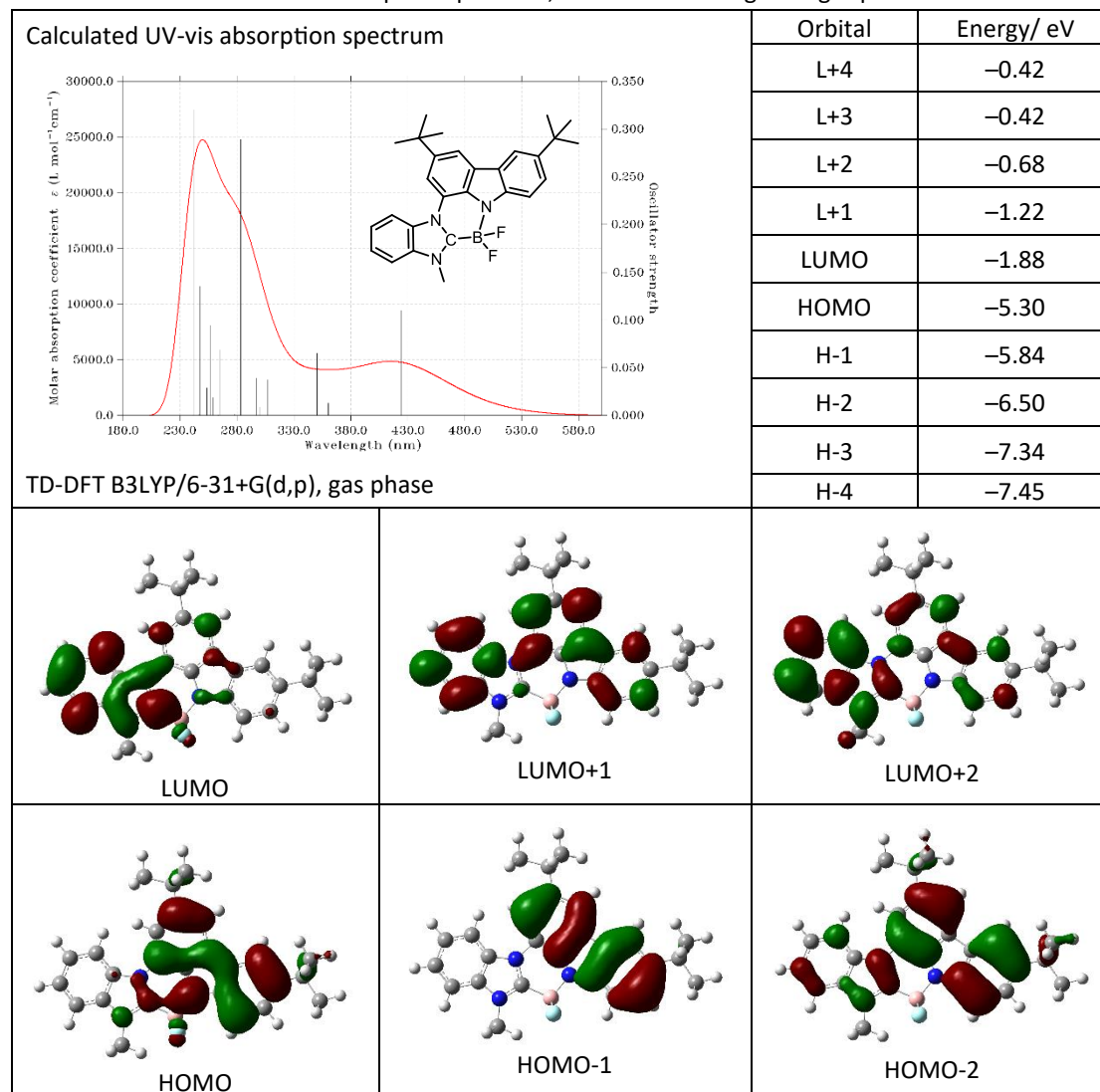


**Table S10.** Transitions of **4** assigned by TD-DFT calculations.

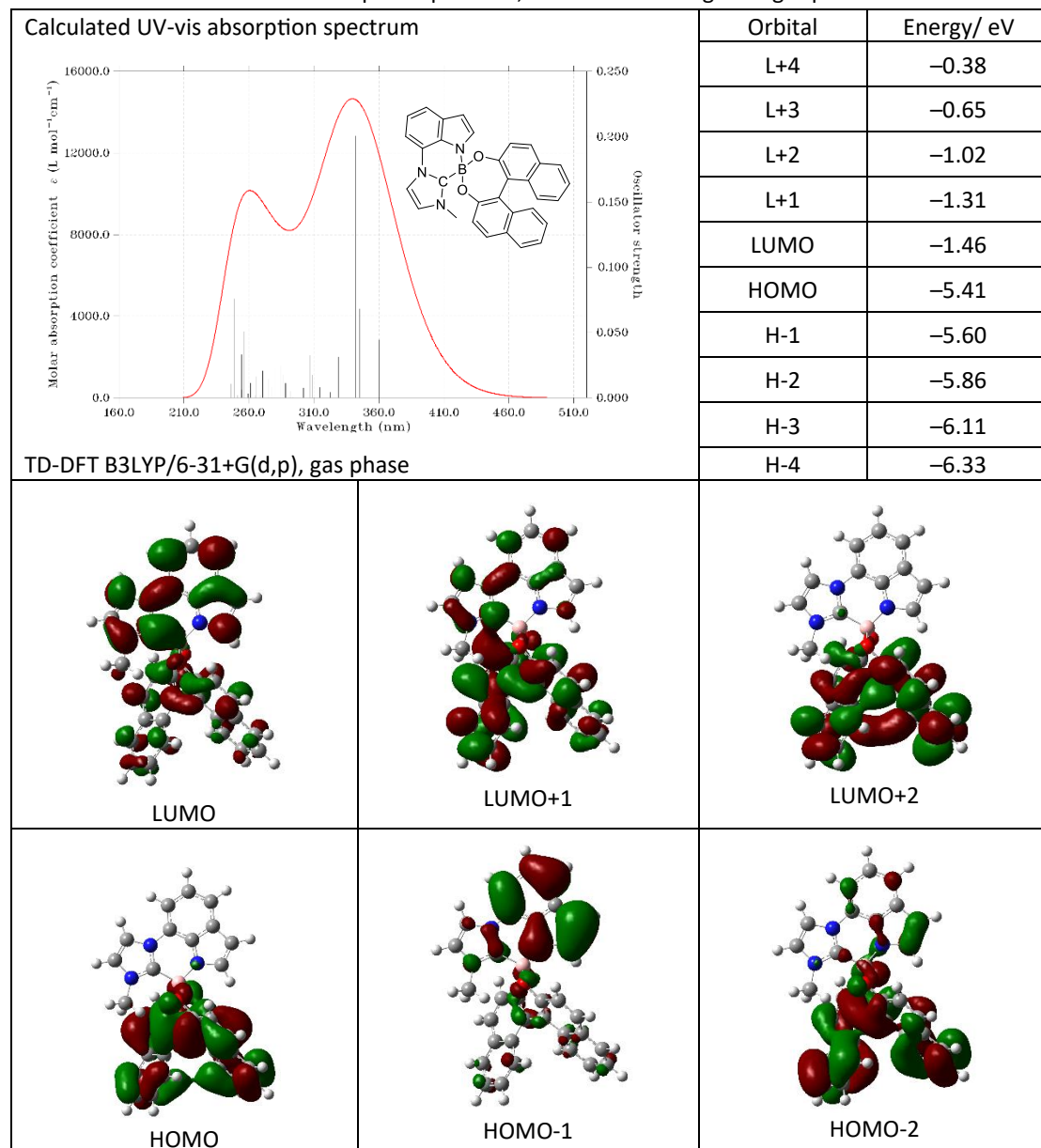
Excited State	E/eV	$\lambda$ /nm	major contributions	$f$
1	3.22	384	H→L	0.0732
2	3.59	345	H-1→L	0.0293
3	3.99	311	H→L+1	0.0692
4	4.38	283	H-1→L+1 (67%); H→L+2 (21%)	0.0372
5	4.42	280	H-1→L+1 (23%); H→L+2 (65%)	0.0523
6	4.72	262	H-2→L	0.0720
7	4.81	258	H→L+3	0.0000
8	4.83	257	H-3→L (14%); H-1→L+2 (73%)	0.0020
9	5.04	246	H-3→L (56%); H-1→L+2 (17%)	0.0926
10	5.08	244	H→L+4	0.0008

**Table S11.** Calculated UV-vis absorption spectrum, orbitals and energies in gas phase of **5**.**Table S12.** Transitions of **5** assigned by TD-DFT calculations.

Excited State	E/eV	$\lambda$ /nm	major contributions	<i>f</i>
1	3.26	380	H→L	0.0915
2	3.52	352	H-1→L	0.0191
3	3.97	312	H→L+1	0.0712
4	4.33	286	H-1→L+1	0.0635
5	4.51	275	H→L+2	0.0198
6	4.76	261	H-2→L	0.0726
7	4.82	257	H-1→L+2	0.0124
8	4.93	252	H-1→L+3	0.0000
9	5.03	247	H-3→L (63%); H-1→L+2 (11%)	0.0926
10	5.24	237	H→L+5	0.1196

**Table S13.** Calculated UV-vis absorption spectrum, orbitals and energies in gas phase of **6**.**Table S14.** Transitions of **6** assigned by TD-DFT calculations.

Excited State	E/eV	$\lambda$ /nm	major contributions	<i>f</i>
1	2.92	424	H→L	0.1101
2	3.44	360	H-1→L	0.0128
3	3.54	350	H→L+1	0.0654
4	4.04	307	H-2→L (44%); H-1→L+1 (29%); H→L+2 (19%)	0.0375
5	4.13	300	H-1→L+1 (26%); H→L+2 (56%)	0.0088
6	4.17	297	H-2→L (51%); H-1→L+1 (18%); H→L+2 (19%)	0.0390
7	4.38	283	H-1→L+1 (20%); H→L+3 (70%)	0.2891
8	4.46	278	H→L+4	0.0009
9	4.67	265	H-2→L+1 (21%); H-1→L+2 (67%)	0.0685
10	4.71	263	H→L+5	0.0006

**Table S15.** Calculated UV-vis absorption spectrum, orbitals and energies in gas phase of **7**.**Table S16.** Transitions of **7** assigned by TD-DFT calculations.

Excited State	E/eV	$\lambda$ /nm	major contributions	<i>f</i>
1	3.44	360	H→L	0.0446
2	3.59	345	H→L+1	0.0680
3	3.62	342	H-1→L	0.2004
4	3.77	329	H-1→L+1 (26%); H→L+2 (48%)	0.0311
5	3.84	323	H-1→L+1 (65%); H→L+2 (21%)	0.0041
6	3.94	314	H-2→L	0.0079
7	4.02	308	H-3→L (23%); H-2→L+1 (50%)	0.0174
8	4.04	307	H-3→L (58%); H-2→L+1 (18%)	0.0322
9	4.11	302	H-2→L+2 (16%); H-1→L+2 (61%)	0.0077
10	4.23	293	H-2→L+2 (12%); H-1→L+2 (25%); H→L+3 (25%)	0.0005

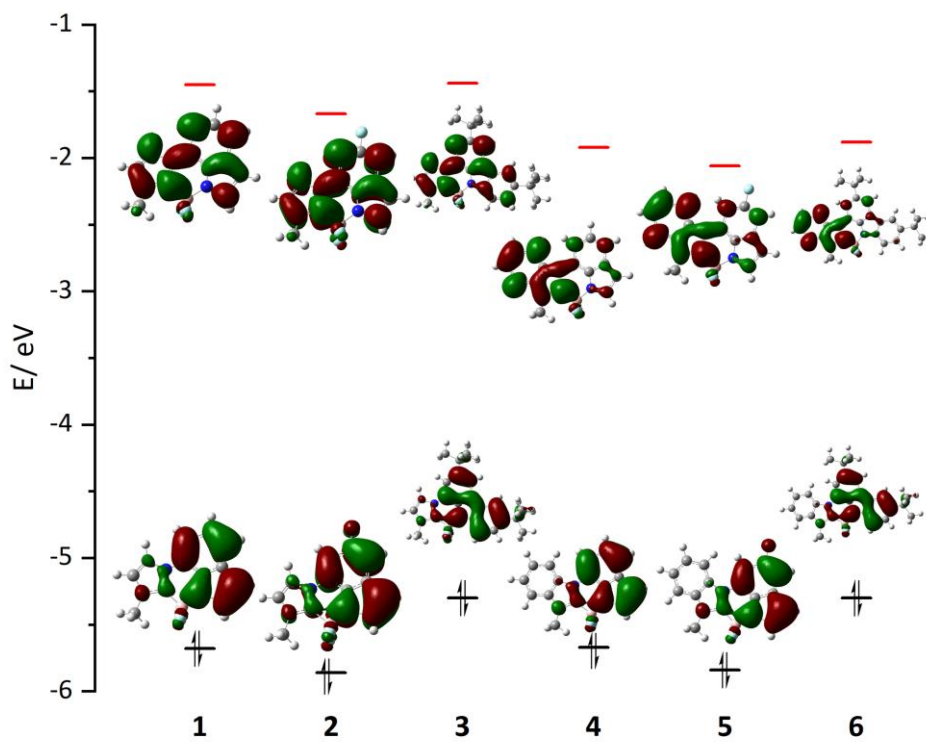


**Figure S106.** Depiction of the HOMOs and LUMOs and corresponding energy levels of 1–6.

**Cartesian coordinates in the structures  
optimized by DFT calculation**

**1** ( $S_0$ ): E(B3LYP) = -852.308924 Hartree

C	-3.10158900	-1.96849100	0.00801400
C	-1.71316400	-2.21823500	0.01049100
C	-0.82560500	-1.14727200	0.00440500
C	-1.33228400	0.15550600	-0.00338800
C	-2.72928100	0.41848800	-0.00698300
C	-3.61655000	-0.67233300	-0.00114100
N	-0.62724300	1.33063900	-0.00987500
C	-1.56119400	2.35290500	-0.01691700
C	-2.84313200	1.85057600	-0.01608900
N	0.59539200	-1.27275000	0.00275300
C	1.36407500	-2.42799300	-0.00097800
C	2.66548200	-2.02806600	-0.01577600
N	2.66730300	-0.64356400	-0.02512900
C	1.40093800	-0.18018200	-0.00929100
B	0.90553200	1.39441200	0.01032600
F	1.40039500	2.01142600	1.17688000
F	1.42848600	2.05551200	-1.12150400
C	3.86047300	0.20700700	-0.00006900
H	-3.78026000	-2.81566000	0.01299500
H	-1.35519800	-3.24233600	0.01689800
H	-4.69110000	-0.51396600	-0.00337600
H	-1.22953600	3.38169100	-0.02225600
H	-3.75421700	2.43221100	-0.02139700
H	0.93426900	-3.41507100	0.00023300
H	3.57666900	-2.60476200	-0.02574300
H	4.64986600	-0.27535800	-0.57919000
H	3.61261300	1.16909600	-0.44625300
H	4.19213000	0.35791800	1.03015100

**2** ( $S_0$ ): E(B3LYP) = -951.547420 Hartree

C	-3.18030500	-1.04207600	0.00435600
C	-1.90968000	-1.63685300	0.00745700
C	-0.79872200	-0.79807400	0.00250400
C	-0.98672500	0.58542300	-0.00455300
C	-2.28359300	1.16946800	-0.00863900
C	-3.40908100	0.32358700	-0.00405300
N	-0.02502700	1.56388000	-0.01016200
C	-0.69343800	2.77328500	-0.01698300
C	-2.05924800	2.58605600	-0.01699900
N	0.54976500	-1.25647200	0.00148600
C	1.02336200	-2.56110400	-0.00256500
C	2.38197200	-2.47894600	-0.01650700

N	2.71056000	-1.13342200	-0.02488000
C	1.59073000	-0.38395400	-0.00945900
B	1.48062000	1.26447200	0.01144600
F	2.10422900	1.74456800	1.17927700
F	2.14452800	1.78314900	-1.11919200
C	4.07176300	-0.58970100	0.00050800
F	-4.25402900	-1.88677300	0.00946800
H	-1.83514500	-2.71735000	0.01327800
H	-4.42556900	0.70166300	-0.00653400
H	-0.13169600	3.69683100	-0.02152200
H	-2.80864900	3.36469400	-0.02243100
H	0.37264200	-3.41893900	-0.00207100
H	3.13142800	-3.25426900	-0.02624900
H	4.72252300	-1.24097700	-0.58549300
H	4.05755300	0.40700200	-0.43807400
H	4.43196700	-0.53008400	1.03038400

**3** ( $S_0$ ): E(B3LYP) = -1320.501913 Hartree

C	-1.33722400	2.71800300	0.00156700
C	-2.36465300	1.75270400	0.00121600
C	-2.07381500	0.38748000	-0.00061100
C	-0.74491400	-0.03500100	-0.00128000
C	0.30658900	0.91640600	-0.00177300
C	0.00003100	2.27775700	-0.00036500
N	-0.27217600	-1.32437600	-0.00256600
C	1.12272800	-1.23489700	-0.00275200
C	1.52631100	0.12810900	-0.00303300
N	-3.06348100	-0.63896500	-0.00419800
C	-4.44595400	-0.51401400	-0.01494600
C	-4.95005900	-1.77899900	-0.02817400
N	-3.87335900	-2.64821100	-0.02980900
C	-2.71779300	-1.95187700	-0.01049700
B	-1.18302900	-2.55376500	0.01734400
F	-1.02231000	-3.32955100	1.18585200
F	-0.99612300	-3.38489300	-1.11084500
C	-3.95788600	-4.11087300	0.00069900
C	-1.63966600	4.23126000	0.00397200
C	-3.15140700	4.53343300	0.00579200
C	-1.02336000	4.88160200	1.26694500
C	-1.02565900	4.88526300	-1.25822400
C	2.07382700	-2.25535600	-0.00270700
C	3.42233900	-1.89650400	-0.00317300
C	3.86060900	-0.55196900	-0.00385200
C	2.88628900	0.45510100	-0.00379000

C	5.35514900	-0.16813000	-0.00466300	C	-1.80050600	-0.87106500	-0.00042200
C	6.28145000	-1.40058200	-0.00440800	C	-2.59459400	0.29195300	0.00058000
C	5.67666200	0.66852400	-1.26729200	N	-1.72535700	1.37619300	0.00151300
C	5.67774000	0.66984400	1.25681000	C	-0.45243400	0.93989700	0.00094000
H	-3.39911600	2.07110300	0.00221400	B	0.88233100	1.91459100	-0.00001100
H	0.80776300	3.00334900	-0.00049000	F	0.83880100	2.73214300	-1.14900900
H	-4.94714000	0.43866200	-0.01950000	F	0.84185600	2.73157500	1.14951000
H	-5.97074200	-2.12687400	-0.04208600	C	-2.14232500	2.77796900	0.00198100
H	-4.83502600	-4.42518700	-0.56765100	C	-2.41127200	-2.13111800	-0.00215800
H	-3.05757700	-4.52171300	-0.45414800	C	-3.80498200	-2.17634500	-0.00231400
H	-4.03631800	-4.46109300	1.03285700	C	-4.58664900	-1.00758700	-0.00090300
H	-3.30817100	5.61720000	0.00761900	C	-3.98948000	0.25006400	0.00041000
H	-3.65016500	4.13270900	-0.88389200	H	2.20838000	-4.23508300	0.00440200
H	-3.64858200	4.12990700	0.89508500	H	0.01359800	-3.18282300	0.00466000
H	-1.22555900	5.95918600	1.27917100	H	4.29679200	-2.89693000	0.00106800
H	0.06162700	4.74615500	1.30550700	H	3.76388300	2.27721800	-0.00265500
H	-1.44627700	4.44432800	2.17788900	H	5.25013600	0.02292500	-0.00279200
H	0.05925600	4.74995500	-1.29918000	H	-2.74217700	2.97985000	0.89342100
H	-1.45025500	4.45065600	-2.16967000	H	-1.25695600	3.40871600	0.00853900
H	-1.22786900	5.96287700	-1.26694600	H	-2.73210500	2.98398300	-0.89522900
H	1.77508900	-3.29793800	-0.00265600	H	-1.84893000	-3.05226800	-0.00416700
H	4.15238700	-2.69725400	-0.00306400	H	-4.29557500	-3.14436100	-0.00369800
H	3.17923800	1.50138800	-0.00421500	H	-5.66888300	-1.08690500	-0.00105900
H	7.32680800	-1.07297600	-0.00496800	H	-4.58204700	1.15834600	0.00103400
H	6.13191000	-2.02407700	0.88364900				
H	6.13124300	-2.02495700	-0.89173800				
H	6.73631400	0.95105000	-1.27997300				
H	5.08591600	1.58905100	-1.30598900				
H	5.46454700	0.09769500	-2.17781800				
H	5.08705800	1.59042900	1.29504700				
H	5.46638000	0.09998200	2.16811100				
H	6.73740900	0.95235500	1.26828600				

**4 (S<sub>0</sub>): E(B3LYP) = -1005.962669 Hartree**

C	2.15653000	-3.15074100	0.00271800
C	0.88291700	-2.54393000	0.00259900
C	0.76781700	-1.15506100	0.00042800
C	1.94883000	-0.39780100	-0.00091400
C	3.23743300	-1.00056800	-0.00095900
C	3.32984800	-2.40236500	0.00090500
N	2.07551600	0.96702600	-0.00173300
C	3.43042700	1.24908000	-0.00235600
C	4.17133200	0.09026200	-0.00193900
N	-0.46459300	-0.42249900	0.00028400

**5 (S<sub>0</sub>): E(B3LYP) = -1105.201435 Hartree**

C	-2.56843700	2.43605600	0.00036300
C	-1.20141200	2.12104200	0.00046500
C	-0.82442500	0.77872200	0.00009600
C	-1.83581600	-0.19127800	-0.00016500
C	-3.21758500	0.14968300	-0.00025800
C	-3.59047400	1.50638000	-0.00001700
N	-1.69503000	-1.55623200	-0.00034700
C	-2.96749900	-2.09327700	-0.00059200
C	-3.92106000	-1.09961100	-0.00057100
N	0.52527000	0.30476900	0.00007400
C	1.74656700	1.00839200	-0.00009600
C	2.75309500	0.02413000	0.00020400
N	2.11345400	-1.21067700	0.00050100
C	0.78070000	-1.03460300	0.00032400
B	-0.33847700	-2.25287500	-0.00000500
F	-0.13744800	-3.04393300	-1.14934900
F	-0.13810300	-3.04411900	1.14934200
C	2.79877300	-2.50312700	0.00063800

F	-2.88628700	3.76551600	0.00069700	C	6.03495300	-0.46746200	-0.00050700
C	2.09584000	2.36417300	-0.00063000	C	6.88362300	-1.75454900	-0.00039500
C	3.45342000	2.68254400	-0.00072200	C	6.40774600	0.34837200	-1.26268600
C	4.44971100	1.69037400	-0.00032800	C	6.40791400	0.34869800	1.26141000
C	4.11237600	0.33961300	0.00011700	C	-4.67174600	0.86114800	-0.00136000
H	-0.49923700	2.93843300	0.00092500	C	-6.04555900	0.62179000	-0.00179600
H	-4.62517000	1.83092900	-0.00007800	C	-6.57313600	-0.68139900	-0.00137600
H	-3.09729700	-3.16635100	-0.00075400	C	-5.73205300	-1.79065700	-0.00057400
H	-4.99222700	-1.24270900	-0.00070600	H	-2.53202900	2.33922500	0.00088200
H	3.42330500	-2.58429900	0.89417000	H	1.71412900	2.97017300	-0.00020300
H	2.05517200	-3.29609000	0.00257700	H	-3.95499800	-4.21088300	-0.89323300
H	3.42061800	-2.58608000	-0.89461000	H	-2.41868100	-4.32931000	0.00053900
H	1.36401300	3.15748200	-0.00104700	H	-3.95435900	-4.21046000	0.89543800
H	3.74382900	3.72812500	-0.00114700	H	-2.22360300	5.85183900	0.00115200
H	5.49504300	1.98141300	-0.00042500	H	-2.66201700	4.39256200	-0.88911100
H	4.87238400	-0.43396000	0.00033000	H	-2.66161000	4.39230300	0.89119400

**6 (S<sub>0</sub>): E(B3LYP) = -1474.155370 Hartree**

C	-0.44540200	2.82891900	0.00029800
C	-1.53538300	1.93445700	0.00041700
C	-1.35503800	0.54781000	0.00014800
C	-0.04945000	0.04470400	0.00000500
C	1.06350100	0.92468900	-0.00015000
C	0.85704000	2.30367400	-0.00006200
N	0.34934500	-1.27005500	0.00003400
C	1.74603700	-1.27028300	-0.00014700
C	2.23202900	0.06366300	-0.00030100
N	-2.41579100	-0.41659400	0.00010700
C	-3.81575300	-0.24765100	-0.00045700
C	-4.35769400	-1.54792100	-0.00017100
N	-3.28806400	-2.43361900	0.00040900
C	-2.12891500	-1.74879600	0.00053200
B	-0.62710700	-2.43445400	0.00085100
F	-0.50822700	-3.24861900	1.14984700
F	-0.50834000	-3.24998500	-1.14720100
C	-3.41328000	-3.89065900	0.00083400
C	-0.65010000	4.35875300	0.00056800
C	-2.13873200	4.76008900	0.00097500
C	0.00655200	4.96938500	1.26304200
C	0.00595800	4.96974100	-1.26204100
C	2.63137700	-2.34846800	-0.00009700
C	3.99942200	-2.07368600	-0.00021700
C	4.51961200	-0.75852800	-0.00037400
C	3.60947100	0.30682400	-0.00040700

C	6.03495300	-0.46746200	-0.00050700
C	6.88362300	-1.75454900	-0.00039500
C	6.40774600	0.34837200	-1.26268600
C	6.40791400	0.34869800	1.26141000
C	-4.67174600	0.86114800	-0.00136000
C	-6.04555900	0.62179000	-0.00179600
C	-6.57313600	-0.68139900	-0.00137600
C	-5.73205300	-1.79065700	-0.00057400
H	-2.53202900	2.33922500	0.00088200
H	1.71412900	2.97017300	-0.00020300
H	-3.95499800	-4.21088300	-0.89323300
H	-2.41868100	-4.32931000	0.00053900
H	-3.95435900	-4.21046000	0.89543800
H	-2.22360300	5.85183900	0.00115200
H	-2.66201700	4.39256200	-0.88911100
H	-2.66161000	4.39230300	0.89119400
H	-0.12492600	6.05790200	1.27403200
H	1.08039500	4.76351000	1.30197200
H	-0.44408200	4.56151700	2.17434100
H	-0.44509800	4.56212200	-2.17324400
H	-0.12553400	6.05826000	-1.27266700
H	1.07978400	4.76388700	-1.30153100
H	2.26885100	-3.37061300	0.00002100
H	4.67888600	-2.91779600	-0.00017800
H	3.96655800	1.33295400	-0.00052500
H	7.94713300	-1.49187000	-0.00050400
H	6.69561000	-2.36793000	0.88739600
H	6.69548800	-2.36816700	-0.88799500
H	7.48270500	0.56554300	-1.27467000
H	5.87442700	1.30334000	-1.30142500
H	6.16167000	-0.20813500	-2.17353600
H	6.16196600	-0.20757400	2.17243700
H	7.48287400	0.56587500	1.27319000
H	5.87460000	1.30367600	1.29997800
H	-4.31169300	1.87857900	-0.00179400
H	-6.72256300	1.46998900	-0.00249800
H	-7.64886000	-0.82413000	-0.00172400
H	-6.12677000	-2.80076400	-0.00031000

**7 (S<sub>0</sub>): E(B3LYP) = -1572.445831 Hartree**

C	6.38456100	0.80207700	0.77267200
C	5.72096800	-0.34752200	0.29515300
C	4.34882900	-0.30101900	0.06891100
C	3.65789300	0.88386100	0.32700500



C	4.31545800	2.04748900	0.81109700	H	0.26461100	-2.43776500	2.39667200
C	5.70347800	1.99190500	1.02862300	H	-1.74285100	-3.91771600	2.39030200
N	2.31624800	1.11649200	0.18005000	H	-1.65364900	4.17927700	-2.27554200
C	2.09989900	2.42488800	0.58409200	H	0.20043800	2.53092900	-2.52397500
C	3.27818100	3.02870800	0.96168200	H	-3.75699000	0.70748300	1.53287800
N	3.57563100	-1.38524100	-0.43975700	H	-5.46781300	2.41891200	1.90208500
C	4.03604700	-2.61126700	-0.89323000	H	-5.47965200	4.51843200	0.54811200
C	2.95166300	-3.27897200	-1.36926900	H	-3.70127800	4.89914000	-1.13578300
N	1.85368900	-2.45279000	-1.20448600	H	-3.95964500	-4.46739300	1.48911400
C	2.22971100	-1.28927100	-0.62400000	H	-5.88094000	-3.93562400	0.01622500
C	0.49341100	-2.81558800	-1.62129100	H	-5.84440400	-1.84624100	-1.35355300
B	1.29937500	0.00690400	-0.15742800	H	-3.96070000	-0.28939400	-1.20255000
O	0.42038700	0.28831800	-1.29771500				
O	0.55551500	-0.26450200	1.08366900				
C	-0.64090800	1.13191600	-1.12188100				
C	-0.59368900	-0.98741100	1.05829100				
C	-0.61703100	-2.19131700	1.81265600				
C	-1.72468200	-3.00344000	1.80216900				
C	-2.85151600	-2.67621800	0.99917000				
C	-2.84586800	-1.44685800	0.25525500				
C	-1.72039900	-0.55237000	0.35933000				
C	-1.70387400	0.79013500	-0.28923200				
C	-2.72627400	1.77734500	-0.04856600				
C	-2.70899200	3.01043400	-0.78487300				
C	-1.65590100	3.25183600	-1.70855100				
C	-0.63426000	2.34607700	-1.85544100				
C	-3.74690300	1.60838900	0.93106500				
C	-4.70879900	2.57452000	1.14056900				
C	-4.71241000	3.76834700	0.37987600				
C	-3.72625400	3.97777600	-0.55891300				
C	-3.96897300	-3.55043300	0.90458700				
C	-5.03558600	-3.25707000	0.08337400				
C	-5.01657900	-2.06884200	-0.68617800				
C	-3.95665700	-1.19025600	-0.60050200				
H	7.45528600	0.74880200	0.94328600				
H	6.28948900	-1.25293000	0.11152400				
H	6.24303800	2.85962600	1.39706100				
H	1.09977400	2.83311900	0.57724700				
H	3.38711100	4.04642800	1.30936500				
H	5.07390400	-2.89437800	-0.85596900				
H	2.86906400	-4.25753000	-1.81470300				
H	-0.05443400	-1.90324400	-1.84720400				
H	0.56356900	-3.43954900	-2.51423000				
H	-0.01425300	-3.36175500	-0.82340100				

## References

- [1] Dolomanov, O. V. Bourhis, L. J. Gildea, R. J. Howard, J. A. K., Puschmann, H. J. *Appl. Cryst.* 2009, 42, 339–341.
- [2] Sheldrick, G. M. *Acta Cryst.* 2015, A71, 3–8.
- [3] Sheldrick, G. M. *Acta Cryst.* 2015, C71, 3–8.
- [4] A. D. Becke, *J. Chem. Phys.* 1993, 98, 5648–5652.
- [5] a) Petersson, G. A. Al-Laham, M. A. *J. Chem. Phys. A* 1991, 94, 6081–6090; b) Petersson, G. A. Bennett, A. Tensfeldt, T. G. Al-Laham, M. A. Shirley, W. A. *J. Chem. Phys.* 1988, 89, 2193–2218.
- [6] Lu, T. Chen, F. W, *Multiwfn: A Multifunctional Wavefunction Analyzer*, *J. Comput. Chem.* 2012, 33, 580–592.